© 2010

Brian Matthew Gaas

ALL RIGHTS RESERVED

RESPONSE AND REGULATION OF CELL-SURFACE HYDROLASES TO NUTRIENT STRESS IN RIVER-INFLUENCED COASTAL AREAS

by

BRIAN MATTHEW GAAS

A dissertation submitted to the

Graduate School-New Brunswick

Rutgers, The State University of New Jersey

in partial fulfillment of the requirements

for the degree of

Doctor of Philosophy

Graduate Program in Oceanography

written under the direction of

James W. Ammerman and Robert Chant

and approved by

_____

_____

_____

_____

_____

New Brunswick, New Jersey

October, 2010

ABSTRACT OF THE DISSERTATION

Response and regulation of cell-surface hydrolases to nutrient stress in river-influenced coastal areas

By BRIAN MATTHEW GAAS

Dissertation Directors: James W. Ammerman and Robert T. Chant

Conceptually, the hydrolysis product of ectoenzyme activity is used to relieve nutrient stress or acquire a type of molecule not immediately accessible in the environment. When properly characterized, ectoenzyme activities can offer greater insight into the nutrient requirements of organisms and how they use organic matter. This dissertation analyzes enzyme activity data from two river-influenced coastal regions, locations of variable inorganic nutrient concentrations, dissolved organic matter concentrations, and biomass. It is the ultimate goal of this dissertation to provide a quantitative means of interpreting ectoenzyme activity or, at the very least, to provide possible interpretations of activity that go beyond the overly-simplistic and qualitative views currently dominant in the ectoenzyme literature. In addition, it highlights the advantages of automated biological measurements, and promotes their use in future work. The first section explores the role of nitrate on LAP expression, and how LAP activities can reflect (and participate in) different biogeochemical regimes within the Hudson River outflow. The second section describes a simple model predicting the influence of leucine aminopeptidase (LAP) activity on a nitrate-limited phytoplankton population. The model includes predictions of the strength of nitrate limitation, ability of LAP to overcome the

limitation, coupling strength between hydrolysis and uptake, and a phytoplankton nitrate requirement. The third section expands upon current research in alkaline phosphatase (AP) activity in the Louisiana shelf. This work provides a first look at high resolution time-series of AP activity and other environmental variables, and how the interpretation of AP activity measurements may be improved by considering a time lag between variables and a temporal control on AP expression.

ACKNOWLEDGEMENTS

My introduction to the world of ectoenzymes came during my undergraduate studies as a biochemistry/genetics major at Texas A&M. I was looking for part-time work in a lab outside of the biochemistry department; at the time, dedicating myself to running gels of DNA and protein extracts didn't seem like exceptionally exciting prospects. Dr. James Ammerman, in the Department of Oceanography and Meteorology, was doing research on alkaline phosphatase, a cell-surface enzyme that responds to low phosphate concentrations and is often used as an indicator of phosphorus stress. I approached Dr. James Ammerman with a request to join his lab to get some research experience. His willingness to take me on was to be a defining moment in my college and post-graduate career.

With help from Dr. Ammerman and his graduate student Jason Sylvan, I learned about ectoenzymes, nutrient limitation in the ocean, and how to pronounce the chemical 4-methylumbelliferyll phosphate. I was given my own project: programming a system to automate the rather tedious alkaline phosphatase measurements Jason was currently making by hand. For the next year and a half, I worked on automating the enzyme assay. While the instrument was never perfected to the degree required to replace the manual measurements, it did give me a strong foundation and understanding in many of the aspects required to make an operational automated enzyme activity system. Perhaps more importantly, it sparked my interest in oceanography and the intersection of technology and science.

I graduated from Texas A&M in 2002, a year after Dr. Ammerman (and Jason) left for Rutgers University. After a 9 month stint as an AmeriCorps volunteer, I rejoined

the Ammerman lab at Rutgers as a Masters of Science student in Oceanography. My project remained the same as when the lab was located in Texas. There was a completely different hardware component based on the principles of flow-injection analysis, which meant learning new programming languages and seeing how the new system would behave differently than the old one. This time, the instrument was developed and successfully deployed in three different trophic regimes. My education in marine science had also advanced to the point where I understood what “trophic regime” meant. With Dr. Ammerman’s approval, I continued my graduate studies at Rutgers University, working on a Ph.D. in oceanography, culminating in this dissertation. In the same way that the following analysis of enzyme activities was made possible through automation, my graduation studies would also have not have been possible without the help of a great many people:

- *Dr. James Ammerman*, for taking me on as an undergraduate and offering his support throughout my studies. Without him, I would have missed out on innumerable opportunities which have strengthened me both as a researcher and as a person.

- *Dr. Jason Sylvan*, for helping me muddle my way through just what it was Dr. Ammerman did in his lab.

- *My thesis committee*, for taking the time to read, comment, and improve the quality of this work. Additionally, many of them allowed me to participate in their own research projects and research cruises, and taught me as part of graduate courses.

- *My fellow graduate students* at Rutgers University, for their friendship and assistance.

- *My family*, for always welcoming me home and not being too upset when I had to spend days doing work instead of interacting with them.

- *Dr-in-progress Karen Routledge*, for her unwavering support and understanding…as well as her excellent cinnamon buns, muffins, and rice.

TABLE OF CONTENTS

LISTS OF TABLES

LIST OF FIGURES

1.0 Introduction

The hydrolysis activity of ectoenzymes is a necessary step in the conversion of otherwise unusable particulate or polymeric organic matter into a form available for uptake. Ectoenzymes are a class of hydrolase that operates on or near the cell surface or in the periplasmic space (Martinez and Azam 1993, 1993b). This definition distinguishes ectoenzymes from intracellular enzymes that reside within the cytoplasm and extracellular enzymes not directly associated with the cell (Chrost and Siuda 2002). Much of the organic matter available to microbes is too large for direct transport into the cytoplasm. Ectoenzymes are used by the cell to convert large and polymeric molecules into smaller, transportable products. This activity plays a major role in dissolved organic matter transformations in both surface and deep waters and can be used to determine dissolved organic matter utilization (Stepanauskas et al. 1999). The linkage between organic and inorganic nutrients and the interrelationship between bacteria and higher trophic levels are two of the primary features of the microbial loop (Azam et al 1983; Azam et al 1994).

The changes ectoenzymes make to the structure of organic matter pools have relevance across a wide range of disciplines, including climate change, eutrophication, and other topics concerned with nutrient availability. There is little reason ectoenzyme activity could not be used to probe some of the interactions between the organic and inorganic matter pools. Ectoenzyme activity is one of a few in situ biological rate measurements, and may be a key element to a deeper understanding of organic matter dynamics.

Despite the important role ectoenzymes play in organic matter cycling, they are overwhelmingly used strictly as indicators of potential nutrient limitation, as their expression has been linked to low inorganic nutrient concentrations. A non-linear increase in many ectoenzymes (e.g. alkaline phosphate, leucine aminopeptidase, glucosidases, lipases) occurs as concentrations of the relevant nutrient moiety (phosphate, leucine, glucose, and lipids in the above examples) decrease. Due to the simplicity of ectoenzyme activity measurements and a straight-forward rational for interpreting the data, ectoenzyme activities have, to some degree, been pigeonholed as indicators of nutrient limitation.

Two types of nutrient limitation are found in aquatic environments (Cullen et al 1992). The first is a limitation on the maximum biomass, also known as Liebig limitation (Liebig 1885). The carrying capacity of the system is defined by the nutrient requirements of the organism and the concentration of available nutrients. Maximum biomass becomes limited, and the carrying capacity reached, when the requirement for a certain nutrient exceeds its availability. By extension, if a source of the limiting nutrient is supplied, the total amount of biomass may increase accordingly. The second type of limitation reduces the instantaneous growth rate of the population (Cullen et al 1992). The addition of a limiting nutrient will increase the speed at which the cell performs functions, but the population does not exhibit the same increase in biomass as found with the relief of Liebig limitation. Generally speaking, techniques used to define nutrient limitation in the field are designed to measure Liebig limitation.

Multiple lines of evidence are usually used together to identify a (Liebig-type) limiting nutrient, including nutrient concentrations, uptake rates of radiolabeled

substrates, nutrient ratios (with or without reference to the Redfield ratio), and nutrient addition experiments (D'Elia et al 1986). Approaches relying on nutrient concentrations do not directly relate to the nutrient status (replete vs depleted) of the biota. Well-adapted organisms may better tolerate lower nutrient concentrations, or access alternative sources of nutrients that are not specifically accounted for. The uptake of radiolabeled substrates is a highly sensitive technique for the analysis of nutrient limitation, but requires special training, protocols, and disposal procedures. Even bioassays, considered perhaps the best identifier of nutrient limitation (D'Elia et al 1986), have multiple factors which can complicate the interpretation of the results (Smith and Hitchcock 1994). In some ways, measuring ectoenzyme activity is a superior method of determining nutrient stress in an aquatic ecosystem because it is specific to the nutrient requirements of the organisms and not the condition of the environment itself.

Despite the relevance of ectoenzyme activity in biogeochemical systems, comparatively little research is currently being performed on the topic of ectoenzyme activities. Many outstanding questions still remain regarding fundamental aspects of ectoenzymes, including their regulation and effect on individual and community dynamics. Ectoenzyme activities are inextricably linked to changes in the dissolved and particulate organic matter pools, inorganic nutrient pools, and some physical forcings. Conflicting reports exist on exactly which environmental parameters control or are related to ectoenzyme expression and activity in different locations and conditions. It is recognized, though often little mentioned, that ecoenzyme activities are a rather simple parameter to measure but much more difficult to interpret. Activity measurements are

notoriously variable and general patterns of activity over spatial and temporal scales can be modified by multiple influences.

The number and complexity of interactions within and between different pools of matter and other environmental variables necessitates the interpretation of enzyme activity be extended beyond the usual statement of “high activity = nutrient-stressed biomass.” In particular, the relationship between ectoenzyme activity, dissolved nutrients, and chlorophyll fluorescence requires a more thorough understanding. The case of two ectoenzymes, alkaline phosphatase and leucine aminopeptidase, are considered in depth here. A new technology, the Enzyme Activity Analysis System, was used to measure the activities of these two enzymes in river-influenced coastal. The following portions of this section will provide background information on alkaline phosphatase and leucine aminopeptidase, and describe the Enzyme Activity Analysis System.

1.1 Alkaline Phosphatase

Alkaline phosphatase (AP) is one of the best characterized of the ectoenzymes. It is known to be induced by low inorganic phosphate concentrations and is produced by both heterotrophic bacteria and phytoplankton (Hoppe 2003).

Much of the conceptual picture of ectoenzyme activities and AP in particular is derived from research of the *pho* regulon of E. coli, a traditional two-component system (Figure 1.1). Inorganic phosphate is transported through the cell membrane by the *pho*A/*pho*C/*pst*S complex. This step may be preceded by the hydrolysis of organic phosphates by alkaline phosphatase (*pho*A). After a series of phosphorylations between *pho*R and *pho*B, an inducer (*pho*B-P) activates the transcription of the *pho* genes, one of

which is *pho*A (alkaline phosphatase). With this mechanism, the concentration of exterior phosphate controls the production of AP; a deficit of phosphate in the environment will lead to an increase in AP production. Assuming sufficient substrate is available to affect the enzyme kinetics, measured AP activity will also increase under phosphate deficient conditions.

The induction of AP by low phosphate is not a linear response. The canonical "induction curve" of AP (and other ectoenzymes) is a decaying exponential. At high inorganic phosphate concentration (in practice, measured as soluble reactive phosphate or SRP), AP activity is minimum. When a minimum threshold is crossed (between 0.1-0.4 uM SRP, Chrost 1991; Chrost and Overbeck 1987; Dyhrman and Palenik 2003; Dyhrman and Ruttenberg 2006; Sylvan 2008), AP activities rapidly increase.

Unfortunately, even with a well-characterized ectoenzyme like AP, the interpretation of bulk activity measurements is not straight-forward. The AP – phosphate relationship is generally not sufficiently resolved to predict AP activity from phosphate concentration (or vice versa). AP activities can range from near zero to above 1.5 uM L^{-1} hr^{-1} (Gaas and Ammerman 2007; Sylvan 2008). This range of activities for a given SRP value limits the functionality of AP activity assays and reduces the usefulness of AP activity in evaluating potential phosphorus stress. AP activity is also potentially controlled by the carbon requirement, induced by the presence of enzyme substrate, and kinetically controlled by substrate concentration (Benitez-Nelson and Buesseler 1999; Hoppe 2003). Patterns in cell-specific ectoenzyme activity can differ from bulk activity (Martinez et al 1996; Dyhrman and Ruttenberg 2006; Hoppe 2003; Strojsova and

Dyhrman 2008; Strojsova et al 2008), making the effects of AP activity more complicated to scale to an ecosystem level.

1.2 Leucine Aminopeptidase

Leucine aminopeptidase (LAP) is often used as an indicator of organic matter usage. LAP is involved in the hydrolysis of amino acids from peptides or amino acid-containing molecules. However, unlike the *pho* regulon of alkaline phosphatase, no distinct genetic mechanism has been found coding for aminopeptidases. Total LAP activity is predominately of bacterial origin, though certain species of dinoflagellates can also contribute (Karner et al 1994; Mulholland et al 2003, Salerno and Stoecker 2009). Importantly, diatoms have not been shown to contribute directly to LAP activity, despite their often assumed role as the dominate photoautroph controlling nutrient uptake in coastal regions.

There is little consensus on the controls of LAP expression- reports show LAP being repressed by dissolved free amino acids, induced or unaffected by dissolved combined amino acids, activated by other ectoenzymes, and constitutively expressed and/or repressed in the presence of high nitrate (Foreman et al 1998; Jorgensen et al 1999; Nausch and Nausch 2000; Donachie et al 2001; Taylor et al 2003; Chrost and Siuda 2006). In addition to nitrogen, LAP activity potentially reflects cellular carbon requirements (Chrost and Rai 1993; Foreman et al 1998; Williams and Jochem 2006). LAP expression in the Hudson River estuary (New York, USA) is controlled by nitrate concentration, implicating LAP activity in relieving nitrogen stress (Taylor et al 2003), at least in that particular location.

1.3 Enzyme Activity Analysis System

In many ectoenzyme assays, activity is measured at a single location using a small volume of water (Hoppe 1983). Since the 1970's (Perry 1972), most bulk ectoenzyme assays have been performed using a fluorometric technique. A highly conjugated organic compound covalently bound to a nutrient moiety is added to an aliquot of water. In the bound state, the complete molecule is an ectoenzyme substrate and exhibits minimal fluorescence. Ectoenzymes in the water hydrolyze the fluorescence compound from the nutrient moiety. The released conjugated compound is highly fluorescent when excited at the proper wavelength. Most ectoenzyme substrates are derivates of methylumbelliferones or methylcoumarins; these classes of substrates are excited by light around 360 nm and fluorescence at ~440 nm. In solution, ectoenzymes in the aliquot of water continually act on unhydrolyzed substrate, increasing the concentration of the fluorophore. Ectoenzyme activity can then be measured as the near instantaneous rate of fluorescence increase over time.

Two main types of instruments currently are used for enzyme activity measurements with fluorescent substrates (Ammerman and Glover 2000; Marx et al. 2001; Huston and Deming 2002; Sylvan et al. 2006): manual fluorometers, and fluorescence microplate readers. Assays done manually or using a microplate reader require the user to manipulate the sample at both the sample acquisition and substrate additions steps. In manual assays, temporary deviations from linearity from settling particles or dispersion may be difficult to identify due to discontinuous measurements and constant handling. A fluorescence microplate reader can run multiple

samples and/or substrates at the same time, including replicates. Incubation times are preset with automated measurements and data logging, providing more freedom for the experimenter. However, the delay between sample acquisition and measurement inherent with spatial ectoenzyme activity surveys may lead to changes in activity.

This work incorporates flow-injection analysis (FIA) technologies to improve fluorometric ectoenzyme assays. FIA has been in use as an analytical technique for ~30 years (Ruzicka 2000) and can be applied to chemical (colorometric), pharmaceutical, and environmental assays (Chen and Ruzicka 2004). Dispersion (from shear mixing and diffusion) between two or more fluids occurs within a system of tubing. A pump and multiple position value control the fluid movement and mixing rates. A flow-through cuvette is placed inside a photometer to measure the concentration of reaction product. In an ectoenzyme assay using FIA protocols, a quartz fluorescent cuvette is coupled with a fluorometer to detect substrate hydrolysis (Gaas and Ammerman 2007; Jeager et al 2009).

With the appropriate computer controls and hardware in place, sample uptake, reagent and substrate mixing, incubation timing, and measurement of reaction product formation can be automated. The reproducibility of sample processing is one of the largest advantages of a FIA system for measurements, especially in comparison to manual and microplate-based enzyme assays (Ruzicka 2000). These advancements have allowed detailed spatial mapping of AP activity in multiple regions, in surface waters as well as at depth (Ammerman and Glover 2000; Gaas and Ammerman 2007). Spatial mapping of AP activity, in turn, has provided information about the causes and extent of eutrophication in coastal areas (Sylvan et al 2006; Gaas and Ammerman 2007).

The Enzyme Activity Analysis System (EAAS) was designed to improve upon existing fluorometric ectoenzyme assays, taking advantage of the automation and stability inherent with FIA systems. A schematic is presented in Figure 1.2. EAAS was designed to measure AP and aminopeptidase activities using the substrates 6,8-difluoro-4-methylumbelliferyl phosphate (dfMUF-P) and L-Leucine-7-amido-4-methylcoumarin (Leu-AMC), respectively. EAAS was run using a stopped-flow protocol. Rather than relying on discrete measurements of fluorescence and interpolating between them, a reaction mixture containing seawater and substrate was incubated directly inside the fluorometer. In this manner, the hydrolysis of substrate over the entire course of the assay is observable.

EAAS runs consisted of 20, 50, or 100 samples, depending on the rapidity of visible detritus accumulation in the syringe. Each run followed the same progression: a five-point external standard curve, substrate baseline, a repeating series of ten samples with one internal standard and one killed control (a series was always ten samples, one internal standard and one killed control), a second substrate baseline, and a second five-point external standard curve. The external standard curves were made using either dfMUF for AP assays, or AMC for aminopeptidase work. The substrate baseline was the steady fluorescence measured after injection of a substrate into distilled water, where no biologically-mediated hydrolysis is expected. The internal standard was the fluorescence of a standard (not substrate) injected into seawater; variation of this value over the course of a run provided corrections for differences in salinity, temperature, colored dissolved matter absorbance, and other changing environmental parameters. Killed controls were

substrate injections into boiled and cooled seawater. Post-run cleaning was done using a 10% HCl solution followed by repeated distilled water flushing.

1.4 Outline of Dissertation

The overarching theme of this work was to further elucidate the relationships and controls on ectoenzyme activities, specifically in eutrophic, river-influenced environments. The high sampling rate available with EAAS matches well with other automated instrumentation, providing a unique opportunity to compare bulk ectoenzyme activities with various environmental parameters on short time and spatial scales.

This dissertation uses data from two river-influenced coastal regions in an attempt to further understand how, when, and to what extent ectoenzymes are induced. A series of research cruises to the Hudson River (New York, USA) and Mississippi River (Louisiana, USA) outflows were conducted between 2004 and 2007.

The Hudson River work focuses on variations in LAP activity around the river plume and along the New Jersey shelf. Measurements of surface LAP activity were taken concurrently with macronutrient concentrations, fluorescence, and salinity data. The analysis describes the relationships between phytoplankton biomass and inorganic nitrogen concentrations and the induction of LAP activity. It also links the magnitude and timing of LAP activity to changes in dissolved organic and inorganic nutrient concentrations as well as other environmental parameters. The ability of LAP to actively support nutrient-depleted phytoplankton biomass is investigated. LAP activity is shown to accurately differentiate biogeochemical states in a coastal environment.

EAAS was reconfigured to measure AP activities for a cruise along the Louisiana shelf. Two biogeochemical process stations were established where multiple environmental parameters were measured during hourly CTD casts. During this time, surface AP activities were measured. The covariance with and possible causative roles of non-nutrient variables in changing ectoenzyme activities are a major focus of this portion of the work. In addition, the temporal variability in different indicators of nutrient limitation (nutrient concentrations, ratios, and AP activities) is characterized, with important ramifications for classifying eutrophic environments.

It is the ultimate goal of this dissertation to provide a quantitative means of interpreting ectoenzyme activity or, at the very least, to provide possible interpretations of activity that go beyond the overly-simplistic and qualitative views currently dominant in the ectoenzyme literature.

2.0 Distribution of aminopeptidase activity in surface waters of the Hudson River plume

2.1 Introduction

Ectoenzymes are a class of hydrolase that operates on or near the cell surface or in the periplasmic space (Martinez and Azam 1993). This definition distinguishes ectoenzymes from intracellular enzymes which reside within the cytoplasm and extracellular enzymes which are not directly associated with the cell (Chrost and Siuda 2002). Much of the organic matter available to microbes is too large for direct transport into the cytoplasm. Ectoenzymes are used by the cell to convert large and polymeric molecules into smaller, transportable products. This activity plays a major role in dissolved organic matter transformations in both surface and deep waters and can be used to determine dissolved organic matter utilization (Stepanauskas et al. 1999).

Leucine aminopeptidase (LAP) is often used as an indicator of organic matter usage. LAP is involved in the hydrolysis of amino acids (leucine) from peptides or amino acid-containing molecules. There is little consensus on the controls of LAP expression-reports show LAP being repressed by dissolved free amino acids, induced or unaffected by dissolved combined amino acids, activated by other ectoenzymes, and constitutively expressed and/or repressed in the presence of high nitrate (Foreman et al 1998; Jorgensen et al 1999; Nausch and Nausch 2000; Donachie et al 2001; Taylor et al 2003; Chrost and Siuda 2006). In addition to nitrogen, LAP activity potentially reflects cellular carbon requirements (Chrost and Rai 1993; Foreman et al 1998; Williams and Jochem 2006). Due to these discrepancies and the overall complexity of biological systems, interpreting

high (or low) LAP activity in a given environment is difficult. Total LAP activity is predominately of bacterial origin, though certain species of dinoflagellates can also contribute (Karner et al 1994; Mulholland et al 2002, Salerno and Stoecker 2009). Importantly, diatoms have not been shown to contribute directly to LAP activity, despite their often assumed role as the dominant photoautroph controlling nutrient uptake in coastal regions.

A standard ectoenzyme assay uses the hydrolysis of an appropriate enzyme substrate and the subsequent production of a fluorescent compound to measure activity (Hoppe 1993). Two main types of instruments are routinely used for ectoenzyme activity measurements with fluorescent substrates (Ammerman and Glover 2000; Marx et al. 2001; Huston and Deming 2002): 1) manual fluorometers, and 2) fluorescence microplate readers. Prior enzyme activity measurements had incubation times ranging from a few hours to multiple days in oligotrophic regions (Perry 1972; Christian and Karl 1995; Taylor et al. 2003; Kirchman et al. 2004; Sebastian et al. 2004). Recent developments using flow-injection analysis (FIA) have allowed automation of ectoenzyme assays (Gaas and Ammerman 2007). The Enzyme Activity Analysis System (EAAS), a fluorometer incorporating sequential injection stopped-flow analysis protocols, can continuously and autonomously measure ectoenzyme activities in 5 minutes. The reproducibility of sample processing is one of the largest advantages of a FIA system for activity measurements, especially in comparison to manual and microplate-based enzyme assays (Ruzicka 2000). Fine-scale resolution is available with an automated system, which allow detailed comparisons to be made between enzyme activity and environmental parameters. In river plumes, where drastic changes can occur over very short time and distance scales, such

high sampling rates are required for detailed analyses. This is especially true on cruises with limited manpower.

The relative simplicity of measuring ectoenzyme activities has lead to a large number of characterized environments over different spatial and temporal scales. However, while previous work has been done in the Hudson River estuary (Arnosti 2003; Taylor et al 2003), little to none has been done in the Hudson River plume. The plume has two general paths along the New Jersey coast, strongly dependent on local winds (Chant et al 2008b). During downwelling favorable conditions, relatively fresh (salinity < 25) plume water can move southward along the coast, forming a narrow (3 km), shallow (5 m) and quick (0.69 m s^{-1}) coastal current (Chant et al 2008). When upwelling winds dominate, freshwater input from contributing rivers is greater than the flux of water into the coastal current. The excess water can form a bulge, stretching 60-70 km from Sandy Hook, New Jersey (Chant et al 2008). There is some uncertainty whether coastal current water, under bulge conditions, consists primarily of river water traveling around the bulge edge or more processed water that has been circulating within the bulge (Fong and Geyer 2002; Chant et al 2008).

This chapter examines the controls and spatial distribution of leucine aminopeptidase (LAP) activity within the Hudson River plume during the presence and relaxation of a freshwater bulge. Differences between the bulge and coastal current in salinity, fluorescence, nitrate, and LAP activities are used to determine if the bulge is biogeochemically distinct from the coastal current. Regulatory effects of various environmental parameters on LAP activity are discussed. LAP activity has the potential

to impact dissolved organic matter transport, metal sequestration and hypoxia formation near the coast.

2.2 Materials and Methods

2.2.1 Sampling

The 2005 Lagrangian Transport and Transformation Experiment (LaTTE) project was conducted using two research vessels deployed simultaneously. LAP activity, salinity, and fluorescence sampling was conducted onboard the R/V Oceanus. Enzyme activity measurements were made by EAAS (described below); the ship's onboard salinometer, thermistor, and fluorometer were used to acquire salinity, temperature, and fluorescence, respectively. Nitrate was measured on the R/V Cape Hatteras with a nutrient analyzer. The two ships, while surveying the same general area, did not consistently overlap cruise tracks. Both ships actively sampled from 9–20 April, 2005.

Seawater samples used for LAP activity measurements were acquired from a sampling line feeding directly from the R/V Oceanus' uncontaminated seawater flow. The ship's seawater input was centered at a depth of 3 m. Water from the same depth was used to acquire environmental parameters: salinity, temperature, and fluorescence readings. Environmental parameters were recorded at a frequency of 6 hr^{-1}. Linear interpolation was used to match these parameters with the slightly sparser EAAS data, measured at a frequency of 5.4 hr^{-1}.

Nitrate was measured with an Autolab automated nutrient analyzer at a frequency of 5.1 hr^{-1} on the R/V Cape Hatteras. Samples were taken from the R/V Cape Hatteras' 2 m depth seawater intake. Nitrate measurements had a detection limit of 0.1 uM and a precision of < 4% RSD. Dissolved organic nitrogen (DON) was approximated as the

difference between total dissolved nitrogen (TDN) and nitrate. TDN was pre-filtered with GFF filters (nominal pre size 0.7 um) and run on a Shimadzu TOC-V. Potassium nitrate standards were run every 24 hr and deionized water blanks run every five samples. DON samples were paired with nitrate concentrations by matching their salinities; any offsets were corrected through linear interpolation. Other aspects of the LaTTE project not used in this study can be found in Chant et al (2008, 2008b) and Moline et al (2008).

2.2.2 EAAS Settings

The instrumental details of EAAS are described elsewhere (Gaas and Ammerman 2007). In brief, a bidirectional syringe pump moved seawater, distilled water, standard, and substrate solutions throughout the system. Mixing between seawater and the substrate occurred within the tubing, increased by the use of a mixing coil. An LED with an output peak at 375 nm was used as the excitation source with an excitation (365 nm) and emission filter (500 nm) to isolate the desired fluorescence signal. Fluorescence was detected by a photomultiplier tube focused on a 100 uL quartz flow cell. The incubation time of substrate within the flow cell (stopped-flow flow-injection analysis protocol) was set to 5 minutes. Each set of 10 samples was followed by a killed control and internal standard. The overall sampling rate was one sample every ~11 minutes. Each run consisted of 20, 50, 100, or 200 samples.

2.2.3 Preparation of Solutions

EAAS used the LAP substrate L-leucine-7-amido-4-methylcoumarin (Leu-AMC) and associated fluorescent standard 7-amino-4-methylcoumarin (AMC) (from Sigma) to

determine LAP activity. Both substances were dissolved in 2-methoxyethanol to a stock concentration of 1 mM. Solutions were diluted using deionized water to a concentration of 200 uM (substrate) or 2 uM (standards). The standards were further diluted to 250, 500, and 1000 nM using deionized water. All deionized water was boiled in a microwave for 4 minutes in polycarbonate Nalgene bottles and cooled in an ice bath before used in the solutions. After preparation, the substrate was kept in a darkened ice bath for the duration of the cruise. Fresh substrate was created from frozen stock solutions every 2 days and fresh standards every 3 days.

2.2.4 Activity Measurement

Peptidases found naturally in seawater hydrolyze the minimally fluorescent substrate Leu-AMC to form the highly fluorescent compound AMC. The rate of substrate hydrolysis, measured as an increase in fluorescence over time, was converted to activity through a standard curve of the hydrolysis product.

Due to dispersion effects, the linear last one-third of each slope measurement was used to determine the rate of fluorescence increase due to activity. Dispersion also increased the apparent dilution experienced by the injected reagents beyond the 10-fold dilution expected by comparing the substrate injection volume (10 uL) to the cuvette volume (100 uL). The final concentrations of solutions within the flow cell during measurement were determined to be 0, 12.4, 24.8, 49.6, 99.2 nM for the fluorescent standards and a substrate concentration of 9.9 uM. LAP kinetics run at the beginning of the cruise identified the saturation point to be closer to 200 nM, so the substrate concentration used here is closer to the K_m (Taylor et al 2003).

LAP activity was measured as the ratio of sample slope to standard slope (units: nmol L^{-1} hr^{-1}). The sample slope was the linear least-squares regression of fluorescence vs. time found in a solution of seawater plus substrate (units: fluorescence sec^{-1}). The standard slope was the linear least-squares regression between the fluorescence of the standards vs. a standard curve made from a solution of deionized water plus fluorescent standard (units: nmol L^{-1} $fluorescence^{-1}$). A correction for environmental effects on fluorescence in the standards (e.g. salinity, particle scattering, chlorophyll and CDOM absorption of excitation light or fluorescence) was applied by subtracting the fluorescence of the blank (0 nM standard) from each internal standards and dividing by the concentration of the last point on the standard curve to arrive at a set of internal standard slopes. The internal standard slopes were applied to each activity calculation by interpolating the internal standard slope across each set of 10 samples (through time); each set was bounded by the measured internal standards.

2.2.5 Computations

An original Matlab (The Mathworks) script was used to calculate LAP activity from EAAS output and interpolating data from the shipboard instrumentation to match EAAS timestamps. The script can be found in the Appendix. Student's t-tests were performed in Microsoft Excel.

2.3 Results

Two regions of high LAP activity (> 250 nmol L^{-1} hr^{-1}) were identified within the Hudson River plume water, corresponding to a freshwater bulge and coastal current

(Figure 2.1). Other locations, notably both off-shore marine waters and plume water to the north of the bulge, had much lower activity. The bulge, a region where salinity was between 20 and 25 (Chant et al 2008), was approximately 50 square nautical miles and extended eastward from the New Jersey coast. The coastal current, located south of the bulge with salinities 25–28, appeared as a thin line running south along the coast.

A linear relationship between LAP activity and salinity is not seen, as might be expected if LAP activity was solely controlled by proximity to the nutrient-ladened river plume (Figure 2.2). Specifically, two peaks were seen at salinities 24.5 and 27.5 with a local LAP activity low around salinity 27. These peaks occurred near the same salinity regions belonging to the bulge and coastal current, respectively. The salinity 27.5 peak, associated with LAP activities in the coastal current, was approximately double the height and much narrower in width than the activity peak associated with the bulge. Output from a regional circulation model (ROMS) was used with LaTTE data to calculate the mean age of water flowing out of the Hudson River (Zhang et al 2010). The LAP activity peaks consisted of water of three different ages. The wide LAP activity peak associated with the bulge (salinity 24.5) was a combination of water with two ages, 10 and 14 days from the model start. The second peak, associated with the coastal current (salinity 27.5), came from water aged 18 days. The fact that the bulge LAP activity peak could be decomposed into two separate and equal height peaks is likely due to a combination of constant nutrient input (Moline et al 2008) and the recirculating nature of the bulge (Chant et al 2008; Chant et al 2008b) differentially aging water closer to the center of the bulge.

The concentration of nitrate at different salinities was also non-linear (Figure 2.3). The nitrate distribution appeared to have three distinct sections. The riverine section (salinity < 22, ‘A’) had consistently high nitrate values. The vast majority of these points came from a geographical region at the same latitude or north of Sandy Hook. A sharp reduction in nitrate concentration was seen in the second section (‘B’) extending from approximately salinity 22–24.8. The boundary between the second and third section was found when nitrate concentrations drop below ~2 uM. Nitrate values within the third section (‘C’), from salinity 24.8 and higher, decreased slightly and linearly. Nitrate concentrations did not drop below 1.01 uM, which may have been a concentration limit for nitrate uptake. The conservative nature of the nitrate-salinity relationship at salinities > 24.8 suggests limited nitrate uptake in section ‘C.’ This is opposed to section ‘B’, where changes in nitrate concentrations were more dominated by uptake.

DON dominated over the inorganic component, averaging 82% of total nitrogen. DON decreased non-linearly with salinity; significant scatter was found below salinity 25. As seen with nitrate, two different slopes could be identified in the DON distribution with the slope changing around salinity 27. If the Hudson River plume DON was refractory (Bronk 2007), the DON concentration would be expected to either remain constant (no removal source) or decrease linearly with salinity. This suggests DON was actively removed as a nutrient source. However, the there were no distinct variations in DON suggesting any specific DON concentration (for instance, the 10.7 and 7.7 uM DON at salinities 24.5 and 27.5, respectively) induced LAP activity, relieved competitive inhibition of LAP, or was otherwise related to LAP activities.

The relationship between LAP activity and nitrate was an induction-like curve similar to that found by Taylor et al (2003) in the Hudson River estuary (Figure 2.4). Activity was normalized by fluorescence (approximating phytoplankton biomass) to compensate for high LAP activity due strictly to biomass effects. An induction curve is common with reversibly repressible enzymes, such as alkaline phosphatase, which are inactivated by the product of their hydrolysis activity (Chrost and Overbeck 1987). Normalizing LAP activity by chlorophyll maintained the same general shape as non-normalized LAP activity, but lowered the amount of scatter in the intermediate to high (2–10 uM) nitrate region. The reduction in scatter by normalization suggests a relationship between LAP activity and phytoplankton, even if it is a secondary effect (Kisand and Tammert 2000; Llewellyn et al 2008). An LAP induction-like curve was found with nitrate, but not with DON.

A plot of fluorescence (in fluorescence units, FU) vs. salinity (Figure 2.5) also demonstrated three distinct sections, including a highly variable freshwater section (‘A’), a rapid decrease from salinity 21.3–27.4 (‘B’), and a slowly decreasing marine section (‘C’). From salinity 27.4 and higher, fluorescence slowly and linearly decreased with further increases in salinity. The boundary between sections ‘B’ and ‘C’ in the fluorescence plot began approximately three salinity units after the B/C boundary in nitrate (Figure 2.3).

The peaks in LAP activity occurred at salinities defining the bulge and coastal current regions. The LAP activity peaks also seemed to correspond to the boundaries between the B/C sections of nitrate and fluorescence, at salinities 24.5 and 27.4 respectively. The B/C boundary was the location where the rapid decrease in each

variable ends. In the case of nitrate, the B/C boundary was also where dilution increased in importance as a nitrate removal mechanism.

The role of autotroph-associated LAP activity was investigated by comparing the amount of LAP activity derived from chlorophyll-containing cells (fluorescence-normalized LAP activity) and bulk LAP measurements (Figure 2.6). Two distinct areas were seen, again separated into the bulge and coastal current regions. The bulge region generally had higher autotroph-associated LAP activity, as shown by lower fluorescence-normalized LAP activities. As total LAP activity increases, normalized LAP activity increased approximately linearly. It should be noted that a comparison with chlorophyll-specific LAP activity does not specify the type of plankton (early bloom diatoms vs. late bloom dinoflagellates), nor distinguish between LAP activity produced by phytoplankton instead of bacteria associated with or responding to the phytoplankton population (Cole et al 1982; Cole et al 1988).

Flow cytometry was used to separate and count diatoms and dinoflagellates at a subset of sampling locations along the NJ shelf. On average, there were 80 times more diatoms than dinoflagellates (Figure 2.7). The distribution of diatoms with salinity did not show any distinguishing features. Diatoms decreased slightly as salinity increased above 25, from ~6000 cells mL^{-1} down to ~4000 cells mL^{-1}. In comparison, dinoflagellates peaked at salinity 27.5, though the peak value is still only 450 cells mL^{-1}. The dinoflagellate peak occurred at the fluorescence B/C boundary, which is also the location of the second LAP activity peak and the fluorescence-normalized LAP activity peak. Dinoflagellates are known to produce LAP, unlike diatoms, so the coincidence of the

dinoflagellate and LAP activity peak and the lack of features with diatoms indicate a dinoflagellate-specific LAP response to low nitrate conditions.

A range of activities was measured over the course of the cruise in the bulge and coastal current (Figure 2.8). Mean LAP activities in the bulge increased towards a maximum of 200 nmol L^{-1} hr^{-1} on 12 April, decreasing to a general value of 80 nmol L^{-1} hr^{-1} for the remainder of the cruise. The coastal current was only sampled during the last two days of the cruise. Mean LAP activity measured in the coastal current was not significantly higher than activity in the bulge on the 12 April activity peak (Student's t-test, $p > 0.10$). LAP activities in the coastal current were significantly higher than those in the bulge on 19-20 April ($p < 0.003$). Mean LAP activity in the coastal current increased over the last two days of the cruise, though the importance of the increase may be diminished when considering the range of coastal current activity values seen on 19 April.

There was no overall pattern in fluorescence seen during the sampling period. Fluorescence in the bulge followed a 2-day increase at the beginning of the cruise on 9 April. After a sharp decline to a minimum level on 13 April, fluorescence increased to its highest value of almost 1100 FU (fluorescence units) on 15 April. Bulge fluorescence again decreased until 19 April. As with LAP activity, only the last two days of sampling occurred in the region of the coastal current. Fluorescence values in the coastal current were lower than any measurement in the bulge except on 13 April. Fluorescence tracked LAP activity fairly well during the first portion of the cruise (9–12 April). The dinoflagellate concentration also increased during this short period, though data was not available to see if dinoflagellate concentration continued to track the LAP activity

decrease towards 17 April. The periods where fluorescence declined did not parallel any distinct trend in bulge activity. In fact, the fluorescence peak on 15 April was reached when mean activity was relatively low. Dinoflagellate numbers increased at the end of the cruise when measurements were made in the coastal current, as did total fluorescence and LAP activity.

Mean nitrate concentrations varied in both the bulge and coastal current regions of the Hudson River plume over the course of the cruise (Figure 2.9). Initial values in the bulge were very high and linearly decreased to a value of ~3 uM on 13 April. Nitrate increased to 7 uM by 17 April, and decreased again to < 2 uM 19–20 April. Nitrate in the coastal current followed the same pattern found in the bulge region, at least in the two days that coastal current nitrate data is available. Mean nitrate values in the early part of the cruise followed an inverse relationship with LAP activity. From 10–13 April, nitrate concentrations decreased while LAP activities increased. As with fluorescence, no consistent relationship was seen after 13 April, with equally low nitrate concentrations later in the cruise not associated with equivalent LAP activities. In addition, the temporal pattern of fluorescence was variable with respect to nitrate. Changes in dinoflagellate concentration, however, did appear to covary (inversely) with decreasing nitrate concentration, despite only making up a small proportion of the total phytoplankton biomass.

2.4 Discussion

The primary objective of this work was to understand LAP dynamics in the Hudson River plume. Data gathered from the LaTTE 2005 experiment was used to

determine the controls and distribution of LAP activity. Ideally, these results can be applied to the Hudson River plume and other systems to assess how LAP and perhaps other ectoenzymes affect the organic component of nutrient cycling.

Water leaving the Hudson River plume formed a bulge between 10–14 April near Sandy Hook (Chant et al 2008, Chant et al 2008b). Formation of the bulge prevented plume water from entering the coastal current directly after release from the river mouth. During formation, freshwater input from the Hudson estuary was diverted into the bulge. This freshwater input is the main source of nitrate to plankton along the shelf (Malone and Chervin 1979; Malone 1983). The bulge had a mean circular motion, which increased the residence time of bulge waters (Zhang et al 2010). The bulge had a residence time of 3–5 days (Chant et al 2008). Beginning on 15 April, an eastward wind pushed the bulge into the New Jersey coast, squirting out part of the fresher bulge water into the coastal current, seen as a salinity decrease from 15 April through 17 April.

LAP activity in the bulge increased during the bulge formation period. Activities in the bulge were much smaller on the last two days than they were in the coastal current. If the two areas were processed to the same degree, activities would likely be similar in both regions. Mean nitrate concentrations alone do not sufficiently account for the difference, since nitrate concentrations on the 17 April were much higher than on the 19-20 April, whereas LAP activity decreased over this range. The fact that LAP activities were significantly different between the bulge and the coastal current suggests that the two water masses behave differently. This indicates that the coastal current was formed primarily from water trapped in the bulge and slowly released. This water was older and more highly processed, as reflected in higher LAP activities.

The spatial differences in LAP activity have potentially large impacts on dissolved organic matter transport, metal sequestration, and hypoxia formation near the coast. Unimpeded transport from the river will quickly move organic particles away from the river plume, reducing the availability of organic and particulate nutrients. High LAP activities near the plume can convert organic and particulate nutrients into inorganic forms that are more bioavailable and hence more quickly removed. The hydrolysis action of LAP could reduce the number and size of particles along the shelf, in turn decreasing the rate and quantity of sinking particles. By lowering the amount of settling organic matter, the formation of bottom water hypoxia may be reduced. Metal sequestration by zooplankton is an important consideration around the Hudson River plume (Moline et al 2008). High LAP hydrolysis rates could lower the availability of metal-containing particles for zooplankton grazing, thereby decreasing the bioaccumulation of metals in higher trophic levels (Mason et al 1996; Wang et al 1996; Chang and Reinfelder 2002).

LAP activity is low nearest to the river mouth. The combination of high total fluorescence and low LAP activity at the lowest salinities suggests that LAP is not constitutively expressed to a great extent. Low specific activity (activity per cell) would likely still result in high bulk activity measurements under these high biomass conditions. However, total fluorescence is likely dominated by non-LAP-producing diatoms, especially in low salinity areas. Using total fluorescence instead of a dinoflagellate-specific value may minimize the actual amount of specific activity. The low salinity region has the highest nitrate concentrations as well as high turbidity. Bio-optical phytoplankton data suggests the high turbidity in this region results in predominantly light-limited conditions (Moline et al 2008), probably allowing nutrient (nitrate or other)

concentrations to remain high despite the high biomass. The ability of the low salinity regions to replenish dissolved nutrients under light-limiting conditions explains the initial flat sections of the nitrate and fluorescence curves seen in Figures 2.3 and 2.5 (section ‘A’). Alternatively, the rate of nitrate input may exceed that of uptake, resulting in the accumulation of nitrate up to the measured high values.

It is assumed that the decrease in nitrate in section ‘B’ (Figure 2.3) is due to biological uptake, and modeling has shown nitrate removal through uptake dominating over dilution (Chapter 3, this dissertation). The coincidence of a major LAP activity peak and the end of the sharp nitrate uptake section (Sections B/C), both around salinity 25, implicates nitrate concentration as a control on LAP production. The rate at which nitrate decreases with salinity (Figure 2.3) does not parallel the increase of LAP activity over the same salinity range; LAP activity does not peak until nitrate concentrations have fallen below 2 uM. This implicates 2 uM as the threshold nitrate concentrations must drop below before LAP is activated. A potential uptake limit seems to exist at 1 uM, as no further removal of nitrate was measured despite further increases in salinity. If so, LAP operates over a relatively small window of 1–2 uM nitrate. This fine-tuning may prevent cells from wasting resources on producing LAP activity if nitrate concentrations are above or below the point where substrate hydrolysis would relieve nitrate stress.

LAP activity is generally considered restricted to the bacterial size fraction, though research shows this to be a simplifying assumption. Some studies have reported changes in bacterial concentrations generally paralleling those of phytoplankton concentrations (Cole 1982, Cole et al 1988). Unfortunately, direct measurements of bacterial abundance, nitrate uptake, or size-fractionated LAP activity were not available.

Phytoplankton-associated activity can be estimated by normalizing total LAP activity to fluorescence. When LAP activity was normalized by chlorophyll fluorescence, only one peak in activity remained, at a salinity of 28 (figure not shown). This suggests that the relevance of the nitrate drawdown at salinity 25 to LAP activity is somehow disconnected to the total fluorescence. Salinity 28 is found only in the coastal current, where a higher proportion of non-autotroph-associated LAP production occurs. Unlike diatoms, dinoflagellates also increase in abundance at salinity 28, and have been shown to produce LAP activity (Mulholland et al 2002, Salerno and Stoecker 2009). Total fluorescence may be dominated by numerically-dominant diatoms (Moline et al 2008), while LAP activity is primarily controlled by dinoflagellates and bacteria. It seems plausible that a change in the community structure is at least partially responsible for the change in LAP-nitrate relationship at salinity 28 (Martinez et al 1996; Cunha 2001). The LAP activity peak at salinity 25 appears driven by bacterial LAP activity, perhaps in response to the declining phytoplankton population. LAP activity may reflect increasing bacterial productivity as the phytoplankton bloom collapses (Llewellyn et al 2008).

The B/C boundaries were locations where LAP activity peaked. The boundaries may also be locations of high physical stability. LAP is concentrated in these areas due to a special combination of low nitrate, sufficient substrate, and environmental perturbations that are slow enough for the bulk population to respond and be measured.

It is difficult to determine whether LAP activity linearly increases with decreasing nitrate concentration after crossing the 2 uM induction threshold. It may be expected that, if LAP activity was induced solely by low nitrate concentration, reducing nitrate values far below the 2 uM threshold would be reflected in even higher activities, even at higher

salinities. This follows from the exponential shape of the LAP induction curve (Figure 2.4). However, LAP activities in oligotrophic environments (where nitrate concentrations are low) are not especially high, even when corrected for low biomass (Fukuda et al 2000; Van Wambeke et al 2001). This may be referred to as the “blue water paradox”- why aren’t specific (biomass-normalized) ectoenzyme activities in the open ocean environment amoung the highest activities globally?

One explanation to the “blue water paradox” is better adaptation to low nutrients, which decreases the nutrient concentration where LAP activity is induced. Nevertheless, assuming nitrate is still limiting at some point, this does not explain why LAP activity does not increase at the new lower nitrate concentration. In fact, neither the K_m nor V_{max} of oligotrophic LAP differs from those of the Hudson River plume (Christian and Karl 1995), imparting no preferential functionality to LAP in low nutrient regions.

Substrate limitation in the open ocean could reduce activities, following Michaelis-Menton kinetics. A kinetic reduction of LAP activity does not decrease the amount of enzyme produced, however, and should not affect potential LAP activity assays (saturating the enzyme with enough substrate to approach V_{max}). However, the existence of a substrate sensor can solve the blue water paradox and explain sub-V_{max} activities in low nutrient waters. Substrate control could limit LAP activity through a mechanism (the substrate sensor) capable of detecting low substrate availability, such as a low constitutive expression of LAP. In this system, if the constitutive expression of LAP cannot hydrolyze some minimal amount of substrate (implying substrate limitation), then the full potential of LAP production does not occur in order to save resources. In

anthropomorphic terms, LAP needs to “know” that sufficient substrate is available to justify the energy expenditure of producing LAP and related proteins.

From an energetics standpoint, this is an improvement on the inducible enzyme argument. If ectoenzymes aren’t made unless the cell has both the need and means of hydrolyzing a lot of substrate, then a cell (with alternatives other than death) might be better off not putting resources into LAP production unless it is able to contribute to relieving nutrient stress. This sort of mechanism also neatly answers the issue of why nitrate (Taylor et al 2003, Ch 2 of this dissertation) and DON/LAP substrate (Chrost 1991; Stepanauskas et al 1999) both appear to influence LAP activity. The constitutive expression of ectoenzymes as a sensor has been suggested before (Chrost 1991). The apparent contradiction of coincidental high biomass/low constitutive LAP activity/low measured bulk LAP activity can be reconciled if only a small portion of the autotroph-associated population produce LAP.

The data contained here were not strictly measuring potential LAP activity; the final substrate concentrations were closer to the K_m than saturation (Taylor et al 2003). In theory, if substrate limitation controlled LAP activity in the Hudson River plume, LAP activity could be increased with a higher substrate concentration. To the extent that DON concentrations (or a constant proportion of DON) represent an appropriate LAP substrate, increasing substrate availability (DON) did not appear to increase LAP activity.

Ectoenzyme activity is most often used as an indicator of nutrient limitation. However, ectoenzymes are also inherently linked to organic matter utilization by way of making complex polymeric organic matter accessible for uptake. In this way, ectoenzyme activity, especially LAP, may be useful as an indicator of organic matter processing.

2.5 Conclusion

This chapter examined the spatial distribution of leucine aminopeptidase (LAP) activity within the Hudson River plume during the presence and relaxation of a freshwater bulge. The results demonstrated that the Hudson River outflow controlled the spatial distribution of intense dissolved organic matter remineralization, as indicated by the distribution of high LAP activity within and outside of the bulge. This can impact dissolved organic matter transport, metal sequestration and hypoxia formation near the coast. Nitrate concentrations appeared to be the primary control of LAP activity. However, the full expression of LAP activity seemed to be co-regulated by substrate concentration. Kinetic regulation controlled the maximum LAP activity, while LAP induction may have required signaling of sufficient substrate availability to make LAP production energetically worthwhile. Total fluorescence was not a good indicator of activity, though LAP activity did follow the concentration of LAP-producing dinoflagellates. Bulk LAP activities suggested that the bulge is biogeochemically distinct from the coastal current that is fed from it. The LaTTE project shows a close correlation between the physical dynamics of a river plume and a biological response: LAP activity. The primary link between these is nitrogen concentration, which must include both the inorganic and organic components. Nitrate forms the basis of biomass increases, the depletion of inorganic nitrogen, and the need and availability of polymeric organic nitrogen.

3.0 Can aminopeptidase activity support nitrate-depleted phytoplankton populations?

3.1 Introduction

Ectoenzymes are a class of hydrolase that operates on or near the cell surface or in the periplasmic space (Martinez and Azam 1993). This definition distinguishes ectoenzymes from intracellular enzymes which reside within the cytoplasm and extracellular enzymes which are not directly associated with the cell (Chrost and Siuda 2002). Much of the organic matter available to microbes is too large for direct transport into the cytoplasm. Ectoenzymes are used by the cell to convert large and polymeric molecules into smaller, transportable products. This activity plays a major role in dissolved organic matter transformations in both surface and deep waters and can be used to determine dissolved organic matter utilization (Stepanauskas et al. 1999).

Leucine aminopeptidase (LAP) is often used as an indicator of organic matter usage. LAP is involved in the hydrolysis of amino acids from peptides or amino acid-containing molecules. LAP expression in the Hudson River estuary (New York, USA) is controlled by nitrate concentration, implicating LAP activity in relieving nitrogen stress (Taylor et al 2003). Total LAP activity is predominately of bacterial origin, though certain species of dinoflagellates can also contribute (Karner et al 1994; Mulholland et al 2003, Salerno and Stoecker 2009). Importantly, diatoms have not been shown to contribute directly to LAP activity, despite their often assumed role as the dominate photoautroph controlling nutrient uptake in coastal regions.

LAP activity is often measured using the non-fluorescent substrate L-leucine-7-amido-4-methylcoumarin (Leu-AMC). After the substrate is added to a water sample and incubated, LAP-mediated hydrolysis of Leu-AMC produces a free leucine molecule and the highly fluorescent compound 7-amino-4-methylcoumarin (AMC). The production of AMC is measured fluorometrically, and is considered proportional to both the rate of substrate hydrolysis as well as LAP activity (Hoppe 1993). Recent developments using flow-injection analysis have allowed automation of ectoenzyme assays (Gaas and Ammerman 2007). The Enzyme Activity Analysis System (EAAS), a fluorometer incorporating sequential injection stopped-flow analysis protocols, continuously and autonomously measures ectoenzyme activities in 5 minutes, depending on the level of activity.

LAP activity (hydrolysis of the leucine side group) and uptake can be coupled tightly or loosely. Tight coupling is energetically more efficient for a cell producing LAP, as the energy of producing and regulating ectoenzyme expression is at least partially offset by nutrient acquisition. However, in bacterial biofilms, aggregates on particles, and some free plankton, a loose coupling has been observed (Hoppe et al 1988; Thompson and Sinsibaugh 2000; Siuda and Chrost 2001; Hoppe 2003; Azam and Malfatti 2007). Nitrogen-limited phytoplankton too may benefit from uncoupled substrate hydrolysis and uptake (Cunha and Almeida 2009). In these situations, the bulk activity of the population creates a “cloud” of nutrients for the benefit of all cells involved. Loose coupling has the potential to increase the available nutrient concentration beyond that of the bulk nutrient concentration, thereby allowing a higher concentration of biomass to survive.

Ectoenzyme activity is most often reported as an indicator of nutrient limitation. There is an implicit assumption that the rate of ectoenzyme activity, possibly in combination with other processes, is capable of relieving nutrient deficiency in a cell or population. This chapter tests the assumption that bulk LAP activities are capable of offsetting nitrate limitation in a natural, eutrophic marine environment.

3.2 Materials and Methods

3.2.1 Sampling

All data were gathered as part of the 2005 Lagrangian Transport and Transformation Experiment field season (9-20 April, 2005). Samples for LAP activity, chlorophyll fluorescence, nitrate concentration, total nitrogen concentration, and salinity were taken at the surface (< 3 m) on either the R/V Oceanus (LAP activity, chlorophyll, salinity) or R/V Cape Hatteras (nitrate, total nitrogen, salinity). LAP activity measurements were made by EAAS at a frequency of 5.4 hr^{-1}. LAP samples were acquired through the uncontaminated seawater line shared by the R/V Oceanus' onboard fluorometer and salinometer. Salinity (both ships) and fluorescence (R/V Oceanus) were measured at a frequency of 6 hr^{-1}. Nitrate samples were taken from the R/V Cape Hatteras' seawater intake and measured with an Autolab automated nutrient analyzer at a frequency of 0.2 hr^{-1}. The nitrate detection limit was 0.1 uM and had an error of < 4% RSD. Discrete total nitrogen samples were pre-filtered through GF/F filters before measurement on a Shimadzu TOC-V analyzer. An approximation of dissolved organic nitrogen (DON) was calculated as the difference between total nitrogen and nitrate. Other

aspects of the LaTTE project not used in this study can be found in Chant et al (2008) and Moline et al (2008).

3.2.2 Preparation of Solutions

An in-depth description of EAAS can be found elsewhere (Gaas and Ammerman 2007). EAAS used the LAP substrate L-leucine-7-amido-4-methylcoumarin (Leu-AMC) and associated fluorescent standard 7-amino-4-methylcoumarin (AMC) (from Sigma) to measure and calculate peptidase activities. Both substances were dissolved in 2-methoxyethanol to a stock concentration of 1 mM. Solutions were diluted using deionized water to a concentration of 200 uM (substrate) or 2 uM (standards). The standards were further diluted to 250, 500, and 1000 nM using deionized water. Dispersion effects within the flow cell reduced the final solution concentrations to 0, 12.4, 24.8, 49.6, 99.2 nM for the fluorescent standards and 9.9 uM for the substrate. All deionized water was boiled in a microwave for 4 minutes in polycarbonate Nalgene bottles and cooled in an ice bath before use in the solutions. After preparation, the substrate was kept in a darkened ice bath for the duration of the cruise. Fresh substrate was created from frozen stock solutions every 2 days and fresh standards every 3 days.

3.2.3 EAAS Settings

A bidirectional syringe pump moved seawater, distilled water, standard, and substrate solutions throughout the system. Mixing between seawater and the substrate occurred within the tubing, increased by the use of a mixing coil. An LED with an output peak at 375 nm was used as the excitation source with an excitation (365 nm) and

emission filter (500 nm) to isolate the desired fluorescence signal. Fluorescence was detected by a photomultiplier tube focused on a 100 uL quartz flow cell. The incubation time of substrate within the flow cell was set to 5 minutes. Each set of 10 samples was followed by a killed control and internal standard. Each run consisted of 20, 50, 100, or 200 samples.

3.2.4 Activity Measurement

LAP activity was measured as the ratio of sample slope to standard slope (units: nmol L^{-1} hr^{-1}). The sample slope was the linear least-squares regression of fluorescence vs. time found in a solution of seawater plus substrate (units: fluorescence sec^{-1}). The standard slope was a standard curve: the linear least-squares regression between the fluorescence of the standards vs. standard concentration (units: nmol L^{-1} $fluorescence^{-1}$). Environmental effects on fluorescence in the standards were corrected by subtracting the fluorescence of the blank (0 nM standard) from each internal standard and dividing by the concentration of the last point on the standard curve to arrive at a set of internal standard slopes. The internal standard slopes were applied to each activity calculation by interpolating the internal standard slope across each set of 10 samples (through time); each set was bounded by the measured internal standards.

3.2.5 Nitrate Deficit Model

The model assumes nitrate concentration is controlled through uptake by phytoplankton with additional nitrate removal through dilution. The model calculates the difference between the predicted removal of nitrate through uptake and dilution, and the

measured change in nitrate concentration. A nitrate deficit is predicted when the sum of nitrate removal mechanisms (uptake and dilution) is greater than the measured removal of nitrate. These conditions imply the presence of in situ nitrate production to overcome the deficit.

Terms with specific meanings are italicized and are defined in the following text. The subscripts indicate which salinity bin the values come from. That is, "$\text{nitrate}_{(n+1)}$" is from the next higher salinity bin than "$\text{nitrate}_{(n)}$." These indices increment through all of the salinity bins. All calculations were performed using Matlab (version 7.5.0). The activity calculations were performed using an original script, as described below.

Nitrate and DON concentrations, fluorescence, and LAP activity data were binned for each salinity unit. Medians of binned data, referred to as the *median* (e.g. *median* nitrate, *median* LAP activity) was used as the average to reduce the weight of exceptionally high values. DON data were linearly interpolated by salinity to correspond with median nitrate. Fluorescence data equal to zero were removed before processing.

Nitrate uptake was calculated from a fixed phytoplankton *nitrate requirement*. The nitrate requirement is the amount of nitrate necessary to support one fluorescence unit of phytoplankton biomass. The nitrate requirement was based on two assumptions: 1) dilution effects are absent where nitrate concentrations do not decrease, and 2) uptake by phytoplankton reduces the nitrate concentration to the minimum value required to support the measured population. The nitrate requirement is then identified as the nitrate : fluorescence ratio over the salinity range where nitrate concentrations are constant and near their lowest value. Data matching these requirements were found at salinities > 29. The nitrate requirement (nitrate : fluorescence ratio) was calculated from the mean of all

nitrate : salinity and fluorescence : salinity ratios found at salinities >29. This approach, rather than a direct nitrate : fluorescence ratio, was required because nitrate and fluorescence were measured on two different vessels.

Additional nitrate removal occurred through *dilution*. In each salinity bin, a conservative mixing line was drawn between the median nitrate value and the median nitrate concentration at salinity 31. The slope of the conservative mixing line is the dilution rate:

[Eq. 1]

$$\textit{dilution}\ \text{rate}_{(n)} = [\textit{median}\ \text{nitrate}_{(31)} - \textit{median}\ \text{nitrate}_{(n)}]\ /\ [\text{salinity}_{(31)} - \text{salinity}_{(n)}]$$

Dilution rates decrease in magnitude linearly ($r^2 = 0.92$) from approximately -1 uM per salinity unit at salinity 18 to zero at salinity 30. This is in accordance with a linear change in nitrate when nitrate concentration is considered proportional to the concentration of freshwater (Zhang et al 2010). Dilution is undefined at salinity 31.

Predicted removal is the change in nitrate concentration resulting from the combined effects of uptake and dilution:

[Eq. 2]

$$\textit{Predicted removal}_{(n)} = \textit{dilution}_{(n)} + \textit{median}\ \text{fluorescence}_{(n)} * \textit{nitrate requirement}$$

The predicted nitrate algorithm is based on the concept that biomass at a given salinity can only access the amount of nitrate present (measured) in the previous salinity bin. The change in median nitrate between increasing salinity bins was calculated as the sum of nitrate removed through uptake and dilution, as described above. Only the removal of nitrate from dilution was considered at each salinity bin and not the associated addition of nitrate to higher salinity bins.

Nitrate deficit was calculated as the difference between the predicted and *measured removal* in nitrate between each salinity bin:

[Eq. 3]

nitrate deficit =

predicted removal – measured removal

Measured removal is the difference in median nitrate between subsequent salinity bins. The nitrate deficit can be interpreted as the amount of in situ production or removal of nitrate required to achieve the measured removal. Positive nitrate deficits occur when the predicted removal is greater than the measured change in median nitrate. In this situation, some mechanism is presumed present to add nitrate to the system. Conversely, a negative nitrate deficiency implies an additional nitrate removal mechanism beyond phytoplankton uptake and dilution. The model does not have a mechanism for increasing median nitrate between salinity bins, so only data where median nitrate decreases was included.

3.2.6 Model Assumptions and Effects

A summary of the model assumptions are as follows:

1) Nitrate removal processes are limited to phytoplankton uptake and dilution. This excludes the removal of nitrate through bacterial uptake, denitrification, and the sinking of non-algal particles. This assumption likely underestimates the amount of removal, especially by ignoring bacterial uptake.

2) The Hudson River and LAP activity are the only sources of nitrate. Additional nitrate sources from other river and sewage outflows are ignored, as is released nitrate from sediments or other advected sources. Nitrate sources that would alter nitrate concentrations in a uniform manner across salinities (like atmospheric deposition) would probably not alter the results of the model.

3) Biogeochemical processes can be averaged by salinity, and changes in a salinity bin control the initial nitrate of next higher salinity bin. This assumption is based on the conception of a parcel of water being initially controlled by river discharge. Part of the water parcel is then shunted off into a different parcel at the next highest salinity, such that the absolute value of the second parcel is limited by the magnitude of nitrate in the first. The Hudson River plume is diluted by taking in high salinity water, so the conceptual picture is erroneous in that regard. However, the fundamental limitation set by a lower salinity bin should still hold.

4) Dilution effects are absent where nitrate concentrations do not change with salinity. Dilution with low nitrate-high salinity water is only occurs if there is a concentration gradient. If the nutrient concentration is the same, then there will not be a change in nitrate concentration. This assumption is valid only if the other assumptions

hold true (particularly that nitrate is only available through the Hudson River and LAP activity) and that LAP hydrolysis operates on a time scale sufficiently fast that nitrate concentrations are held constant over the time scale of dilution.

5) Phytoplankton reduce the nitrate concentration to the minimum required to support the population. This is the same as assuming there is no rapid internal cycling of nitrate.

6) The nitrate : fluorescence ratio (the nitrate requirement) is constant across all salinities. This is almost certainly not the case, as the proportion of diatoms decrease as salinity increases (Moline et al 2008).

3.3 Results

Median nitrate decreased sharply until salinity 25 and was much shallower at higher salinities (Figure 3.1). Median nitrate approximated an exponential decay or a three-part piecewise linear function, though significant scatter in nitrate data existed below salinity 25. Nitrate values were a near constant 1.01 uM above salinity 29, and never decreased below 1.00 uM. DON was six times higher at salinity 19 than at salinity 31. DON generally declined exponentially, most of which occurred at salinity 19-24. Median DON was usually ~19 uM higher than median nitrate, with more variability seen at lower salinities.

As salinity approached 31 (the end point), nitrate removal through dilution approached zero. When there was no longer a concentration gradient, all nitrate removal was presumed to occur through uptake. The constant nitrate region above salinity 29 was used to calculate the amount of nitrate required to support the extant phytoplankton

population (the nitrate requirement). Although nitrate remained constant, fluorescence varied more widely. The nitrate requirement was 96.2 ± 11 (standard error) fluorescence units per uM nitrate. An intermediate relationship between nitrate : salinity and fluorescence : salinity was required to compare nitrate : fluorescence at each salinity and is included in the uncertainty.

Dilution contributed less than 13% of predicted removal over the entire salinity range while the rest was biological uptake (Figure 3.2). Uptake and total nitrate removal remained fairly constant until salinity 23 where both decline sharply. Predicted removal was less influenced by dilution as salinity increases. Dilution was more linearly related to predicted removal ($r^2 = 0.84$) than uptake ($r^2 = 0.74$), despite uptake having a larger effect.

All of the calculated nitrate deficits were positive, implying an in situ source of nitrate or nitrate equivalents was responsible for balancing nitrate input from the river with uptake and dilution, at least at higher salinities (Figure 3.3). The predicted nitrate removal in each salinity bin is independent of the prior bin, so excess nitrate required to compensate for the nitrate deficit could not come from the river. Nitrate deficits ranged from 0.9 – 6.1 uM nitrate with a mean of 3.2 uM nitrate. A nitrate deficit was not calculated for salinity 20 due to a positive change in median nitrate. A single peak existed at salinity 23, which did not directly correspond with either a peak or trough in dilution, uptake, or median nitrate concentration. The nitrate deficit was not predicted especially well by a linear relationship with dilution rate ($r^2= 0.64$), but was best explained by uptake ($r^2=0.83$). This is not surprising since over 85% of the predicted removal came from biological uptake. Nitrate concentration is coupled to the dilution rate (increased

nitrate increases dilution rate), and so was not considered a separate influence. The nitrate deficit decreased slower above salinity 25 than at 23-25. Median nitrate, dilution, and uptake all decreased above salinity 25. The change in slope appeared primarily related to median nitrate and, to a lesser extent, uptake.

It seems possible that positive deficiencies near the freshest waters were related to the chemostat nature of the plume (Chant et al 2008; Moline et al 2008). Nitrate may have been continually pumped into the plume at a rate faster than uptake and dilution could remove it, effectively replacing nitrate. However, this would result in a nitrate disequilibrium, at least without invoking another removal mechanism such as sinking or denitrification.

If nitrate concentrations were in steady-state and uptake is significantly faster than dilution processes, the salting rate could be used to derive the nitrate uptake rate. Mean salting times of 25 hrs have been measured on the shelf during the LaTTE project (Houghton et al 2008). Salting time (the inverse of salting rate) is the amount of time required to increase the salinity by 1 salinity unit. The rate of freshwater dilution should be the same as that of nitrate (Zhang et al 2010), so the rate of dilution is also around 25 hours. The nitrate uptake rate is then equal to the calculated uptake divided by 25 hours. The distribution of the uptake rate with salinity is the same as uptake in Figure 3.2. The uptake rate remained a relatively constant 250 nmol L^{-1} hr^{-1} from salinity 18-23, after which it declined to a minimum of 50 nmol L^{-1} hr^{-1}. Estimated uptake rates from the Hudson River plume decreased logarithmically with decreasing nitrate concentration, following the same pattern as in other high nutrient, mixed assemblage locations (e.g. Kudela and Dugdale 2000). Similar values have been found in upwelling regions with a

mixed phytoplankton assemblage (Mercado et al 2008), though these rates are three times lower than seen in the Columbia River plume (Kudela and Peterson 2009).

LAP activity was presumed to create nitrate equivalents, a functional replacement for nitrate. LAP production is often considered a response to nitrate limitation (Hoppe 1983, Taylor et al 2003), and so may also be a possible mechanism to compensate for nitrate deficiencies. Median LAP activity varied from 49-156 nmol L^{-1} hr^{-1} (Figure 3.4). Mean LAP activity across all salinities was 105 nmol L^{-1} hr^{-1}. LAP activity peaked at salinity 24, with substantially lower LAP activities at salinities 20 and 30. LAP activities generally decreased from salinity 24 and higher.

Interestingly, median LAP activity was not proportional to the nitrate deficiency, nor did it follow the usual exponential increase common to ectoenzyme induction (Figure 3.5). Instead, LAP activity increased in a logarithmic fashion compared with nitrate concentration, dilution, uptake, and nitrate deficiency. The curvature changed around 100 nmol L^{-1} hr^{-1}, at a nitrate deficiency of ~1.5 uM. This suggests that LAP activity was not induced solely by a large nitrate deficiency but had some additional regulating factor. For instance, LAP activity may have been substrate limited above a nitrate deficiency of 2 uM.

The amount of time required for median LAP activity to create sufficient nitrate equivalents to offset the nitrate deficiency in each salinity bin is the deficiency time. Deficiency times ranged widely, from 13 - 60 hours (Figure 3.6). The mean deficiency time was 29.5 hours, which is close to the mean salting time of 25 hours. Times decreased with increasing salinity, but did so in a saw-tooth manner. Deficiency times followed more closely the pattern of nitrate deficiency rather than LAP activity. The

shortest times were collocated with the smallest nitrate deficiency, at salinity > 28. Deficiency times above salinity 28 averaged 16.6 hours. The deficiency time was highest at salinity 19, though the greatest nitrate deficiency was at salinity 23. In comparison, nitrate deficiency was at a local (between salinity 18-23) low at salinity 19.

Over time, LAP activity could reduce the nitrate deficiency through the production of nitrate equivalents. LAP activity must operate at median values for 13 hours before the nitrate deficiency in any single salinity bin would be compensated for. After 13 hours of constant LAP production at the measured values, some proportion of the phytoplankton biomass (divided by salinity bin) would become replete with nitrate-equivalents. The percentage of salinity bins where LAP activity could compensate for the nitrate deficiency increases by 3.5% per hour during hours 13 - 30 of constant LAP production at measured rates (Figure 3.7). This is not the same as the proportion of the entire phytoplankton population, as certain bins contained a greater concentration on biomass than others. No further alleviation of the nitrate deficiency would occur until 43 hours, where the rate decreases to 1.8% per hour. A significant amount of time would be necessary for LAP activity to produce sufficient nitrate equivalents to offset the nitrate deficiency: 19 hours for 25%, 26.5 hours for 50%, and 44 hours for 75% of the deficiency.

If LAP substrate is considered a constant fraction of the total DON concentration, an approximate coupling strength and direction can be determined. The coupling strength is the fraction of the nitrate-equivalents required by the uptake rate capable of being supplied by LAP activity. If the uptake rate exceeds LAP activity, then the system is uncoupled and an additional nutrient source is assumed. Alternatively, if LAP exceeds

uptake, then the system is also considered uncoupled and excess nitrate-equivalents are available to organisms. Similar rates imply a tightly coupled system, with LAP supplying the necessary nitrate-equivalents to support biological requirements. An estimation of coupling strength based on assumed substrate (fraction of DON) concentration and LAP activity predicted the potential for loose coupling would be strongest at both ends of the nitrate and salinity spectrum (Figure 3.8). Uptake exceeded LAP activity by a factor of 2 when nitrate was >7 uM (below salinity 23), and LAP activity exceeded uptake by a factor of 2 when nitrate was ~ 1 uM (above salinity 28). The relationship was linear and positive (r^2=0.67; 0.85 removing the high point), which is in accordance with Hoppe et al (1988).

3.4 Discussion

LAP activity is often portrayed as a mechanism for cells to overcome nitrate limitation. Indeed, ectoenzyme activity is often (almost entirely) used to indicate nutrient stress. It is commonly accepted that LAP activity responds to decreasing nitrate concentration. However, nutrient concentration alone is not sufficient to diagnose nutrient stress. Nitrate concentration is the amount of nitrate present in the system, and is not inherently indicative of nutrient status. For instance, an oligotrophic organism well-adapted to low nutrient concentrations may not be nutrient stressed at nitrate concentrations found in eutrophic waters (Sunda and Hardison 2007). For this reason, nutrient concentration ratios are more often employed to indicate nutrient limitation. The model described here defines the lack of nitrate in terms of the nitrate deficiency and not measured nitrate concentration. Nitrate deficiency is a measure of the amount of nitrate

required but not available to the population, and hence should be useful as an indicator of nutrient stress.

The model used in this analysis assumes that the hydrolysis product of LAP activity is functionally equivalent to nitrate. By the same token, LAP is thought to be expressed for the purpose of assisting in the acquisition of nitrogen from the environment (Martinez and Azam 1993b). The ability of bacteria to transform DON into usable inorganic nitrogen species has already been established (Berman et al 1999). The relationship between LAP activity and nitrate is similar to other ectoenzymes that are known to be induced by a lack of dissolved inorganic nutrients. This suggests that LAP activity is activated in order to counteract a lack of nitrate (Hoppe 1983). While the hydrolysis product of LAP is not chemically identical to nitrate, it seems reasonable to assume that the hydrolysis product of LAP activity fulfills the same role of nitrate, and the LAP hydrolysis product can be thought of as a nitrate equivalent. The coefficient of determination (r^2) between nitrate and fluorescence increases by 0.12 when LAP activity is added to nitrate. The additional strength in the nitrate-fluorescence relationship gained when including LAP activity suggests that LAP activity directly affects nitrate concentration, presumably by increasing the concentration of nitrate equivalents.

LAP activity peaked near the salinity bin where the nitrate deficiency is largest. This is the expected response if LAP activity increases in response to nitrate stress. However, LAP activity did not linearly increase with nitrate deficiency, but had a logarithmic relationship. As the nitrate deficiency increases, the shallow coincident increase in LAP activity resulted in deficiency times also increasing. Given sufficient substrate and time, any amount of nitrate equivalents could be produced given any

positive LAP activity. The salting time is one way of constraining the number of nitrate equivalents produced by LAP. The mean salting time was 25 hours, which is within the range ectoenzyme activities can remain relatively stable (Bochdansky et al 1995). During this time, LAP activity could produce only enough nitrate equivalents to compensate for 46% of the nitrate deficiency. Considering only time limitation, LAP activity completely compensates for nitrate deficiencies at or above salinity 25; at lower salinities, more time would be required to fully offset the nitrate deficiency. An average phytoplankton doubling time of 24 hours results in the same percent compensated.

There is potential for insufficient substrate limiting production of nitrate equivalents. Decreasing the substrate availability quickly reduces the nitrate equivalents capable of being produced by LAP activity. Approximately 15% of measured DON in each salinity bin may be an acceptable LAP substrate (Bronk 2002). At this substrate concentration, 77% of the salinity bins have insufficient substrate for LAP activity to fully overcome the nitrate deficiency, including all salinities between 21 and 29. The range of salinities where the deficiency time is short enough for LAP activity to compensate for the nitrate deficiency is opposite from where substrate limitation is potentially inhibiting. This greatly increases the difficulty in LAP activity compensating for nitrate deficiency in marine waters. It should be recognized that DON and natural LAP substrates with rapid turnover were not specifically measured, and the pool of suitable LAP substrates may be larger than assumed here. For instance, available DON could be masked if there is tight coupling between DON usage and release (Seitzinger and Sanders 1997; Bronk et al 2007). Specific conditions (such as bloom senescence) can also modify river-derived DON and LAP substrate concentration.

Generally speaking, high LAP activities corresponded to higher DON concentrations. This could mean LAP activity is enhanced at higher substrate concentrations, following Michaelis-like enzyme kinetics, and may explain the logarithmic relationship between LAP activity and nitrate deficiency. LAP kinetics in the plume show that V_{max} is around 500 nmol L^{-1} hr^{-1}, much higher than the LAP activity plateau value of 120 nmol L^{-1} hr^{-1} (Gaas, unpublished). The K_m is ~10 uM, at which the expected LAP activity is ½ V_{max}, or 250 nmol L^{-1} hr^{-1}. Since activities were lower than 250 nmol L^{-1} hr^{-1}, this places the substrate concentration below 10 uM. Given a mostly linear relationship between substrate concentration and LAP activity below the K_m (10 uM), the substrate concentration associated with LAP activities of 120-160 nmol L^{-1} hr^{-1} is estimated at 4.8-6.4 uM. Median DON concentrations for these LAP activities are mostly between 10-20 uM, which means ~40% of DON may be an acceptable LAP substrate. If so, LAP activity becomes substrate limited (over the course of a 25 hour deficiency time) only at salinities 23 and 24.

LAP activity is generally considered restricted to the bacterial size fraction, though research shows this to be a simplifying assumption. There is currently no evidence that diatoms, the dominant phytoplankton found in low salinity regions of the Hudson River plume (Moline et al 2008), produces a cell surface LAP. Dinoflagellates, found at higher salinities, can produce an LAP (Karner et al 1994; Mulholland et al 2003, Salerno and Stoecker 2009). This results in total LAP coming from the dinoflagellate population, bacteria, and/or phytoplankton (diatom and dinoflagellate)-associated bacteria. The repletion time calculations implicitly require total uncoupling between LAP producers and nitrate uptake, allowing the LAP-produced nitrate equivalents to become

available to the entire phytoplankton population. Presumably, bacteria and dinoflagellates would have greater access to the LAP hydrolysis product, and loose coupling is only required to support the diatom population.

The coupling strength of LAP hydrolysis and amino acid uptake can vary with both the inorganic or organic nitrate concentration (Hoppe et al 1988; Nausch et al 1998; Cunha and Almeida 2009). Experiments (e.g. Hoppe et al 1988) show that coupling strength decreases with increasing substrate concentration, though Cunha and Almeida (2009) found increasing LAP : leucine uptake ratios with increased nitrogen availability. DON on the NJ shelf decreased in a decaying exponential fashion, and nitrate concentrations also decreased with increasing salinity (Figure 3.1). Uptake exceeded LAP activity by a factor of 2 below salinity 23, and LAP activity exceeded uptake by a factor of 2 above salinity 28. If leucine is used as an alternative nitrogen source to nitrate, then the inverse relationship found by Cunha and Almeida (2009) also matches this data. Diatoms are more likely to be found at lower salinities where freshwater stratification and nutrient concentrations are higher. These low salinity areas are also where nitrate uptake exceeds LAP activity and uncoupling is high. Higher uptake values (compared to LAP activity) imply LAP activity is not required to support the diatom-dominated phytoplankton population, and hence offers an explanation for why LAP has not been found in coastal diatom species.

It is worth noting that an opposite relationship is found if one considers the nitrate deficiency instead of the nitrate concentration compared to the coupling strength. If the figure showing coupling strength (Figure 3.8) is altered such that the nitrate deficiency is on the X-axis instead of nitrate concentration, then at low salinities, a greater amount of

LAP is produced than is being taken up, supplying diatoms with nitrate. This is further evidence that diatoms may rely on the LAP production of other organisms for their nitrate needs without the requirement of producing LAP themselves.

In addition to uptake uncoupling, LAP activity could be a fundamental mechanism for supporting non-LAP producing species during periods of nitrogen stress if grazing is present. In this scenario, nitrogen is acquired from DON through LAP activity and incorporated into biomass. Grazing activity can transfer the nitrogen to the next higher trophic level, where it is eventually released through exudation. Alternatively, sloppy feeding could release the nitrogen directly into the water. In either case, the nitrogen becomes available for phytoplankton uptake (Gruber et al 2006).

Biological uptake and dilution terms were the only nitrate removal mechanisms considered to change nitrate concentration. Loss of nitrogen through particle sinking is another possible mechanism. Nitrate associated with phytoplankton particles is implicitly dealt with in the fluorescence to nitrate conversation. Nitrate that is taken up to support biomass is reflected in an increase in fluorescence. Likewise, nitrate loss from sinking phytoplankton particles is incorporated through reduced total fluorescence. Denitrification could also contribute to decreasing nitrate concentration, though is probably limited to lower salinities. Nitrate, fluorescence, and LAP activity were all measured at the surface, so nitrate would probably need to be removed from the highly aerated surface by sinking before denitrification (an anaerobic process) could occur. Advection within the sampling region is reflected in the dilution calculations. Though implied, the model was not inherently constrained to the sampling area. Loss of nitrate from advection outside of the sampling region is possible, and was not compensated for.

There is no source of nitrate defined in the model except for the initial median nitrate values. Remineralization was not included in the model. Remineralization would have an in-model effect of reducing the nitrate requirement, such that higher fluorescence (more phytoplankton) could be present without increasing median nitrate. A reduced nitrate requirement decreases the nitrate deficiency. The nitrate requirement in the model was uniform at all salinities. This is already a simplificiation as varying proportions of organisms with different nitrate requirements are likely present in different salinity bins (Moline et al 2008). The reduction in the nitrate requirement due to remineralization would be dependent on the strength of remineralization, and would probably not be constant at all salinities (Cunha et al 2001). Perhaps a better approach than the nitrate : fluorescence ratio used here would be a particulate organic nitrogen (PON) : fluorescence ratio. PON data was not immediately available at the time of this analysis, but would provide a more direct measurement of the nitrogen content per phytoplankton. However, nitrogen incorporated into cells are more likely to be in an ammonium-like form than nitrate. With nitrate dominating the total nitrogen of the system, the change in redox state of nitrogen is not of obvious concern.

True dilution (in a closed system) would lower the initial nitrate concentration and add an equal amount to the high salinity (low nitrate) end point. The model only included the initial removal and not this redistribution of nitrate to higher salinities.

Predicted nitrate calculations treat dilution and uptake as operating independently. Dilution in particular is sensitive to the starting nitrate concentration, which controls the nitrate gradient. Over the time uptake and dilution processes are operating, uptake is continually lowering the starting nitrate concentration, thereby reducing the dilution rate

and making the dilution rate a function of uptake rate. Though uptake rates are 87% faster than the dilution rates in the model, fluorescence increase is related to the doubling rate of phytoplankton, and so uptake was not considered to affect the initial nitrate concentration.

Nitrate deficiency measurements are independent, such that neither the magnitude nor direction of the nitrate deficiency in one salinity bin affects the nitrate deficiency in any other bin. By uncoupling the salinity bins, erroneous assumptions made about the dynamics of the plume system (e.g. no internal nitrate source, entirely nitrate-limited growth, constant fluorescence : nitrate ratio) are only applied to individual salinity bins, and not compounded through all of the bins. Treating the salinity bins as independent underestimates the magnitude of negative deficiencies (surpluses), since the initial nitrate concentration is reset to the mean nitrate value at each salinity bin.

3.5 Conclusion

Ectoenzyme activity is often used as an indicator of organic matter usage. Conceptually, the hydrolysis product of ectoenzyme activity is used to relieve nutrient stress or acquire a type of molecule not immediately accessible in the environment. LAP activity is most likely not entirely sufficient to support a nitrate-starved population due to substrate limitation and insufficient decoupling at high salinities, and time constraints at low salinities. The nitrate uptake rate is the primary remover of nitrate, though at rates comparable to the production of nitrate equivalents by LAP. LAP activity was neither proportional to the magnitude of the nitrate deficiency, nor did it increase exponentially when the deficiency increased. Rather LAP activity exhibited a logarithmic increase with nitrate deficiency. LAP supplied by bacteria and dinoflagellates may be sufficient to

sustain diatom populations lacking LAP, explaining the current lack of identified LAP-producing genes in these species.

4.0 Short-term phosphatase dynamics in the Mississippi River plume

4.1 Introduction

Alkaline phosphatase (AP) is one of the best characterized of the ectoenzymes. AP hydrolyses polymeric organic matter containing a terminal phosphate monoester, releasing a molecule of phosphate and the remaining organic compound into solution. The released phosphate group is then available for cellular uptake. AP is known to be induced by low inorganic phosphate concentrations and is produced by both heterotrophic bacteria and phytoplankton (Hoppe 2003). The presence of high AP activity is overwhelmingly used as an indicator of phosphorus stress and has been employed in that capacity in a diverse range of ecosystems including lakes, upwelling zones, coastal environments, and the open ocean (Chrost and Overbeck 1987; Ammerman et al 2003; Sebastian et al 2004; Dyhrman and Ruttenberg 2006; Gao et al 2006; Sylvan et al (2006); Gaas and Ammerman 2007). Spatial mapping of AP activity has provided information about the causes and extent of eutrophication in coastal areas. The Louisiana shelf region of the Gulf of Mexico is one location where AP activity has been used successfully to implicate phosphate as a limiting nutrient (Sylvan et al 2006). AP activity measurements are relatively easy to make, given the development of fluorescent AP substrates and automated methods of sampling (Ammerman and Glover 2000; Sylvan et al 2006; Gaas and Ammerman 2007; Jeager et al 2009). These advancements enable detailed studies of spatial and temporal variation in AP activity in multiple regions, in surface waters as well as at depth.

In surface mapping projects often done with ectoenzymes, a single measurement is made along a ship track and the spatial distribution of activity is used to identify areas of nutrient stress. The relationship between the degree of nutrient stress and rate of AP activity is difficult to quantify, and even the canonical decaying exponential relationship between AP activity and phosphate concentration has not been well characterized. Rather, a more qualitative approach is used where a semi-arbitrary “high” AP activity is used to identify locations with potential phosphate stress.

Multiple lines of evidence are usually used together to identify a limiting nutrient, including nutrient concentrations, nutrient ratios (with or without reference to the Redfield ratio), and nutrient addition experiments (D’Elia et al 1986). Approaches relying on nutrient concentrations do not directly relate to the nutrient status (replete vs depleted) of the biota. Well-adapted organisms may tolerate lower nutrient concentrations better, or access alternative sources of nutrients that are not specifically accounted for. Even bioassays, perhaps considered the best identifier of nutrient limitation (D’Elia et al 1986) have multiple factors which can complicate the interpretation of the results (Smith and Hitchcock 1994). In some ways, AP activity is a better way of determining phosphorus stress in an aquatic ecosystem because it can, in theory, represent the integrated nutrient sufficiency or limitation of the organisms rather than an instantaneous dissolved phosphorus concentration or DOP of uncertain bioavailability. AP activity provides insight into the link between an external environmental parameter (phosphate concentration) and the internal nutrient requirement.

Unfortunately, even with a well-characterized ectoenzyme like AP, the interpretation of bulk activity measurements is not straight-forward. The phosphate

concentration at which AP activity begins to increase can be identified and may indicate the threshold defining phosphorus stress. However, the AP—phosphate relationship is not sufficiently resolved to predict AP activity from phosphate concentration or conclusively identify phosphate stress (Cao et al 2010). This limits how much AP activity assays can be interpreted. For example, AP activity is also potentially controlled by the carbon requirement, induced by the presence of enzyme substrate, and kinetically controlled by substrate concentration (Benitez-Nelson and Buesseler 1999; Hoppe 2003). Patterns in cell-specific ectoenzyme activity can differ from bulk activity (Dyhrman and Ruttenberg 2006; Strojsova and Dyhrman 2008; Strojsova et al 2008), making the effects of AP activity more complicated to scale to an ecosystem level.

In many ectoenzyme assays, activity is measured at a single location using a small volume of water (Hoppe 1983). Automated shipboard instrumentation, while increasing the sampling rate, is also primarily a single point measurement (Gaas and Ammerman 2007). By virtue of a large sample number, single point measurements over a survey area can identify patterns and potential discontinuities. Time-series of ectoenzyme activity can reveal how quickly ectoenzymes respond to changes in nutrient concentration (or other environmental variable) and how much variability may be expected in a spatial survey due to evolving conditions at a survey station.

The overarching theme of this chapter is to evaluate the robustness of AP as an indicator of phosphorus limitation and to quantify the variability in AP activity over a 24 hour period. An automated instrument for AP activity and hourly CTD casts are used to identify the basic relationships between AP activity and environmental variables. The data will be put into the context of a known spatial distribution of AP activity and

phosphate dynamics. The addition of time as a variable may offer further insight into AP expression and regulation. This information is important when interpreting single AP activity measurements during a spatial survey.

4.2 Methods

4.2.1 Sampling

AP activity and environmental parameters were measured at two time-series stations along the Louisiana (USA) shelf in late March 2007. Both stations were 24 hours long. Station TS1 was sampled on 23 March and TS2 on 28 March. Ship drift was minimal during the time-series. The maximum drift was $2 * 10^{-4}$ degrees latitude and $3 * 10^{-4}$ degrees longitude.

AP activities were measured with the Enzyme Activity Analysis System (EAAS), an automated instrument using stopped-flow injection in combination with fluorescence substrates to measure enzyme-mediated hydrolysis. EAAS was connected to a sampling arm deployed 3 m from the port side of the R/V Pelican. The arm sampled seawater from a depth of 0.5 m. Specific details about EAAS can be found in Gaas and Ammerman (2007). The substrate 6,8-difluoromethylumbelliferyl phosphate (Invitrogen/Molecular Probes) was added to a small aliquot of seawater taken with the sampling arm to produce a final substrate concentration of 10 uM. The incubation time was set for 5 minutes with a total sampling frequency of 4.6 hr^{-1}. AP activities were binned by hour for comparison with hourly environmental data.

Surface water samples were collected once per hour for 24 hours. Additional samples were collected every other hour at depths of 2, 5, 12, and 18 m using a rosette

sampler for environmental parameters. Parameters included phosphate (soluble reactive phosphate or SRP), nitrate, nitrite, ammonia, chlorophyll a fluorescence, and salinity. Total dissolved inorganic nitrogen (DIN) was the summation of nitrate, nitrite, and ammonia and was numerically dominated by nitrate concentrations. Each nitrogen species plus SRP was measured by a Techicon Autoanalyzer II. Chlorophyll *a* fluorescence and salinity were measured using a Sea-bird Electronics SBE 911 CTD and Turner Designs SCUFA fluorometer attached to the rosette. Dissolved oxygen and a BSI QSP-200L PAR sensor were also attached to the rosette.

Linear interpolation was used to estimate the values of subsurface samples during non-sampling periods. Values were only interpolated horizontally in time and not vertically by depth. This is due to the expected vertical stratification from freshwater derived from the Mississippi River. Data processing for both EAAS data (AP activities) as well as environmental parameters (nutrients, rosette instruments) was done using original Matlab (Mathworks, v.2007b) scripts (see Appendix for EAAS script).

4.2.2 Identification of Phosphorus Limitation

Sylvan et al (2006) did an extensive set of experiments in the Mississippi River plume and Louisiana shelf region documenting the seasonal phosphorus limitation of phytoplankton. They combined multiple metrics to demonstrate phosphorus limitation along the shelf in March and May 2001. These metrics included SRP concentrations and DIN : SRP ratios. Based on work by Dortch and Whitledge (1992), Sylvan et al (2006) define phosphorus limitation along the Louisiana shelf as the following: SRP

concentration ≤ 0.2 uM and DIN : SRP ratio > 30. All measurements were made in surface waters.

The time-series stations TS1 and TS2 were located close to Sylvan et al's (2006) stations 2A and 1B (Figure 4.1). The time-series stations were located to identify potentially different sources of surface shelf water. TS1 (and Sylvan et al's station 2A) was presumably dominated by Mississippi River water exiting Southwest Pass. Water found at TS2 (and 1B) may also have been influenced by the Mississippi River plume, but is likely to have additional properties determined by the Atchafalaya River and off-shore marine waters. In the nomenclature of Sylvan et al (2006), TS1 and 2A were both in the Plume Box, while TS2 and 1B were in the shelf box. Table 4.1 shows the range of values of Sylvan et al measurements (based on their contour plots) and the corresponding range and mean of the time-series stations from this work. Note that station 1B was measured in March 2001, while 2A was measured in May 2001. All of the contours were from May 2001 as well.

The contour range in Sylvan et al (2006) must be treated with caution, as the range is both very wide and not especially selective. For example, contours at station 1B exhibited a DIN range of 0 - 30 uM, though nitrate concentration measured for their nutrient addition experiment at this station was 5 uM. For this reason, discrete surface nutrient measurements at station 2A and 1B are recreated in Table 1. Hereafter, the Sylvan et al (2006) stations 2A and 1B will collectively be referred to as "contour stations."

4.3 Results

For reference, approximate nutrient loadings from the Mississippi River during the three measurement periods (March 2001, May 2001, March 2007) are given in Table 4.2. Despite having the highest flow rate of three periods, March 2007 (the year of the time-series stations) nutrient loads fell between the values for the other two years.

During the time period of the cruise, the Mississippi River plume followed the anticyclonic movement typical for the season (Walker et al 2005). Satellite imagery of sediment transport showed a wider plume north of Southwest Pass on 23 March compared to the 28th (Figure 4.2). The greater sediment load seen near the coast around Terrebonne Bay (north of station TS2) and further west on 23 March was indicative of westerly winds. This apparently shifted to easterly-dominant winds by the end of the week, as seen by the reduction in sediment north of TS2 and at TS1. Sediment from neither the Atchafalaya nor the Mississippi River appeared to reach as far as TS2. However, it is likely that the Mississippi River was the dominant influence on both sets of stations.

The flow rate from the Mississippi River (measured at Tarbert Landing, MS) during this study was 15,900 m^3 sec^{-1}, compared to 14,500 m^3 sec^{-1} during the Sylvan et al (2006) survey of station 2A and 28,000 m^3 sec^{-1} at station 1B (Table 4.2). Salinity is an indicator of freshwater concentration and hence the proximity and magnitude of the primary surface nutrient source. Flow rate partially determines the spatial extent of the river plume as well as the rate at which river-influenced environmental properties can change. The measured salinity ranges and means of time-series stations TS1 and TS2 fit within the salinity range of contour stations 2A and 1B, allowing the two to be compared.

Station 1B is further away from the mouth of the Mississippi River than station 2A and hence was potentially more impacted by variations in Mississippi River flow rates.

SRP concentrations at the time-series stations were consistently an order of magnitude higher than at the contour stations. Maximum SRP concentrations were also much higher at both of the time-series stations than at the contour stations. SRP reached its lowest level when river flow rates and DIN concentrations were at their highest value. Conversely, DIN concentrations were not any different between the time-series and contour stations, which increase the likelihood of a nitrogen-limited Louisiana shelf during the time-series measurements. DIN : P ratios at the time-series stations average 12-fold lower than at the contour stations.

Both contour stations exhibited strong uncoupling between phosphate uptake and phosphate production through AP activity. The uncoupling favored excess production of phosphate by AP activity. SRP uptake rate is the reciprocal of the turnover time (times the SRP concentration or radiolabeled phosphate) and was 67 nM hr^{-1} at station 2A and 14 nM hr^{-1} at station 1B. The uptake rate was highest at the station with a more direct Mississippi River plume influence, as indicated by the lower salinity range. The amount of SRP capable of being produced by AP activity over the course of the turnover time was between 45 - 138 nM at Station 2A and 124 - 332 nM at 1B. This resulted in a 2 - 24 times excess of AP-produced SRP. Uncoupling between AP activity and uptake was many times higher at station 1B than 2A.

Based on the criteria laid out above (SRP $\leq$ 0.2 uM; DIN : SRP > 30), the contour stations 2A and 1B were definitively phosphorus-limited (Dortch and Whitledge 1992). None of the time-series stations were phosphorus-limited if one considers only the mean

SRP values given in Table 4.1. However, at various points during the time-series, both time-series stations met the low phosphate requirement. Many times during the sampling period, station TS1 meets both the SRP and DIN : SRP requirements for phosphorus limitation. In contrast, the DIN : SRP ratio at TS2 was about one-half the amount required to meet the definition of phosphate limitation. Interestingly, despite differences in phosphate concentration and the DIN : SRP ratio, mean AP activities at the time-series and contour stations were similar, though the range of activities at both sets of stations is very large.

4.3.1 Station TS1

Surface SRP concentrations varied over the course of the time-series at station TS1 (Figure 4.3a). From 16:00 until 05:00, SRP remained between 0.2 - 0.3 uM. SRP peaked three times, at 06:00, 08:00, and again at 14:00. SRP increased beyond 0.7 uM in both cases. The first and third peaks had durations (rise, peak, and fall) of about 4 hours. The largest single change in SRP (0.62 uM) occurred as part of the second peak, between 08:00 - 09:00. Almost equivalent changes in magnitude occurred as an SRP increase between 03:00 – 04:00. The changes in SRP concentrations in the first and third peaks were very similar in magnitude. Previous 4 hour patterns of change in nutrients (DOC, dissolved free amino acids) have been found during short-term observations; these were considered to be due to the coupled production by primary producers and subsequent usage by heterotrophs (Meyer-Reil et al 1979).

SRP concentrations below 12 m oscillated between 12 - 18 m water every ~10 hours, though this value varied. SRP was much more concentrated in deeper water

compared to the surface. One tongue of water with increased SRP extended from the 12 m depth region at 17:00 and into the 2 m depth region. There did not appear to be a related increase in surface SRP. A second lesser upwelling originating with 18 m water at 19:00 extended into the 2 m depth region by 04:00. The rate of SRP upwelling was calculated by tracing local increases in SRP towards the surface. SRP in the 17:00 tongue was advected vertically at a rate of 7 m hr^{-1}, decreasing to 3 m hr^{-1} by the 2 m depth region. The tongue originating at 19:00 was transported at rates between 7 m hr^{-1} to 1 m hr^{-1}. The fastest advection occurred between 5 m and 12 m and declined as depth decreases. The average advection rate was about 3 m hr^{-1} in the vertical.

Salinity along the second tongue originating at 19:00 followed the upwelling of SRP to at least the 5 m depth region (Figure 3b). This manifested as an upwelling of high salinity water, decreasing in salinity as depth decreases. A similar but weaker salinity signal was present at 2 m as well. However, the salinity peak at 2 m occurred at 07:00, which is 3 hours later than the SRP peak at 06:00 at the same depth. Neither subsurface SRP nor salinity appeared to impact surface waters. Salinity increased by 6 just below the surface (< 2 m), suggesting very strong stratification from freshwater input. Such stratification may have prevented upwelled water from 12 and 18 m from reaching the surface. A similar separation between river-derived CDOM and sub-surface CDOM input has been found in the Louisiana shelf (Chen and Gardner 2004; Chen et al 2004). The SRP peak at 06:00 occurred at the same time as a salinity low, supporting the notion that changes in surface SRP were primarily due to riverine transport along the surface and not from upwelling. Based on the Brunt-Väisälä frequencies between 0 - 2, 2 - 5, 5 - 12, and 12 - 18 m, the buoyant restoring force limits the displacement of entrained water from the

shallower depth to mean (harmonic) periods of 0.1, 0.1, 0.2, and 0.4 minutes, respectively. This rapid rate is indicative of the strong stratification (Goebel et al 2005). The period is much less than the minimum two hour period which could be detected in the time-series, which invalidates advection through instability/density inversion as a mechanism for causing variations in the environmental parameters.

The timing of the subsurface changes are highly suggestive of tidal forcing. The tidal range of the Louisiana shelf is relatively small, but internal changes could be much higher. The 10 hour oscillating period is close to the strong semi-diurnal (M2) tide found in Terrebonne Bay and along the Louisiana shelf (DiMarco and Reid 1998; Inoue and Wiseman 2000). The tidal influence is much stronger in the along-shelf direction close to the coastline, with tidally driven currents of ~54 m hr^{-1} (DiMarco and Reid 1998). This is significantly faster than the upwelling velocity seen at TS1 (Figure 4.3). The continuity equation ($\delta X/\delta t + \delta Y/\delta t + \delta Z/\delta t = 0$) requires a very slight vertical velocity gradient of -3.1 m hr^{-1} per meter (-0.086 cm s^{-1} m^{-1}) in order to create the average upwelling velocities found at TS1. However, it seems more likely that an upwelling event is not occurring but rather the internal wave motion of the tide advecting the entire water column.

Surface DIN : SRP ratios at station TS1 varied widely, from 52 - 240 (Figure 4.3c). The highest DIN : SRP values (> 170) were concentrated during a 5 hour period in the middle of the time-series, which ended more abruptly than it began. DIN : SRP declined as a decaying exponential function (1/X) with increasing SRP, meaning the DIN : SRP ratio at the surface was primarily driven by low SRP concentrations rather than DIN. No distinct function was apparent between the DIN : SRP ratio and SRP at 12 or 18

m. At these depths, DIN concentrations decreased and SRP concentrations increased concurrently.

The relationship between fluorescence and SRP was opposite that found in the Hudson River plume between fluorescence and nitrate (figure not shown; see Chapter 2). In the Hudson River plume, high nitrate concentrations generally parallel high fluorescence. Likewise, fluorescence at TS2 decreased in a similar manner to nitrate as salinity increases. This type of relationship exemplifies nutrient-focused control (akin to bottom-up control, extended to nutrients) of phytoplankton biomass. At station TS1, the relationship between fluorescence and SRP was a decaying exponential (fluorescence decreases as SRP increases). This is a result of uptake-focused control (related to top-down control), where SRP concentrations are primarily controlled by the amount of biological uptake.

AP is characterized by an exponential increase in activity when SRP decreases below a threshold value (Chrost and Siuda 2002). This shape reflects the induction of AP by low SRP concentrations. The specifics of this relationship (SRP concentration at the threshold, rate of increase in activity with decreasing SRP) vary with the environment and species (Lomas et al 2004; Ranhofer et al 2009). An induction curve was found in station TS1 surface waters (Figure 4.4). Low AP activities (< 20 nmol L^{-1} hr^{-1}) were present at SRP concentrations above 0.35 uM. When SRP dropped below 0.35 uM, AP activity increased. Though generally describing an exponential decay, the initial portion (low SRP) of the AP activity/SRP curve did not have a 1 to 1 correspondence; in this and other cases (e.g. Nausch 1998; Dyhrman and Ruttenberg 2006) both high and low AP activities could be found at identically low SRP concentration. This degeneracy prohibits

AP activity from serving as a reliable indicator of phosphate stress. The pattern presented here was further skewed by two high AP activity points at relatively high SRP concentrations of 0.62 and 0.95 uM.

The decaying exponential relationship between AP activity and SRP concentration is usually interpreted as activity being initiated when the SRP concentration drops below a given low value (the induction point). However, the overall shape does not indicate what additional factors may control the expression of AP activity. For instance, the rate of SRP removal or amount of SRP removal could be important. Alternatively, AP induction may have a temporal requirement, such that AP activity may not be induced when phosphate concentrations are increasing. This would act as a second level of regulation on AP activity and could affect the interpretation of AP activities in some systems.

The relevance of the magnitude of SRP removal to AP activity was evaluated by determining the rate of phosphate removal through mixing, calculated as the change in SRP with salinity. If AP activity was strictly a response to low SRP concentration, then AP activity should be invariant with the SRP removal rate. Alternatively, the rate or direction of change in SRP may be important, and must be determined by a time-series approach. A conservative mixing line was calculated from coastal and marine endpoints. The coastal endpoint was the highest surface SRP concentration and its associated salinity. The lowest salinity was not a unique value, so the endpoint was based on the unique highest SRP concentration. The marine endpoint used the minimum SRP (0.18 uM) and highest surface salinity (35) from both time-series stations. This results in a

conservative mixing slope of -0.047 uM SRP sal^{-1}. For each two consecutive data points, the change in SRP and salinity was calculated, producing an SRP – salinity slope.

AP activity increased linearly with SRP removal when the SRP – salinity slope was between -0.04 and -0.2 uM sal^{-1} (Figure 4.5). AP activities were generally low when SRP removal was outside this range. No pattern was apparent when comparing the rates of SRP removal and SRP concentrations, though SRP concentrations were generally higher when the magnitude of the removal rate was larger than -0.2 uM sal^{-1} (figure not shown).

There may be special meaning behind the SRP removal rate boundaries of -0.04 and -0.2 uM SRP sal^{-1}. The conservative mixing slope, -0.047 uM SRP sal^{-1}, is close to the upper SRP removal rate of -0.04 uM SRP sal^{-1}. At removal rates greater (more positive) than the conservative mixing slope, AP activity may be unnecessary as SRP is presumably being added to the system. The cutoff at -0.2 uM SRP sal^{-1} is near the minimum concentration of SRP found at the time-series stations. SRP concentrations increased above 0.35 uM when the SRP removal rate had a magnitude greater than -0.2 uM sal^{-1}. The decline in AP activity beyond -0.2 uM SRP sal^{-1} is explained most easily by SRP concentrations exceeding the minimum threshold required for AP induction. A more complicated explanation is based on the idea that -0.2 uM SRP sal^{-1} is the highest removal rate of SRP which does not exceed the total SRP at each salinity. A hypothetical cellular mechanism could exist which prevents AP expression when the SRP removal rate exceeds SRP concentrations.

The time-series of SRP and AP activity highlights the need for an additional AP regulation mechanism beyond a low SRP induction threshold (Figure 4.6). Periods with

low SRP concentrations did not correspond often with high AP activities. There were long stretches of time (20:00 - 03:00) where low SRP (< 0.35 uM) and low AP activity (< 25 nmol L^{-1} hr^{-1}) coincide. A more complicated pattern was apparent when considering all but the final two hours of the time-series. AP consistently peaked when SRP concentrations decrease below ~0.4 uM. Specifically, SRP must decrease past this level; other periods when SRP < 0.4 uM but were either increasing or staying level over time did not produce AP activity. The same pattern held when using chlorophyll (fluorescence)-specific activity, which should partially correct for differences in bulk AP activity due to population size changes.

AP activity may have a “temporal chirality” where equivalent SRP concentrations do not necessarily elicit an AP response. The term temporal chirality here harkens to the chirality of organic molecules. In chemistry, chirality is a handedness, whereby a molecule exhibits different chemistry from a molecule with the same components but alternate configuration (e.g. D- and L-amino acids). Temporal chirality is the concept that, for conditions with the same measured SRP concentration, a different response is expected depending whether the SRP concentrations are decreasing in time or not. There is evidence for an additional layer of control over AP activities from both the conservative mixing analysis and the temporal chirality of the time-series. Both lines of evidence associate high AP activities with the process of SRP removal as opposed to only low SRP concentrations. There is undoubtedly a close relationship between SRP removal and SRP concentration, which maintains the consistency of the decaying exponential profile.

AP activity is a possible mechanism for increasing the concentration of SRP without relying on advection, and has the ability to respond within the time span seen with the SRP peaks. Any significant increase in SRP requires AP to have enough time to create the SRP and slow enough uptake to allow hydrolyzed SRP to accumulate. The second SRP peak increased by 0.61 uM, which would take about 15 hours for the measured AP activity (40 nM hr^{-1}) to generate (Figure 4.6). However, the uptake rate at station 2A was measured at 67 nM $hour^{-1}$, which would negate any possible SRP accumulation from AP activity, assuming the uptake rate was similar during March 2007.

Similar calculations with the 0.66 uM change in SRP concentration and a peak activity of 169 nM hr^{-1} found at the third SRP peak (including 14 nM hr^{-1} uptake found at station 1B), would require over 4 hours to generate. This is longer than the duration of the peaks in SRP concentration. It is unlikely that much of the second peak in SRP is due to AP activity, though some of the third peak may be. The first peak was associated with zero AP activity. Using AP activity to produce measurable increases in SRP in phosphate-limiting conditions seems inefficient; tight coupling between hydrolysis and uptake would increase the efficiency but decrease the apparent change in SRP concentration. This said, higher AP activities between stations 2A and 1B were found in the location with lower uptake rate. Unfortunately, uptake rates are not available for the time-series stations. The uptake rates reported at the two contour stations were likely to be under more phosphorus-limiting conditions, and may be unrealistically fast for the time-series stations.

The relationship between environmental variables and AP activity is not necessarily constant in time. For instance, changes in fluorescence from growth may lag

changes in the availability of SRP. The change in the relationship between surface SRP, fluorescence, and AP activity was examined by lagging either fluorescence or AP activity behind SRP, and lagging AP activity behind fluorescence (Figure 4.7). The coefficient of determination (linear r^2) was calculated for each lag period, starting with a lag of zero (the value of the variables when they were originally measured). A linear r^2 value was used specifically to test the evolution of a linear relationship, especially from the primarily (negative) exponential relationships found between SRP and fluorescence, and SRP and AP activity seen at lag = 0. Data from only where SRP $\leq$ 0.3 uM was considered when calculating the r^2 between SRP and AP activity, as this is the SRP range where AP induction occurs.

The best linear regression (r^2 = 0.28) between SRP and fluorescence occurred when fluorescence values were lagged behind SRP by 14 hours. This is a 10% improvement on the predictability of fluorescence based on a linear relationship with SRP. The lag may indicate the average generation time of phytoplankton along the shelf. However, no single lag period offered an overwhelming increase in linearity. The linearity between SRP concentration ($\leq$ 0.3 uM) and AP activity peaked at r^2 = 0.33 and occurred with a lag of 11 hours. An almost equivalent r^2 value was found with a lag of 4 hours. The time difference between the two lagged peaks is very close to the to the 5 hour difference between two peaks in SRP concentration (Figure 4.6), suggesting the correlation is driven by alignment with these two peaks rather than an improved overall fit. The low coefficients of determination with SRP : fluorescence and SRP : AP activity also suggests that the fundamental relationship between these pairs of environmental variables are not inherently linear but have some additional controls.

Linearity between fluorescence and AP activity greatly increased when AP activity was lagged by 7 hours; r^2 values jump from 0.09 to 0.59. The linearity steadily improved with increased lag until the peak at 7 hours lag time, after which the linearity slowly declined. The strength of the increase and the existence of a single peak value implies a fundamental change in the fluorescence : AP activity relationship when a time lag is implied.

4.3.2 Station TS2

The time-series began at 21:00 with an SRP concentration of 0.26 uM, which increased to 0.33 by 01:00 (Figure 4.8a). Surface SRP decreased in a mostly linear fashion from 01:00 until 08:00 when SRP concentrations approached their minimum value of ~0.2 uM. After this, mean SRP remained low. This same linear decrease in SRP between was found at all of the depths. The upper 3 depths (surface, 2, 5 m) had similar SRP concentrations. This differs from station TS1 where SRP was much lower in the surface layer than at any other depth. The highest SRP at station TS2 (0.6 uM) was at 18 m, indicating a subsurface SRP source. Water at 18 and 12 m depths at station TS1 also contained significantly higher SRP than elsewhere in the water column. As with the other depths, SRP at 18 m decreased over time with no indication of advection upwards into shallower water. Overall SRP concentrations varied between 0.18 and 0.34 uM, with most of the measurements < 0.3 uM.

Salinity at station TS2 was higher than TS1 throughout the water column during the entire time-series (Figure 4.8b). Surface salinity ranged from 30 - 33, and from 30 - 36 when considering all depths. This matches the surface salinities seen at contour station

2B. A large increase in salinity was seen between the surface and 2 m depth. This indicates a very thin cap of residual freshwater from the Mississippi River plume. Salinity at 2 m decreased to a minimum value of 32.2 at 11:00, and then increased again. From hour 00:00 - 17:00, the trends in surface salinity were opposite that found in the 2m depth layer. The magnitude of the salinity decrease in the 2m layer was larger than the opposing trend seen at the surface. As with SRP concentrations, salinity did not appear to be upwelled to the surface. The harmonic periods of the buoyant restoring force were 0.1, 0.4, 0.8, and 0.7 minutes for the associated depth regions of 0 - 2, 2 - 5, 5 - 12, and 12 - 18 m. As with TS1, such a short period precluded variations in the time-series due to density inversions and instability (and associated water parcel movement). Overall lower freshwater concentrations compared to TS1 resulted in less stratified conditions directly below the freshwater surface lens.

DIN : SRP ratios throughout the water column did not meet the requirement used to define phosphate limitation (Figure 4.8c). Surface values were consistently much higher than at any other depth, including 2m below the surface. However, even these values did not exceed a DIN : SRP ratio of 25. DIN : SRP ratios were at their lowest at the end of the time series between 2 and 5 meters. The DIN : SRP ratio increased to 11.5 at 12 and 18 m depth and was higher earlier in the time-series. Unlike station TS1, the surface DIN : SRP ratio was controlled by both TN (05:00 peak) and P (17:00 peak). In contrast to the SRP distribution, the highest DIN values were in the surface layer, with intermediate low values and an increase in nitrate at 18 m (not shown). This suggests a freshwater surface transport dominated by nitrate.

Oxygen concentrations did not drop below 2 mg O_2 L^{-1} and so were neither anoxic nor considered hypoxic (Rabalais et al 1994). However, a good correlation exists between oxygen concentration and SRP (r = -0.87) suggesting the release of SRP through redox reactions. Released SRP may have been advected from anoxic waters elsewhere. Significant nutrient release from sediments can occur within the short (hour to semi-diurnal) time periods found here (Grunwald et al 2007).

The relationship between SRP concentration and fluorescence was also different than at TS1 (figure not shown). Unlike the uptake-focused control at TS1 where fluorescence was inversely (and non-linearly) related to SRP, fluorescence at TS2 was positivity and linearly related to SRP. This relationship was also found in the Hudson River and indicates nutrient-focused control of phytoplankton biomass, assuming phosphate-limitation of maximum growth potential. The primary differences between the two time-series stations were the higher DIN and fluorescence values at TS1 compared to TS2. Despite much lower DIN concentrations at TS2 than at TS1, a similar linear and positive trend was seen with surface nitrate as with SRP.

AP activity did not exhibit the same profile with SRP as was found at station TS1 (Figure 4.9). As with fluorescence, AP activity generally increased linearly with increasing SRP concentration. The activity range during the linear portion was about 100 nmol L^{-1} hr^{-1} and increased to 400 nmol L^{-1} hr^{-1}. This pattern does not fit the canonical induction model of AP activity. SRP concentrations were always below the 0.35 uM AP induction threshold identified at station TS1, so increasing AP activities with decreasing SRP concentrations were expected. The relationship is indicative of biomass effect on activity— each cell producing some AP activity contributes to the total, so total AP

activity increases with total biomass. When AP activity is normalized by fluorescence (specific AP activity), the direction of the activity changed with respect to SRP and a negative linear trend was produced. In effect, though more cells are available to produce AP activity, each cell is producing less as SRP concentration increases. The shape of the AP activity : SRP relationship at station TS1 was not altered when AP activity was normalized by fluorescence.

Using the same conservative mixing values from TS1, the mixing rate of SRP with salinity was calculated to be -0.034 uM sal^{-1}. This is smaller than at station TS1, presumably due to the lower SRP concentration at station TS2. A boundary of sorts was formed at the removal rate from conservative mixing; almost all of the data had removal rates in excess of the conservative mixing rate (Figure 4.10). This is interpreted as input of SRP. Normalized AP activity was consistently at an elevated level, despite having positive removal rates (SRP addition). No data was available to test whether the linear increase in AP activity occurred between the removal rate of conservative mixing (-0.034 uM sal^{-1}) and -0.2 uM sal^{-1}, which were the boundaries identified at station TS1. It is apparent that negative SRP removal rates were not necessary for AP induction.

Throughout almost the entire time-series of station TS2, normalized AP activity followed a pattern opposite of SRP concentration (Figure 4.11). The exception to the pattern was a single point at 17:00. Unlike the time-series at station TS1, SRP concentrations never increased above 0.35 uM. As such, there was no indication for or against temporal chirality as an additional level of control on AP activity. The time-series began with SRP concentrations decreasing below 0.35 uM, which fulfilled the two necessary conditions identified for the presence of AP activity following the temporal

chirality concept. If the induction threshold is adjusted downward to 0.28 uM, then almost all of the changes in normalized AP activity are accounted for by the direction of SRP concentration changes.

The uptake rate at contour station 1B was 14 nM hr^{-1} during May 2001, a period likely to be more strongly phosphate-limited than when the time-series stations were measured. AP activity during May 2001 could produce between 124 - 332 nM hr^{-1} at station 1B. This resulted in a 9 - 24 times excess of SRP produced by AP activity compared to phosphate uptake. This amount of uncoupling could allow significant quantities of AP-derived SRP to accumulate in the water. The changes in SRP concentration during the time-series were sufficiently small that the measured AP activity could almost instantly account for the entire change. This may be one reason why AP activity is relatively invariant with the removal rate. The close tracking of normalized AP activity and SRP may be a result of phosphate production through enzyme activity.

The coefficient of determination (r^2) changed in a sinusoidal pattern when surface environmental parameters at station TS2 were time-lagged relative to each other (Figure 4.12). Every variable combination examined—SRP : fluorescence (SRP : Fluor); SRP : AP activity (SRP : AP); SRP : fluorescence-normalized AP activity (SRP : norm. AP); and fluorescence : AP activity (Fluor : AP)—exhibited the same pattern. Moreover, the phase of the waveform was also very consistent between each variable pair. The maximum r^2 values for the variable pair were 0.54, 0.50, and 0.31 for SRP : Fluor, SRP : AP, and Fluor : AP respectively.

The Fluor : AP activity pair was unusual in that the third peak, at lag 19 hr, was of unequal height compared to the other peaks of that variable pair. The middle peak of that

variable pair was also divided into two modes, with the major mode peaking after the peaks of all other variable pairs. Unlike station TS1, the initial configuration of the variable pairs (lag = 0 hr) was at least as high as is produced using any other lag period. There was almost no difference between the fluorescence-normalized and non-normalized AP activity in either the magnitude or phase of the highest r^2 value. The SRP : Fluor pair had consistently lower r^2 values compared to SRP : AP and reached a minimum after an additional 1 - 2 hour lag. Despite the offset in the troughs, peak r^2 values occurred simultaneously with SRP : norm. AP and 1 hour before SRP : AP. The average frequency was 12 hours (peak r^2 occurs 12 hours apart). No semi-diurnal variations were noticed in any of the surface environmental data, though subsurface semi-diurnal variations were seen at TS1 (Figure 4.3).

4.4 Discussion

Alkaline phosphatase activity is routinely used to indicate phosphorus limitation in aquatic environments (Hoppe 2003). The basis of this approach is the approximately exponential increase in AP activity found with decreasing inorganic phosphate concentrations (Chrost 1991). Nutrient addition experiments are perhaps the most reliable means of identifying a limiting nutrient, but also require the most infrastructure and time to run, hence restricting the times and locations where data can be gathered. Though other measures of phosphorus limitation (SRP concentration; DIN : SRP ratios) are used most often for the number and simplicity of the data, these values do not inherently reflect the biological requirement or need for phosphorus (Beardall et al 2001). In this regard, AP activity is a superior indicator of phosphorus limitation as activities directly reflect the

need for phosphate and not just phosphate availability. Even so, a multitude of environmental conditions have the potential to affect AP activities, including varying biomass and SRP concentration.

This manuscript focuses on how AP activities and environmental parameters along the Louisiana shelf analyzed as a time-series may differ from measurements taken at a single point in time. Of primary importance was to: 1) determine the amount of variability within a 24-hour period, 2) identify and characterize the environmental parameters that may have an effect on AP activities along the Louisiana shelf, and 3) evaluate the robustness of AP as an indicator of phosphorus limitation.

4.4.1 24 hour variability

The identification of phosphorus limitation was based on two criteria, both of which relied, at least in part, on the concentration on phosphate (SRP) in the water. The SRP concentration at the time-series and contour stations, in turn, was based on input from the Mississippi River, possible advection from subsurface or shelf water, and removal through uptake (Chen et al 2000). The Mississippi River was expected to be a source of SRP, advection to either increase or reduce SRP, and uptake to decrease SRP concentration. The combination of these three processes resulted in the measured SRP concentration at a given point and time.

None of the processes were instantaneous and likely operated on different time scales. Prior work in the Mississippi River plume identified phytoplankton growth rate on order of 1 - 3 day^{-1}, while the advection of plume water took 1 - 2 days (Lohrenz et al 1992). In contrast, the formation and relaxation of temporary turbidity fronts can occur

between 2 - 6 hours (Hitchock 1997), which is a time scale similar to phytoplankton growth rates. It is important to take the relative time scale of changes into account when considering the relationship between environmental parameters.

Contrary to the rather static picture of sub-seasonal nutrient limitation often presented in the Louisiana shelf, time-series analysis of two stations influenced by the Mississippi River showed large amounts of variation in all environmental variables at all depths during the course of 24 hours. Of particular note was the variability in SRP concentrations, since both inequalities used to define phosphate limitation (SRP $\leq$ 0.2 uM; DIN : SRP > 30, Dortch and Whitledge 1992) are related to SRP. Surface SRP values at station TS1 ranged from 0.18 to 1.1 uM and 0.18 to 0.33 uM at stations TS2. Variation in SRP (and other variables) was highest at the surface, though the maximum concentration was often in deeper water. SRP values could peak and return to original values in 4 hours or less.

The range of SRP values was wide enough that over the course of both 24 hour time-series, SRP concentrations occasionally met the low SRP requirement for being phosphate-limited. For instance, the variation in surface SRP at station TS1 caused a change to phosphorus limitation and back again on three different occasions in 24 hours. This sort of variation could undermine the determination of phosphorus limitation if only a single time point is used (Strojsova and Vrba 2007). It is suggested that future indices of nutrient limitation incorporate a measure of the temporal variability in nutrient concentration. Such an index would not only be a meaningful indicator of uncertainty (in addition to the deviation between replicate measurements), but also the magnitude and/or frequency of events which may temporarily relieve nutrient limitation. A similar

argument is valid for non-nutrient indicators of nutrient stress, such as enzyme activity (Beardall et al 2001).

The relevant timescales of environmental changes can be calculated using the variation in the strength of the correlation between two parameters over time (e.g. Lui et al 2007; Moreno-Ostos et al 2009). This concept is similar to the cross-correlation of a Fourier time-series analysis. By identifying how a correlation varies through time, a better picture of the interrelationship between environmental variables is available, and some compensation can be made for the different rates at which elements of the environment respond.

The optimal lag times differed for each variable at TS1. The relationship between fluorescence and SRP, and AP activity and SRP remained low at each lag time, suggesting a fundamental non-linearity of these variables (Putland et al 2004; Hoover et al 2006). Interestingly, the overall non-linear relationship between SRP and chlorophyll was established over the course of 1 day, rather than the multiple day experiments cited above. However, it is possible that the changes in fluorescence and/or nutrients were from advected water. In this case, the relationship between SRP and fluorescence could be based on a long-term equilibrium established elsewhere, rather than a rapid and non-linear response to changing nutrient concentrations. Of course, there is a chance the relationship is inherently non-linear.

The best linear fit between fluorescence and SRP occurred after 14 hours. If SRP removal was associated with the 1 -3 day^{-1} growth rate estimated in the Mississippi River plume (Lohrenz et al 1992), the lag time between fluorescence and SRP may be an indication of phytoplankton generation time. In contrast to fluorescence and SRP, a

significant increase in the linearity of the fluorescence : AP activity relationship was found with 7 hours lag time; this value is half of the proposed generation time. The drastic increase in linearity between AP activity and fluorescence when including a lag period implies that low nutrient concentrations themselves may not be as important for AP production as the phytoplankton “noticing” that nutrient concentrations have changed. It also suggests that phosphate is not continually required at the same rate over time but varies with fluorescence, presumably in relation to growth rate (Maguer et al 2007; Jauzein et al 2008). Small, rapid changes in SRP concentration may not be as important as changes which last multiple hours. Normalizing AP activity by fluorescence to create a phytoplankton-specific activity should perhaps be done when the fluorescence value is lagged by one-half of the generation time.

Surface values were apparently dominated by surface processes, with little to no influence from the subsurface. This comes despite evidence of upwelling and advection between 2 – 18 m depth, highlighting the strength of the rive plume signal, even during a moderate flow period. The high stratification may make the tidal signal an internal wave, isolating tidally-mediated processes from shallow areas. Isolation of surface water from the rest of the water column greatly simplifies the possible processes affecting surface SRP concentrations. Strong surface stratification also increases the importance of processes which affect the stability of the water column when considering how likely SRP concentrations are to change over time (e.g. Yin et al 1997; Goebel et al 2005). Increased shallow mixing could supply relatively large concentrations of nutrients to the surface layer, especially during periods where they might not be quickly removed (Hetland and DiMarco 2008). The difference in stratification strength between surface (<

2 m) and subsurface waters necessitates analyses of Louisiana shelf hypoxia consider subsurface measurements of nutrient concentrations and biomass. In many cases, models predicting the timing and extent of hypoxia do include subsurface processes (Donner and Scavia 2007; Green et al 2008; Hetland and DiMarco 2008).

The advection of SRP in the subsurface water column could be traced using salinity. A comparison of salinities as part of a spatial survey, even using a single time point, should provide a means of identifying subsurface advection of SRP, though not the time scale (Hitchcock et al 1997). However, salinity did not track surface SRP concentrations well, most likely due to the role of uptake in changing SRP concentration. DIN was more linearly related with salinity than SRP, presumably because of either a lesser nitrogen demand or greater riverine supply of nitrogen. Conservative mixing of nitrate, phosphate, and silicate has been identified previously for low salinity waters during high flow periods (Hitchcock 1997). Given the difference in ability to identify advection through salinity changes between surface waters (poor) and subsurface (good, especially in 12 and 5 m depths) it seems reasonable to be able to use a conservative mixing approach to determine initial surface SRP concentrations.

4.4.2 Environmental Effects on AP Activity

The canonical relationship between AP activity and SRP concentration is a decaying exponential. However, in this data set and other measurements of the AP activity – SRP relationship, existing uncertainty precludes using AP activities to quantitatively predict phosphate limitation (Tanaka et al 2006; Cao et al 2010). Part of

this uncertainty stems from a partial understanding of how SRP and other environmental parameters affect AP activity, and the extent to which they do so.

Phosphate concentration is likely the primary control of AP activity (Chrost and Overbeck 1987 and others). Numerous experiments have confirmed the induction of AP activity with low SRP. The exact value at which this happens is not uniform, however (Lomas et al 2004; Tanaka et al 2006; Ranhofer et al 2009). Some degree of scatter may be expected, as the genetic regulation of AP production is based on phosphate (Vershinina and Znamenskaya 2002), and very linear fits can be found when phosphate (and not SRP) are considered (Tanaka et al 2006). However, AP activities were approximately equal at both time-series stations as well as the contour stations, despite an order of magnitude higher concentration of SRP at the time-series stations. The similarity in activities with different SRP concentrations mentioned here and elsewhere (e.g. Nausch 1998; Dyhrman and Ruttenberg 2006) suggests the presence of other factors that control bulk AP activities.

The first additional factor considered here is the rate of phosphate removal (change in SRP with salinity) with relation to the conservative mixing rate. Close to the river mouth (station TS1), only low AP activities were found when the removal rate was slower than that predicted by conservative mixing. AP activity linearly increased when the removal rate exceeded the mixing rate, suggesting AP activity responds to decreasing SRP and not just low values. This relation only held when the removal of SRP (per unit salinity) was less than the minimum SRP concentration (0.2 uM). However, most of the AP activities further away from terrestrial nutrient courses (station TS2) were found

when the removal rate was not only above the conservative mixing rate, but when the removal rate was positive (SRP concentration increased with salinity).

One possible explanation is that the increases in SRP away from the river originate from AP activity itself (Song et al 2006; Cao et al 2010). Uptake rates were much slower away from the Mississippi River plume, so most of the phosphate produced by AP activity may have been able to accumulate in the water. Unfortunately, uptake rates for the time-series stations were not available, and further work will be required to test this hypothesis.

Temporal chirality is a possible additional control on AP activity. In the time-series of AP activity, low SRP concentrations did not always correspond with high AP activity as predicted. Except at the very end of the time-series, AP only increases when SRP concentrations decrease to the SRP induction point. After crossing this value, if SRP does not continue to decrease, AP activities remain low. AP activity is also low when SRP concentration increases. As with the removal rate, temporal chirality would impose a second set of conditions on top of SRP concentration to further specify the circumstances which AP activity will be produced.

The two proposed controls (SRP removal rate and temporal chirality) are interrelated. Though temporal chirality does not specifically invoke changes with salinity, it seems likely that many of the largest SRP concentration increases are due to advection (Hitchock et al 1997; Lohrenz et al 1999; Chen et al 2000), possibly with prior uptake of nutrients. When SRP increases from additional riverine (or subsurface) input, there is an inherent change in salinity. Hence, the notion of AP activity not responding to increasing SRP concentrations over time is physically equivalent to AP activity not being produced

when the SRP removal rate (change in SRP over change in salinity) is above the conservative mixing rate.

A reason for adding a second layer of control to AP activity is to increase the efficiency of AP producers. It is energetically expensive to produce ectoenzymes, and a competitive advantage would lay with those organisms that only do so when the production of AP would offset phosphorus limitation. At high phosphate concentrations, AP is not required to meet the phosphorus requirement of the organism, and so is not produced. When the induction threshold is crossed, phosphate concentrations are low enough that phosphorus may become limiting. Temporal chirality prevents AP activity from being produced when phosphate concentrations are rising. This could enhance efficiency by preventing the production of phosphate when phosphate is already being added from an outside source (such as advection).

Fluorescence, as an indicator of phytoplankton biomass, can play two primary roles regarding bulk AP activity. Many phytoplankton can produce AP (Chrost and Siuda 2002; Hoppe 2003), and so larger populations have the potential to contribute to a higher total activity. In this role, fluorescence can be used to produce a “specific activity,” AP activity normalized by fluorescence, indicating the average activity per fluorescence unit. Multiple sources have shown a positive relationship between phytoplankton concentration and associated bacteria concentrations (Fuhrman et al 1980; Cole et al 1982; Cole et al 1988). Bacteria also produce AP (Chrost and Overbeck 1987), enhancing the apparent specific activity. High biomass will also reduce the phosphate concentration, leading to the production of AP activity once the induction threshold is crossed.

Two different patterns of fluorescence and SRP were found along the Mississippi River-influenced section of the Louisiana shelf. The first is an exponential decrease in fluorescence with increasing SRP. When SRP is ~0.35 uM, further increases in SRP do not affect fluorescence. These univariate changes above 0.35 uM SRP suggest a change from phosphorus limitation to a different nutrient, such as light (Lohrenz et al 1999). The near river system was uptake-focused: a large phytoplankton population (fluorescence) depletes most of the nutrients (SRP). When the phytoplankton population is smaller, the requirement for SRP also decreases, allowing SRP concentrations to remain high. The residence time of the Mississippi River plume near the river mouth (salinity 0 - 18) has been estimated at 1 day (Breed et al 2004). Fast advection near the Mississippi River plume means nutrients do not stay localized and are depleted in transit (Chen et al 2000). The change in SRP measured during the time-series is mechanistically different than the reduction of SRP that occurs during the residence time, so the two are not directly comparable.

The negative exponential relationship seen in low salinity Mississippi River plume water is almost exactly reversed from the nitrate – fluorescence relationship found in the bulge portion of Hudson River plume (Chapter 2). The Hudson River, acting as a chemostat (Moline et al 2008), allowed high phytoplankton growth while continually replenishing the nutrient supply. The system could be considered nutrient-focused: a high nutrient (nitrate) supply supported a large phytoplankton population (fluorescence), and as the nutrient supply dwindled, phytoplankton concentrations also decreased. A linear and positive relationship existed between SRP and fluorescence in mid- and high salinity Louisiana shelf waters as well. Phytoplankton biomass away from the river was

potentially sufficient reduced in number (median value is 7-fold lower than in low salinity water) in comparison to the nutrient concentration that additional DIN and/or SRP had a positive effect on growth. Similar differences between in-plume and out-of-plume dynamics have previously been predicted and found along the Louisiana shelf (Lohrenz et al 1999; Green et al 2008; Eldridge and Roelke 2010).

The relationship between AP activity and fluorescence had varying importance depending on the time-series station. Normalizing AP to fluorescence did not change the AP – SRP relationship at TS1. Likewise, no distinct pattern was present when comparing AP activities to fluorescence. However, at TS2, the use of specific AP activity instead of measured activity profoundly changed the nature of the relationship. Measured AP activity increased with increasing SRP concentration. When AP activity was normalized by fluorescence, the trend reversed and normalized AP decreased quite linearly with increasing SRP. In part, the role of fluorescence normalization on AP activity may reflect the relationship between fluorescence and SRP. At TS1 and at times where SRP > 0.35 uM, fluorescence values did not change, and so normalized AP activity also would not vary. At TS2, fluorescence increased with SRP linearly with the effect of lowering normalized AP activity. While the idea of cell-specific normalization is sound, it remains to be seen if the result is actually specific to population size or to the low SRP concentration that results from high biomass. Extra consideration for the direction of energy transfer (nutrient-focused vs. uptake-focused) may be required in spatially large environments with point sources of nutrients. Another explanation for the effect of fluorescence normalization on AP activity is a change in the AP-producing species composition (e.g. Dyhrman and Ruttenberg 2006; Meseck et al 2009; Chapter 2 of this

dissertation). Unfortunately, the data required to examine this aspect of community AP dynamics was not available.

Another environmental parameter known to have an effect on ectoenzyme activity is UV radiation (Garde and Gustavson 1999; Espeland and Wetzel 2001). UV radiation can act as an enzyme inhibitor through photolysis of the enzyme complex. UV radiation can also potentially increase activity through photolysis of relatively refractory organic matter into enzyme substrates (Bano et al 1998; Minor et al 2007). No indication of UV inhibiting or enhancing AP activity was seen at either station, based on the poor linear regression between the AP activity and PAR (TS1: $r = 0.33$; TS2: $r = 0.22$). The Mississippi River plume had a mean average PAR attenuation of 3.4 m^{-1} at TS1, which may interfere with processes requiring UV absorption.

4.4.3 AP Activity as Phosphorus Limitation Indicator

A formal set of inequalities with nutrient concentrations and ratios was used by Sylvan et al (2006) to identify nutrient limitation along the Louisiana shelf, supported by nutrient addition experiments and AP activities. Based on these identifiers, the contour stations were definitively phosphate-limited in March and May of 2001. In contrast to the contour stations, the mean values of the time-series stations did not meet the phosphorus limitation requirements at any of the time-series stations. However, both time-series stations met the low SRP requirement at some point during their respective measurement periods. Only TS1 additionally met the DIN : SRP ratio requirement; station TS1 was always > 30, while station TS2 was consistently below 25. Unfortunately, nutrient

addition data was not available with time-series stations to verify the phosphate limitation status of the time-series stations.

Despite the borderline position regarding phosphorus limitation based on SRP concentration and DIN : SRP ratios, AP activity at both time-series stations were approximately the same as the contour stations. This highlights the primary problem in using AP activity to indicate phosphate stress—how to match measured AP activity to a quantitative indicator of phosphorus stress.

The general paradigm of ectoenzyme activity induction (Chrost and Siuda 2002), and of AP specifically, was represented at the time-series stations. An SRP concentration was present which marked the approximate induction threshold for AP activity. Likewise, decreasing SRP past the threshold occasionally resulted in an increase in AP activity. Additional regulation of activity through temporal chirality may fine-tune the periods when AP is expressed, but did not alter the overall SRP – AP relationship.

Many environmental factors beyond phosphate concentration have the potential to modify AP activities. AP activity was not correlated with DIN, suggesting that AP activity was not used to acquire nitrogen from the environment. This was the case even when the DIN : SRP ratio was low. The inhibitor (PO_4) to substrate (DOP) ratio is an important factor in controlling AP activity (Chrost and Siuda 2002). Also, there is evidence that bulk AP activity is reduced at extremely high substrate concentrations (Sebastian et al 2004). The effect of biomass on SRP and AP production in general has already been mentioned as contributing to higher activities. Of these, the kinetic effect of substrate concentration on AP activity is probably the most difficult to identify and account for in interpreting AP activities. Dissolved organic phosphate, which is the

organic matter pool AP substrates are a part of, was not measured as part of the time-series work. Additionally, substrate structure, quality, and differences in the enzyme-producing capacity of the microbial population can all contribute to variations in how SRP is remineralized in the water column (Arnosti 2004) though some of these are not relevant to the potential (saturating) AP assays used here.

AP is perhaps better thought of as an indication of what a cell is doing to adapt to low phosphorus surroundings rather than an indication of low phosphorus conditions. AP activity can change significantly in 24 hours, sometimes up to an order of magnitude difference (Chrost and Siunda 2002; Strojsova and Vrba 2007), and internal pools of phosphorus can change in a matter of minutes (Ault-Riche et al 1998). Likewise, ectoenzymes that function as carbon scavengers can also vary greatly in a few hours (Arnosti 2004). AP activities are an easily measured mechanism of determining current and potentially rapidly changing phosphorus stress in aquatic biomass. An accurate interpretation of AP activity requires the separation of biomass effects, substrate kinetics, and the effects of additional regulation like temporal chirality. Despite the added complexity in interpreting AP activities compared to measuring nutrient concentrations, the explicit relationship between AP activity and phosphorus should make AP activity assays a primary methodology for quantitatively defining phosphorus stress.

4.5 Conclusion

This chapter focuses on the response of alkaline phosphatase activities to short-term (24 hr) environmental changes at two places along the Louisiana shelf. The first time-series station (TS1) experienced uptake-focused control, with phytoplankton

biomass lowering SRP concentration. The basic induction curve was present at the first time-series station. A threshold value of ~0.35 uM SRP was identified as the concentration necessary to induce AP activity. This threshold was asymmetrical; AP activity appeared to be induced only when nutrient concentrations were decreasing, creating a temporal chirality in activity. Related to this concept is the activation of AP by the magnitude of the SRP removal rate, rather than absolute SRP concentration. The linearity of the fluorescence : AP activity relationship improved drastically when lagging AP activity at the first time-series station. The second time-series station (TS2) had nutrient-focused control, with high SRP reflected by high fluorescence. An AP induction curve was not seen, but was replaced by a positive linear relationship with SRP and fluorescence. Normalizing AP activity by fluorescence changed the direction of the AP : SRP relationship, displaying nutrient-focused control at TS2. The linearity of SRP, fluorescence, and activity pairs each demonstrated a strong cyclical pattern when lagged with each other, but the strength of the relationships were not enhanced compared to initial values. At both time-series stations, SRP, salinity, and the DIN : SRP ratio changed during the time-series at all depths. Cyclical upwelling or tidal oscillations were seen from 12-18 m depth, but did not appear to influence surface values. Both stations were borderline phosphorus-limited, though SRP concentration varied during the course of the time-series. The addition of an index for variability in nutrient concentration over time is suggested when using nutrient concentrations and ratios to determine limitation. AP activity is uniquely positioned as an explicit indicator of the phosphorus requirements of a population. The use of AP activities to define phosphate stress should be routinely measured as part of any survey exploring aquatic phosphate limitation.

5.0 Conclusion

Conceptually, the hydrolysis product of ectoenzyme activity is used to relieve nutrient stress or acquire a type of molecule not immediately accessible in the environment. As such, ectoenzyme activities have been used primarily to indicate nutrient stress. Unlike nutrient concentrations and nutrient ratios, ectoenzyme production is a direct cellular response to environmental conditions. When properly characterized, ectoenzyme activities can offer great insight into the nutrient requirements of organisms and how they use organic matter. Proper characterization of ectoenzymes in the environment includes identifying the induction point of activity, assessing the linearity at inorganic nutrient concentrations below the induction point, and assessing how variability in activity over time and space relates to changes in the strength of nutrient limitation. While a very useful tool for analyzing potential nutrient stress, ectoenzymes are a primary mechanism for converting particulate organic matter into dissolved matter and dissolved organic nutrients into dissolved inorganic nutrients and hence have an importance far beyond that of just a stress response. A detailed analysis of variability in ectoenzyme activity is necessary in order to move beyond the limited and highly qualitative "'high' activity = 'strong' nutrient limitation" paradigm currently in use.

5.1 Specific Conclusions

This dissertation analyzed data from two different ectoenzymes commonly measured and thought to be important in the marine environment. The data came from two river-influenced coastal regions, locations of variable inorganic nutrient concentrations, dissolved organic matter concentrations, and biomass. Each chapter

described the relationships found between phytoplankton biomass and inorganic nutrient concentrations and the induction of ectoenzyme activity. It also linked the magnitude of ectoenzyme activity to changes in dissolved organic and inorganic matter concentrations. The covariance and possible roles of non-nutrient variables in changing ectoenzyme activities were explored.

Inorganic nutrient concentrations appeared to be the primary control of both LAP and AP activities, though some degree of co-regulation by substrate concentration (kinetic and substrate-limited activity) was apparent. Ecoenzyme induction may require signaling of sufficient substrate availability to make production energetically worthwhile. Total fluorescence was a good indicator of ectoenzyme activity only in nutrient-focused planktonic ecosystems. Normalization of activity by fluorescence drastically altered the relationship between ectoenzyme activity and environmental parameters and should be done only when the microbial ecosystem is dominated by autotrophic ectoenzyme producers. Large variations in inorganic nutrient concentration and ectoenzyme activity are possible in a relatively short amount of time, limiting the scope of statements that can be made with sparse temporal data sets. Ectoenzyme activities did not appear to be influenced by subsurface advection when measurements were taken within the two buoyant river plumes. The distribution of ectoenzyme activities was used to identify biogeochemically distinct areas. The production of nitrate equivalents by LAP was similar to the nitrate uptake rate in the Hudson River plume. LAP activity was not proportional to the magnitude of the nitrate deficiency but exhibited a logarithmic increase with nitrate deficiency, possibly due to kinetic effects with varying substrate concentrations. LAP supplied by bacteria and dinoflagellates may be sufficient to sustain

diatom populations lacking LAP, explaining the current lack of identified LAP-producing genes in these species. LAP activity was most likely not entirely sufficient to support a nitrate-starved phytoplankton population due to substrate limitation and insufficient decoupling at high salinities, and time constraints at low salinities. A threshold value of ~0.35 uM SRP was identified as the concentration necessary to induce AP activity. The induction threshold was asymmetrical; AP activity appeared to be induced only when nutrient concentrations were decreasing, creating a temporal chirality in activity. AP activity may be influenced by the magnitude of the SRP removal rate, rather than absolute SRP concentration. AP activity is uniquely positioned as an explicit indicator of the phosphorus requirements of a population. Attempts to define inorganic nutrient stress should routinely include ectoenzyme measurements to account for in situ production of inorganic nutrients. The addition of an index for temporal variability is suggested when using nutrient concentrations, ratios, or ectoenzyme activities to determine nutrient stress.

5.2 Future Work

Many opportunities exist to enhance the work presented in this dissertation. All ectoenzyme work would be improved if cells were enumerated, nutrient uptake rates were available, kinetics curves run on natural waters, and phytoplankton were separated from bacteria. Cell counts would eliminate the uncertainty inherent with fluorescence (packing effects, photobleaching, etc). Uptake rates are necessary to determine production/uptake coupling, indicating how available hydrolyzed polymeric organic matter is to the population as a whole. Ectoenzyme kinetics run in natural water samples would indicate the amount of substrate available (compared to a laboratory reference). It

could validate suspicions of substrate limitation on ectoenzyme activities. Through standardization with a pure enzyme extract, the average quantity of enzymes per unit biomass in a volume of natural water could also be determined. Size fractionation or pigment analysis to separate autotrophs from heterotrophs would highlight the ability of different populations to produce ectoenzymes, which is extremely important in all bulk ectoenzyme assays. These issues are so integral to the function of the microbial ecosystem, any project neglecting these aspects will be inherently limited in scope.

Some determination of nutrient limitation in the Hudson River plume would be useful. The assumption was made that the plume system was primarily nitrate-limited, but no experimental determination was available. There was limited time-series data as part of the Hudson River plume work (Chapter 2). Combining all the necessary instrumentation on one ship to measure salinity, nutrients, biomass, and ectoenzyme activity would simplify the analysis and increase the amount of useful data.

The LAP model (Chapter 3) would be improved if the nitrate requirement were determined by the PON : fluorescence ratio, instead of a nitrate concentration. The list of assumptions required by the current formulation of the model is extensive. Verification of many of the assumptions listed in the model description should be performed before applying the model results to the ecosystem.

The Eularian approach to AP activities was original, especially along the Louisiana shelf. Profiling AP activities with the other environmental variables could be useful. A 3D approach using a towed undulating vehicle connected to EAAS has been done in the Louisiana shelf (Gaas and Chen, in progress). As with the Hudson River, direct experimentation would increase the validity of statements made concerning the

potential for nutrient limitation along the Louisiana shelf. When evaluating the effect of lag on the coefficient of determination, only linear regressions were used. A non-linear (specifically an exponential) formulation for calculating the coefficient of determination would be a useful addition to the linear case already considered. An index of temporal stability in assessing nutrient limitation should be created. With so much importance placed on the nutrient-limited growth of phytoplankton and the role of eutrophication in the Gulf, increasing the robustness of limiting nutrient evaluations appears a valid and worthy goal. The concept of temporal chirality requires more controlled conditions, where advection is removed as a mechanism for changing phosphorus concentration. A simple experiment consisting of AP measurements of a phytoplankton culture going from phosphate replete to depleted and back to replete status should validate or invalidate the temporal chirality hypothesis.

REFERENCES

Ammerman, J. W., and W. B. Glover. 2000. Continuous underway measurement of microbial ectoenzyme activities in aquatic ecosystems. Mar Ecol Prog Ser 201: 1–12.

Ammerman, J.W., Hood, R.R., Case, D.A., and Cotner, J.B. 2003. Phosphorus deficiency in the Atlantic: an emerging paradigm in oceanography. Eos 84(18): 165-167.

Arnosti, C. 2003. Microbial extracellular enzymes and their role in dissolved organic matter cycling, p. 315-342. In S. E. G. Findlay and R. L. Sinsabaugh [eds.], Aquatic ecosystems: Interactivity of dissolved organic matter. Academic Press.

Arnosti, C. 2004. Speed bumps and barricades in the carbon cycle: substrate structural effects on carbon cycling. Mar Chem 92: 263-273.

Ault-Riche, D., Fraley, C.D., Tzeng, C.M., and Kornberg, A. 1998. Novel assay reveals multiple pathways regulating stress-induced accumulations of inorganic polyphosphate in Escherichia coli. J Bacterio 180(7): 1841-1847.

Azam, F., Fenchel, T., Field, J.G., Gray, J.S., Meyer-Reil, L.A., and Thingstad, F. 1983. The ecological role of water-column microbes in the sea. Mar Ecol Prog Ser 10: 257-263.

Azam, F., and Malfatti,F. 2007. Microbial structuring of marine ecosystems. Nature Rev Micro 5: 782-792.

Azam, F., Smith, D.C., Steward, G.F., and Hagstrom, A. 1994. Bacteria-organic-matter coupling and its significance for oceanic carbon cycling. Micro Ecol 28(2): 167-179.

Bano, N., Moran, M.A., and Hodson, R.E. 1998. Photochemical formation of labile organic matter from two components of dissolved organic carbon in a freshwater wetland. Aquat Micro Ecol 16: 95-102.

Beardall, J., Berman, T., Heraud, P., Kadiri, M.O., Light, B.R., Patterson, G., Roberts, S., Sulzberger,B., Sahan, E., Uehlinger, U., and Wood, B. 2001. A comparison of methods for detection of phosphate limitation in microalgae. Aquat Sci 63(1): 107-121.

Benitez-Nelson, C.R., and Buesseler, K.O. 1999. Variability of inorganic and organic phosphorus turnover rates in the coastal ocean. Nature 389: 502-505.

Berman, T., Bechemin, C., and Maestrini, S.Y. 1999. Release of ammonium and urea from dissolved organic nitrogen in aquatic ecosystems. Aquat Micro Ecol 16: 295-302.

Bochdansky, A.B., Puskaric, S., and Herndl, G.J. 1995. Influence of zooplankton grazing on free dissolved enzymes in the sea. Mar Ecol Prog Ser 121: 53-63.

Breed, G.A., Jackson, G.A., and Richardson, T.L. 2004. Sedimentation, carbon export and food web structure in the Mississippi River plume described by inverse analysis. Mar Ecol Prog Ser 278: 35-51.

Bronk, D. 2002. Dynamics of DON. In: Hansell, D., Carlson, C. (Eds.), Biogeochemistry of Marine Dissolved Organic Matter. Academic Press, San Diego, pp. 153-247.

Bronk, D.A., See, J.H., Bradley, P., and Killberg, L. 2007. DON as a source of bioavailable nitrogen for phytoplankton. Biogeosci 4: 283-296.

Cao, X., Song, C., and Zhou, Y. 2010. Limitations of using extracellular alkaline phosphatase activities as a general indicator for describing P deficiency of phytoplankton in Chinese shallow lakes. J Appl Phycol 22: 33-41.

Chang, S.I., and Reinfelder, J.R. 2002. Relative importance of dissolved versus trophic bioaccumulation of copper in marine copepods. Mar Ecol Prog Ser 231: 179-186.

Chant, R. J., Glenn, S. M., Hunter, E., Kohut, J., Chen, R. F., Houghton, R. W. , Bosch, J., Schofield, O. 2008. Bulge Formation of a Buoyant River Outflow. J Geophy Res 113: C01017, doi:10.1029/2007JC004100.

Chant, R.J., Wilkin, J., Zhang, W., Choi, B-J., Hunter, E., Castelao, R., Glenn, S., Jurisa, J., Schofield, O., Houghton, R., Kohut, J., Frazer, T., and Moline, M. 2008(b). Disperal of the Hudson River plume on the New York Bight. Oceanogr 21 (4): 148-161.

Chen, R.F., Bissett, P., Coble, P., Conmy, R., Gardner, G.B., Moran, M.A., Wang, X., Wells, M.L., Whelan, P., and Zepp, R.G. 2004. Chromophoric dissolved organic matter (CDOM) source characterization in the Louisiana Bight. Mar Chem 89: 257-272.

Chen, R.F., and Gardner, G.B. 2004. High-resolution measurements of chromophoric dissolved organic matter in the Mississippi and Atchafalaya River plume regions. Mar Chem 89: 103-125.

Chen, X., Lohrenz, S.E., and Wiesenburg, D.A. 2000. Distribution and controlling mechanisms of primary production on the Louisiana-Texas continental shelf. J. Mar Syst 25: 179-207.

Chen, Y., and J. Ruzicka. 2004. Accelerated micro-sequential injection in lab-on-valve format, applied to enzymatic assays. Analyst 129: 597–601.

Christian, J. R., and D. M. Karl. 1995. Bacterial ectoenzymes in marine waters: activity ratios and temperature responses in three oceanographic provinces. Limnol Ocean 40: 1042–1049.

Chrost, J.R. 1991. Environmental control of synthesis and activity of aquatic microbial ectoenzymes, p. 29-59. In R. J. Chrost [ed.], Microbial enzymes in aquatic environments. Springer-Verlag.

Chrost, R.J., and Overbeck, J. 1987. Kinetics of alkaline phosphatase activity and phosphorus availability for phytoplankton and bacterioplankton in Lake Plubsee (north German eutrophic lake). Micro Ecol 13: 229-248.

Chrost, R.J. and Rai, H. 1993. Ectoenzyme activity and bacterial secondary production in nutrient-impoverished and nutrient-enriched fresh-water mesocosms. Micro Ecol 25(2): 131-150.

Chrost, R.J., and Siuda, W. 2002. Ecology of Microbial Enzymes in Lake Ecosystems, p. 35-72. In R. G. a. D. Burns, R.P. [ed.], Enzymes in the Environment. Marcel Dekker, Inc.

Chrost, R.J. and Siuda, W. 2006. Microbial production, utilization, and enzymatic degradation of organic matter in the upper trophogenic layer in the pelagial zone of lakes along a eutrophication gradient. Limnol Ocean 51: 749-762.

Cole, J.J. 1982. Interactions between bacteria and algae in aquatic ecosystems. Ann Rev Ecol Syst 13: 291-31.

Cole, J.J., Findlay, S., and Pace, M.L. 1988. Bacterial production in fresh and saltwater ecosystems- a cross-system overview. Mar Ecol Prog Ser 43: 1-10.

Cullen JJ, Yang X, MacIntyre HL. 1992. Nutrient limitation of marine photosynthesis. In: Falkowski PG, Woodhead AD (eds) Primary Production and Biogeochemical Cycles in the Sea. Plenum Press, New York.

Cunha, A., and Almeida, A. 2009. Inorganic nutrient regulation of bacterioplankton heterotrophic activity in an estuarine system (Ria de Aveiro, Portigal). Hydrobio 628: 81-93.

Cunha, M.A., Almeida, M.A., and Alcantara, F. 2001. Short-term responses of the natural planktonic bacterial community to the changing water properties in an estuarine environment: Ectoenzymatic activity, glucose incorporation, and biomass production. Micro Ecol 42(1): 69-79.

D'Elia, C. F., Sanders, J G , and Boynton, W. R. 1986. Nutrient enrichment studies in a coastal plain estuary: phytoplankton growth in large-scale, continuous culture. Can J Fish Aquat Sci 43: 397-406.

DiMarco, S.F. and Reid, R.O. 1998. Characterization of the principle tidal current constituents on the Texas-Louisiana shelf. J Geophy Res 103(C2): 3093-3109.

Donachie, S.P., Christian, J.R., and Karl, D.M. 2001. Nutrient regulation of bacterial production and ectoenzyme activities in the subtropical North Pacific Ocean. Deep-Sea Res II 48(8-9): 1719-1732.

Donner, S.D., and Scavia, D. 2007. How climate controls the flux of nitrogen by the Mississippi River and the development of hypoxia in the Gulf of Mexico. Limnol Ocean 52(2): 856-861.

Dortch, Q., and Whitledge, T.E. 1992. Does nitrogen or silicon limit phytoplankton production in the Mississippi River plume and nearby regions? Cont Shelf Res 12(11): 1293-1309.

Dyhrman, S.T., and Palenik, B. 2003. Characterization of ectoenzyme activity and phosphate-regulated proteins in the coccolithophorid Emilianaia huxleyi. J. Plank. Res. 25(10): 1215-1225.

Dyhrman, S.T., and Ruttenberg, K.C. 2006. Presence and regulation of alkaline phosphatase activity in eukaryotic phytoplankton from the coastal ocean: implications for dissolved organic phosphorus remineralization. Limnol Ocean 51(3): 1381-1390.

Eldridge, P.M., and Roelke, D.L. 2010. Origins and scales of hypoxia on the Louisiana shelf: importance of seasonal plankton dynamics and river nutrients and discharge. Ecol Model 221(7): 1028-1042.

Espeland, E.M., and Wetzel, R.G. 2001. Complexation, stabilization, and UV photolysis of extracellular and surface-bound glucosidase and alkaline phosphatase: implications for biofilm microbiota. Microb Ecol 42: 572-585.

Fong, DA, Geyer, W.R. 2002. The alongshore transport of freshwater in a surface trapped river plume. J Phys Ocean 32: 957-972.

Foreman, C.M., Franchini, P., and Sinsabaugh, R.L. 1998. The trophic dynamics of riverine bacterioplankton: Relationships among substrate availability, ectoenzyme kinetics, and growth. Limnol Ocean 43(6):1344-1352.

Fuhrman, J.A., Ammerman, J.W., and Azam, F. 1980. Bacterioplankton in the coastal euphotic zone: distribution, activity and possible relationships with phytoplankton. Mar Bio 60: 201-207.

Fukuda, R., Sohrin, Y., Saotome, N., Fukuda, H., Nagata, T., and Koike, I. 2000. East

west gradient in ectoenzyme activities in the subarctic Pacific: possible regulation by zinc. Limnol Ocean 45(4): 930-939.

Gaas, B.M., and Ammerman, J.W. 2007. Automated high resolution ectoenzyme measurements: instrument development and deployment in three trophic regimes. Limnol Ocean Meth 5: 463-473.

Gao, G., Zhu, G.W., Qin, B.Q., Chen, J., and Wang, K. 2006. Alkaline phosphatase activity and the phosphorus mineralization rate of Lake Taihu. Science China Ser D- Earth Sci 49: 176-185.

Garde, K., and Gustavson, K. 1999. The impact of UV-B radiation on alkaline phosphatase activity in phosphorus-depleted marine ecosystems. J Exp Mar Bio Ecol 238(1): 93-105.

Goebel, N.L., and Wing, S.R., and Boyd, P.W. 2005. A mechanism for onset of diatom blooms in a fjord with persistent salinity stratification. Estuar Coast Shelf Sci 64: 546-560.

Green, R.E., Breed, G.A., Dagg, M.J., and Lohrenz, S.E. 2008. Modeling the response of primary production and sedimentation to variable nitrate loading in the Mississippi River plume. Cont Shelf Res 28: 1451-1465.

Gruber, D.F., Simjouw, J-P., Seitzinger, S.P., and Taghon, G.L. 2006. Dynamics and characterization of refractory dissolved organic matter produced by a pure bacterial culture in an experimental predator-prey system. App Envir Micro 72(6): 4184-4191.

Grunwald, M., Dellwig, O., Liebezeit, G., Schnetger, B., Reuter, R., and Brumsack, H.J. 2007. A novel time-series station in the Wadden Sea (NW Germany): first results on continuous nutrient and methane measurements. Mar Chem 107(3): 411-421.

Hetland, R.D., and DiMarco, S.F. 2008. How does the character of oxygen demand control the structure of hypoxia on the Texas-Louisiana continental shelf? J Mar Sys 70: 49-62.

Hitchcock, G.L., Wiseman, W.J., Boicourt, W.C., Mariano, A.J., Walker, N., Nelsen, T.A., and Ryan, E. 1997. Property fields in an effluent plume of the Mississippi River. J Mar Sys 12: 109-126.

Hoppe, H-G. 1983. Significance of exoenzymatic activities in the ecology of brackish water: measurements by means of methylumbelliferyl-substrates. Mar Ecol Prog Ser 11: 299-308.

Hoppe, H-G. 1993. Use of fluorogenic model substrates for extracellular enzyme activity

(EEA) measurement of bacteria, p. 423-431. In P. F. Kemp, B. F. Sherr, E. B. Sherr and J. J. Cole [eds.], Handbook of methods in aquatic microbial ecology. Lewis Publishers.

Hoppe, H-G. 2003. Phosphatase activity in the sea. Hydrobio 493: 187-200.

Hoppe, H-G, Kim SJ, Gocke K. 1988. Microbial decomposition in aquatic environments: combined process of extracellular enzyme activity and substrate uptake. Appl Environ Microbio 54: 784–790.

Hoover, R.S., Hoover., D., Miller, M., Landry, M.R., DeCarlo, E.H., and Mackenzie, F.T. 2006. Zooplankton response to storm runoff in a tropical estuary: bottom-up and top-down controls. Mar Ecol Prog Ser 318: 187-201.

Houghton, R.W., Chant, R., Rice, A., and Tilburg, C. 2008. Salt flux into coastal river plumes: dye studies in the Delaware and Hudson River outflow. In prep.

Huston, A.L. and Deming, J.W. 2002. Relationships between microbial extracellular enzymatic activity and suspended and sinking particulate organic matter: seasonal transformations in the North Water. Deep-Sea Res II 49(22-23): 5211-5225.

Inoue, M., and Wiseman, W.J. Jr. 2000. Transport, mixing and stirring processes in a Louisiana estuary: a model study. Estuar Coast Shelf Sci 50: 449-466.

Jaeger, S.A., Gaas, B.M., Klinkhammer, G.P., and Ammerman, J.W. 2009. Multiple Enzyme Analyzer (MEA): Steps toward the in situ detection of microbial community ectoenzyme activities. Limnol Ocean: Method 7: 716-729.

Jauzein, C., Collos, Y., Garces, E., Vila, M., and Maso, M. 2008. Short-term temporal variability of ammonium and urea uptake by Alexandrium catenella (Dinophyta) in cultures. J Phyco 44(5): 1136-1145.

Jorgensen, N.O.G., Kroer, N., and Coffin, R.B. 1999. Relations between bacterial nitrogen metabolism and growth efficiency in an estuarine and an open-water ecosystem. Aquat Micro Ecol 18(3): 247-261.

Karner, M., Ferrierpages, C., and Rassoulzadegan, F. 1994. Phagotrophic nanoflagellates contribute to occurrence of alpha-glucosidase and aminopeptidase in marine environments. Mar Ecol Prog Ser 114(3): 237-244.

Kirchman, D.L., Dittel, A.I., and Findlay, S.E.G. 2004. Changes in bacterial activity and community structure in response to dissolved organic matter in the Hudson River, New York. Aquat Micro Ecol 35(3): 243-257.

Kisand, V. and Tammert, H. 2000. Bacterioplankton stategies for leucine and glucose

uptake after a cyanobacterial bloom in an eutrophic shallow lake. Soil Bio Biochem 32: 1965-1972.

Kudela, R.M., and Dugdale, R.C. 2000. Nutrient regulation of phytoplankton productivity in Monterey Bay, California. Deep-Sea Res II 47: 1023-1053.

Kudela, R.M., and Peterson, T.D. 2009. Influence of a buoyant river plume on phytoplankton nutrient dynamics: what controls standing stocks and productivity? J Geophy Res 114: C00B11.

Liebig J. 1885. Die Grundsatze der Agricultur-Chemie mit Rucksicht auf die in England angestelten Untersuchungen., Vol. F. Vieweg und Sohn, Braunschwieg.

Llewellyn, C.A., Tarran, G.A., Galliene, C.P., Cummings, D.G., de Menezes, A., Rees, A.P., Dixon, J.L., Widdicombe, C.E., Fileman, E., and Wilson, W.H. 2008. Microbial dynamics during the decline of a spring diatom bloom in the northeast Atlantic. J Plank Res 30(3): 261-273.

Lohrenz, S.E., Fahnenstiel, G.L., Redalje, D.G., Lang, G.A., Dagg, M.J., Whitledge, T.E., Dortch, Q. 1999. Nutrients, irradiance, and mixing as factors regulating primary production in coastal waters impacted by the Mississippi River plume. Cont Shelf Res 19(9): 1113-1141.

Lohrenz, S.E., Wiesenburg, D.A., Rein, C.R., Arnone, R.A., Taylor, C.D., Knauer, G.A., and Knap, A.H. 1992. A comparison of in situ and simulated in situ methods for estimating oceanic primary production. J Plank Res 14(2): 201-221.

Lomas, M.W., Swain, A., Shelton, R., and Ammerman, J.W. 2004. Taxonomic variability of phosphorus stress in Sargasso Sea phytoplankton. Limnol Ocean 49(6): 2303-2310.

Lui, G.C.S., Li, W.K., Leung, K.M.Y., Lee, J.H.W., and Jayawardena, A.W. 2007. Modeling algal blooms using vector autoregressive model with exogenous variables and long memory filter. Ecol Model 200: 130-138.

Maguer, J. L., Helguen, S., Madec, C., Labry, C., and Le Corre, P. 2007. Nitrogen uptake and assimilation kinetics in Alexandrium minutum (Dynophyceae): effect of N-limited growth rate on nitrate and ammonium interactions. J. Phycol 43(2): 295-303.

Malone, T.C., and M.B. Chervin. 1979. The production and fate of phytoplankton size fractions in the plume of the Hudson River New-York Bight. Limnol and Ocean 24: 683–696.

Malone, T.C., Falkowski, P.G., Hopkins, T.S., Rowe, G.T., and Whitledge, T.E. 1983.

Mesoscale response of diatom populations to a wind event in the plume of the Hudson River. Deep-Sea Res 30(2A): 149-170.

Martinez, J. and Azam, F. 1993. Aminopeptidase activity in marine chroococcoid cyanobacteria. App Env Micro 59(11): 3701-3707.

Martinez, J. and Azam, F. 1993b. Periplasmic aminopeptidase and alkaline phosphatase activities in a marine bacterium: implications for substrate processing in the sea. Mar Ecol Prog Ser 92: 89-97.

Martinez, J., Smith, D.C., Steward, G.F., and Azam, F. 1996. Variability in ectohydrolytic enzyme activities of pelagic marine bacteria and its significance for substrate processing in the sea. Aquat Micro Ecol 10: 223-230.

Marx, M.C., Wood, M., and Jarvis, S.C. et al. 2001. A microplate fluorimetric assay for the study of enzyme diversity in soils. Soil Bio Biochem 33(12-13): 1633-1640.

Mason, R.P., Reinfelder, J.R., and Morel, F.M.M. 1996. Uptake, toxicity, and trophic transfer of mercury in a coastal diatom. Environ Sci Tech 30: 1835-1845.

Mercado, J.M., Ramirez, T., Cortez, D., Sebastian, M., Liger, E., and Bautista, B. Partitioning the effects of changes in nitrate availability and phytoplankton community structure on relative nitrate uptake. Mar Ecol Prog Ser 359: 51-68.

Meseck, S.L., and Alix, J.H., Wikfors, G.H., and Ward, J.E. 2009. Differences in the soluble, residual phosphate concentrations at which coastal phytoplankton species up-regulate alkaline-phosphatase expression, as measured by flow-cytometric detection of ELF-97 fluorescence. Estuar Coasts 32: 1195-1204.

Meyer-Reil, L-A,. Bolter, M., Liebezeit, G., and Schramm, W. 1979. Short-term variations in microbiological and chemical parameters. Mar Ecol Prog Ser 1: 1979.

Minor, E.C., Dalzell, B.J., Stubbins, A., and Mopper, K. Evaluating the photoalteration of estuarine dissolved organic matter using direct temperature-resolved mass spectrometry and UV-visible spectroscopy. Aquat Sci 69: 440-455.

Moline, M.A., Frazer, T.K., Chant, R., Glenn, S., Jacoby, C.A., Reinfelder, J.R., Yost, J., Zhou, M., and Schofield, O.M.E. 2008. Biological Responses in a Dynamic Buoyant River Plume. Oceanogr. 21(4): 70-78.

Moreno-Ostos, E., Cruz-Pizarro, L., Basanta, A., and George, D.G. 2009. Spatial heterogeneity of cyanobacteria and diatoms in a thermally stratified canyon-shaped reservoir. Intern Rev Hydrobio 94(3): 245-257.

Mulholland, M.R., Gobler, C.J., and Lee, C. 2002. Peptide hydrolysis, amino acid

oxidation, and nitrogen uptake in communities seasonally dominated by Aureococcus anophagefferens. Limnol Ocean 47(4): 1094–1108.

Mulholland, M.R., Lee, C., and Glibert, P.M. 2003. Extracellular enzyme activity and uptake of carbon and nitrogen along an estuarine salinity and nutrient gradient. Mar Ecol Prog Ser 258: 3-17.

Nausch, M. 1998. Alkaline phosphatase activities and the relatioinship to inorganic phosphate in the Pomeranian Bight (southern Baltic Sea). Aquat Microb Ecol 16(1): 87-94.

Nausch, M., and Nausch, G. 2000. Stimulation of peptidase activity in nutrient gradients in the Baltic Sea. Soil Bio Biochem 32(13): 1973-1983.

Nausch, M., Pollehne, F., and Kerstan, E. 1998. Extracellular enzyme activities in relation to hydrodynamics in the Pomeranian Bight (southern Baltic Sea). Micro Eco 36: 251-258.

Perry, M. J. 1972. Alkaline phosphatase activity in subtropical Central North Pacific waters using a sensitive fluorometric method. Mar Biol 15: 113-119.

Putland, J.N., Whitney, F.A., and Crawford, D.W. 2004. Survey of bottom-up controls of Emiliania huxleyi in the Northeast Subarctic Pacific. Deep-Sea Res I-Ocean Res Papers 51(12): 1793-1802.

Rabalais, N.N., Wiseman, W.J., and Turner, R.E. 1994. Comparison of continuous records of near-bottom dissolved oxygen from the hypoxia zone along the Louisiana coast. Estuaries 17(4): 850-861.

Ranhofer, M.L., Lawrenz, E., Pinckney, J.L., Benitez-Nelson, C.R., and Richardson, T.L. 2009. Cell-specific alkaline phosphatase expression by phytoplankton from Winyah Bay, South Carolina, USA. Estuar Coast 32(5): 943-957.

Ruzicka, J. 2000. Flow Injection: From Beaker to Microfluidics. Anal Chem 72: 212A 217A.

Salerno, M. and Stoecker, D.K. 2009. Ectocellular glucosidase and peptidase activity of the mixotrophic dinoflagellate Procentrum minimum (dinophyceae). J Phyco 45(1): 34-45.

Sebastian, M., J. Aristegui, M. F. Montero, J. Escanez, and F. X. Niell. 2004. Alkaline phosphatase activity and its relationship to inorganic phosphorus in the transition zone of the North-western African upwelling system. Prog Ocean 62: 131–150.

Seitzinger, S.P., and Sanders, R.W. 1997. Contribution of dissolved organic nitrogen from rivers to estuarine eutrophication. Mar Ecol Prog Ser 159: 1-12.

Siuda, W., and Chrost, RJ. 2001. Utilization of selected dissolved organic phosphorus compounds by bacteria in lake water under non-limiting orthophosphate conditions. Pol Jour Env Studies 10 (6): 475-483.

Smith, S.M. and Hitchcock, G.I. 1994. Nutrient enrichments and phytoplankton growth in the surface waters of the Louisiana Bight. Estuar 17(4): 740-753.

Song, C., Cao, X., Li, J., Li, Q., Chen, G., Zhou, Y. 2006. Contributions of phosphatase and microbial activity to internal phosphorus loading and their relation to lake eutrophication. Sci China Ser D-Earth Sci 49(s1): 102-113.

Stepanauskas, R., H. Edling, and L. J. Tranvik. 1999. Differential dissolved organic nitrogen availability and bacterial aminopeptidase activity in limnic and marine waters. Microb Ecol 38:264–272.

Strojsova, A., and Dyhrman, S. 2008. Cell-specific beta-N-acetylglucosaminidase activity in cultures and field populations of eukaryotic marine phytoplankton. FEMS Micro Ecol 64(3): 351-361.

Strojsova, A., Nedoma, J., Strojsova, M., Cao, X., and Vrba, J. 2008. The role of cell surface-bound phosphatases in species competition within natural phytoplankton assemblage: an in situ experiment. J. Limnol 67(2) 128-138.

Strojsova, A., and Vrba, J. 2007. Short-term variation in extracellular phosphatase activity: possible limitations for diagnosis of nutrient status in particular algal populations. Aquat Ecol 43: 19-25.

Sunda, W.G., and Hardison, D.R. 2007. Ammonium uptake and growth limitation in marine phytoplankton. Limnol Ocean 52(6): 2496-2506.

Sylvan, J.B. 2008. Assessing multiple indicators of nutrient limitation in marine phytoplankton on the Louisiana continental shelf. Ph.D. dissertation. Rutgers University, New Brunswick, New Jersey.181 pgs.

Sylvan, J.B., Dortch, Q., Nelson, D.M., Brown, A.F.M., Morrison, W., and Ammerman, J.W. 2006. Phosphorus limits phytoplankton growth on the Louisiana shelf during the period of hypoxia formation. Environ Sci Technol 40: 7548-7553.

Tanaka, T., and Henriksen, P., Lignell, R., Olli, K., Seppala, J., Tamminen, T., and Thingstad, T.F. 2006. Specific affinity for phosphate uptake and specific alkaline phosphatase activity as diagnostic tools for detecting phosphorus-limited phytoplankton and bacteria. Estuar Coasts 29(6): 1226-1241.

Taylor, G.T., Way, J., Yu, Y., and Scranton, M.I. 2003. Ectohydrolase activity in surface

waters of the Hudson River and eastern Long Island Sound estuaries. Mar Ecol Prog Ser 263: 1-15.

Thompson, A.J., and Sinsabaugh, R.L. 2000. Matric and particulate phosphatase and aminopeptidase activity in limnetic biofilms. Aquat Micro Ecol 21: 151-159.

Torriani-Gorini A. 1994. Introduction: the pho regulon of *Escherichia coli*. In: Torriani-Gorini A, Yagil, E & S Silver (ed) Phosphate in Microorganisms: Cellular and Molecular Biology. ASM Press, Washington DC, p 1-4.

Van Wambeke, F., Goutx, M., Striby, L., Sempere, R., and Vidussi, F. 2001. Bacterial dynamics during the transition from spring bloom to oligotrophy in the northwestern Mediterranean Sea: relationships with particulate detritus and dissolved organic matter. Mar Ecol Prog Ser 212: 89-105.

Vershinina, O.A., and Znamenskaya, L.V. 2002. The Pho regulons of bacteria. Microbiol 71(5): 497-511.

Walker, N.D., Wiseman, W.J., Rouse, L.J. Jr. and Babin, A. 2005. Effects of river discharge, wind stress, and slope eddies on circulation and the satellite-observed structure of the Mississippi River plume. J Coast Res 21(6): 1228-1244.

Wang, W-X., Reinfelder, J.R., Lee, B-G., and Fisher, N.S. 1996. Assimilation and regeneration of trace elements by marine copepods. Limnol Ocean 41(1): 70-81.

Williams, C.J., and Jochem, F.J. 2006. Ectoenzyme kinetics in Florida Bay: Implications for bacterial carbon source and nutrient status. Hydrobio 569: 113-127.

Yin, K., Goldblatt, R.H., Harrison, P.J., St. John, M.A., Clifford, P.J., and Beamish, R.J. 1997. Importance of wind and river discharge in influencing nutrient dynamics and phytoplankton production in summer in the central Strait of Georgia. Mar Ecol Prog Ser 161(2): 173-183.

Zhang, W., Wilkin, J., and Schofield, O. 2010. Simulation of water age and residence time in New York Bight. J Phys Ocean doi: 10.1175/2009JPO4249.1.

APPENDIX OF TABLES

Values and ranges of time-series and contour stations

	DIN	SRP	DIN : SRP	AP activity	SRP turn-over time	Salinity
(units)	(uM)	(uM)	(unitless)	(nmol L^{-1} hr^{-1})	(min)	(unitless)
2A	30-50 [24]	0-0.03 [0.03]	1024-2048 [876]	100-250 [--]	27	15-20 [--]
1B	0-30 [5]	0-0.03 [0.02]	0-256 [272]	100-250 [--]	83	30-40 [--]
TS1	27-76 (45)	0.18-1.1 (0.41)	52-240 (125)	0-340 (71)	--	13-20 (17)
TS2	4-8 (5)	0.18-0.33) (0.25)	11-25 (16)	1-444) (307)	--	30-33 (31)

Table 4.1 SRP is soluble reactive phosphorus, considered equivalent to phosphate concentration. DIN is total dissolved inorganic nitrogen, which is the sum of nitrate, nitrite, and ammonium. Stations 2A and 1B (the “contour stations”) are derived from the contour and nutrient addition data from Sylvan et al (2006). Stations TS1 and TS2 are the time-series stations from this work. The range of values are the appropriate contour interval (Sylvan et al) or the range of surface values from the time-series. Numbers in parenthesis are the mean values for the variables. Numbers in brackets are the measured values from Sylvan et al (2006). (--) indicates the values are not available for that station.

Approximate nutrient fluxes for the Mississippi River

Variables	March 2001	May 2001	March 2007
Flow rate ($m^3 s^{-1}$)	28,000	14,500	15,900
NO_3 +NO_2 (uM)	2.84	4.19	3.34
PO_4 (uM)	0.06	0.08	0.07
~DOP (MT)	18600	8490	8920

Table 4.2 The dates include the two months considered in Sylvan et al (2006) – March and May 2001— and the time-series data from this chapter (March 2007). Original data is based on the LOADEST AMLE predicted load and was derived from metric tons of the nutrient. DOP was not converted into micromolar units since an average molecular weight is not available. Data is from the U.S. Geological Survey (http://toxics.usgs.gov/hypoxia/mississippi/flux_ests/delivery/index.html).

APPENDIX OF FIGURES

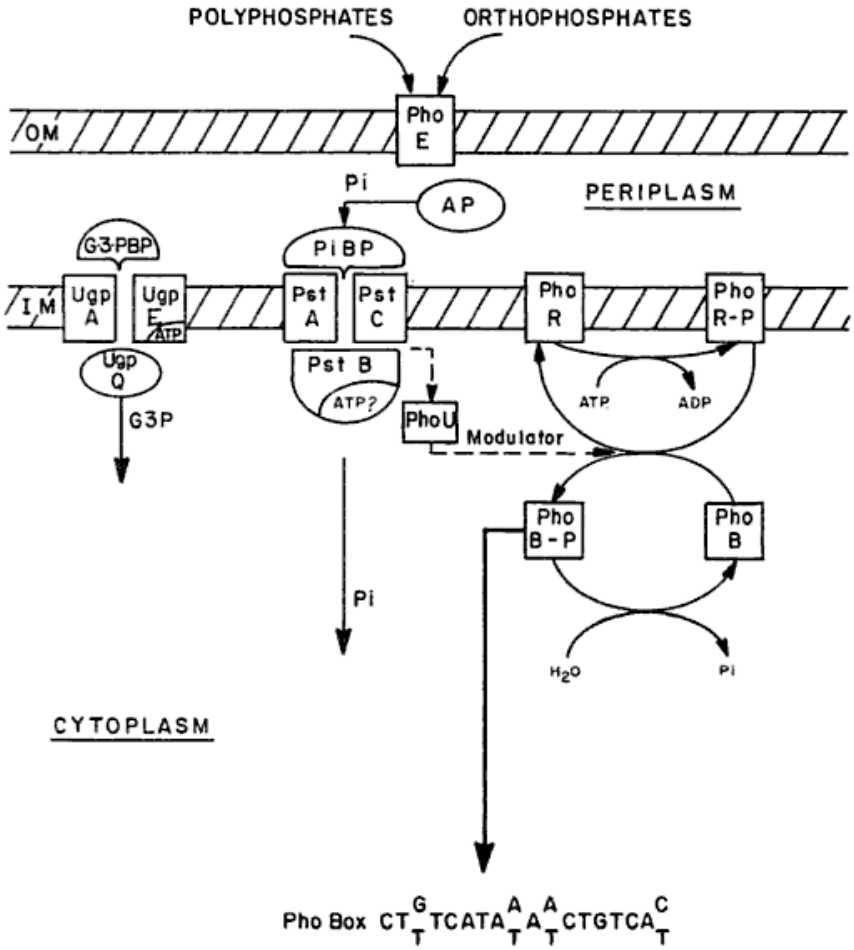

Figure 1.1 *pho* regulon of E. coli. The two component system is defined by the phosphorolation of *pho*R and *pho*B. The product of *pho*A produces alkaline phosphatase (AP). From Toriani-Gorini (1994).

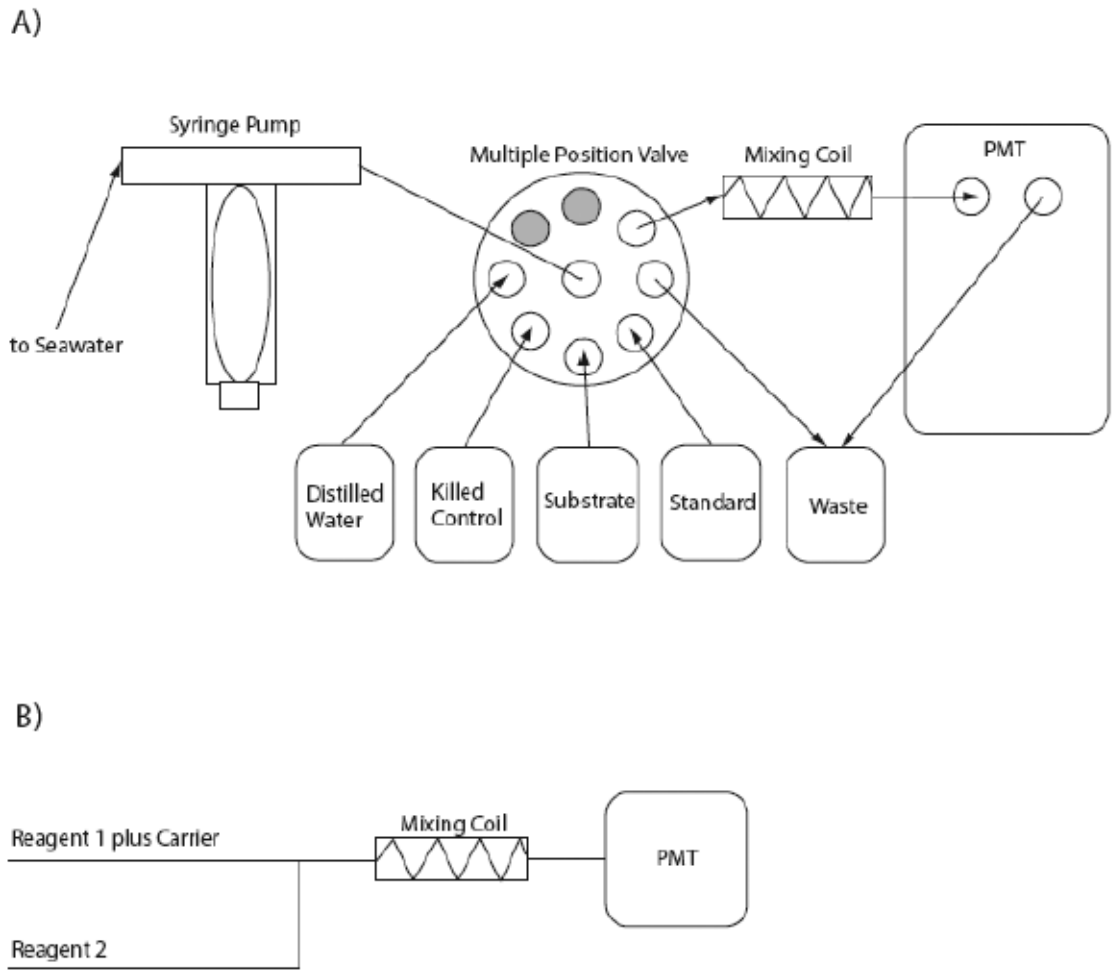

Figure 1.2 Schematic of EAAS plumbing. A) Schematic of fluid flow. The direction of the arrows represents the direction of fluid flow during normal sampling. The line connecting the syringe pump to the multiple position valve accepts fluids in both directions, depending on whether EAAS is aspirating reagents toward the syringe or pushing fluid toward the detector. Grey ports in multiple position valve were not used.
B) Fluid wiring diagram. The following analytes are created by switching Reagent 1 (R1) and Reagent 2 (R2): standard curve (R1 = distilled water, R2 = standard), substrate baseline (R1 = distilled water, R2 = substrate), sample (R1 = seawater, R2 = substrate), killed control (R1 = killed control, R2 = substrate), internal standard (R1 = seawater, R2 = standard). From Gaas and Ammerman (2007).

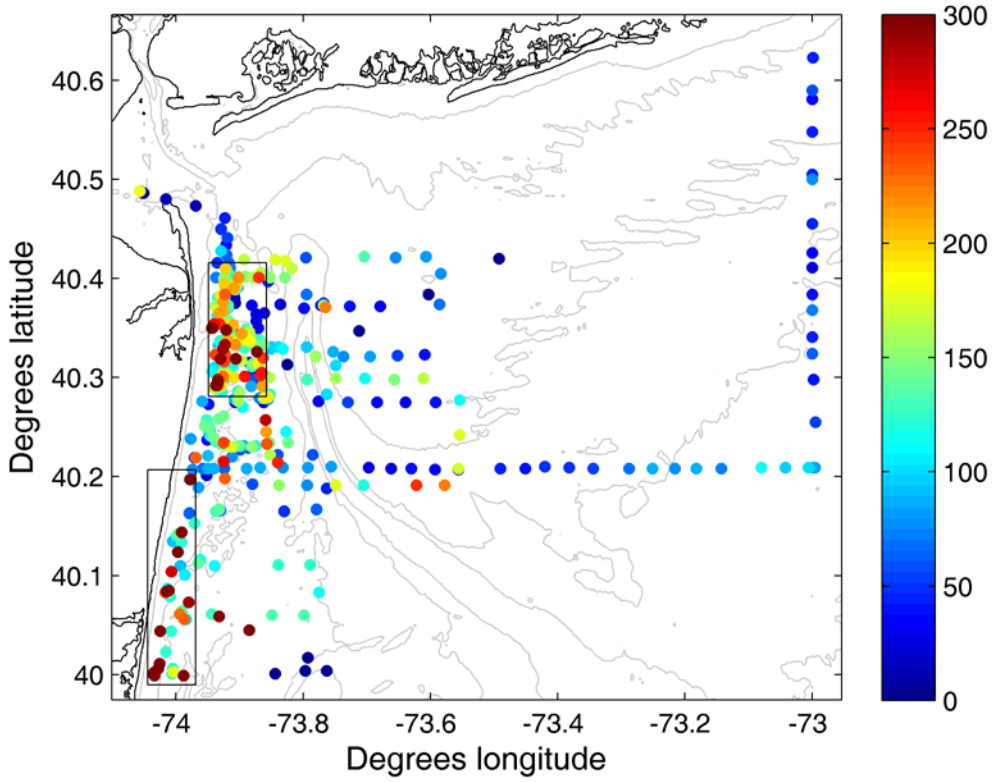

Figure 2.1 Spatial distribution of LAP activity. The left coastline is New Jersey, and the Hudson River exits onto the shelf from the northwest corner. Light grey lines off-shore are isobaths in 10m depth increments. Colored dots are locations and magnitudes of LAP activity measurements as made by EAAS. Color scale is in units of nmol L^{-1} hr^{-1}. Upper black rectangle marks the bulge, and the lower rectangle identifies the points within the coastal current.

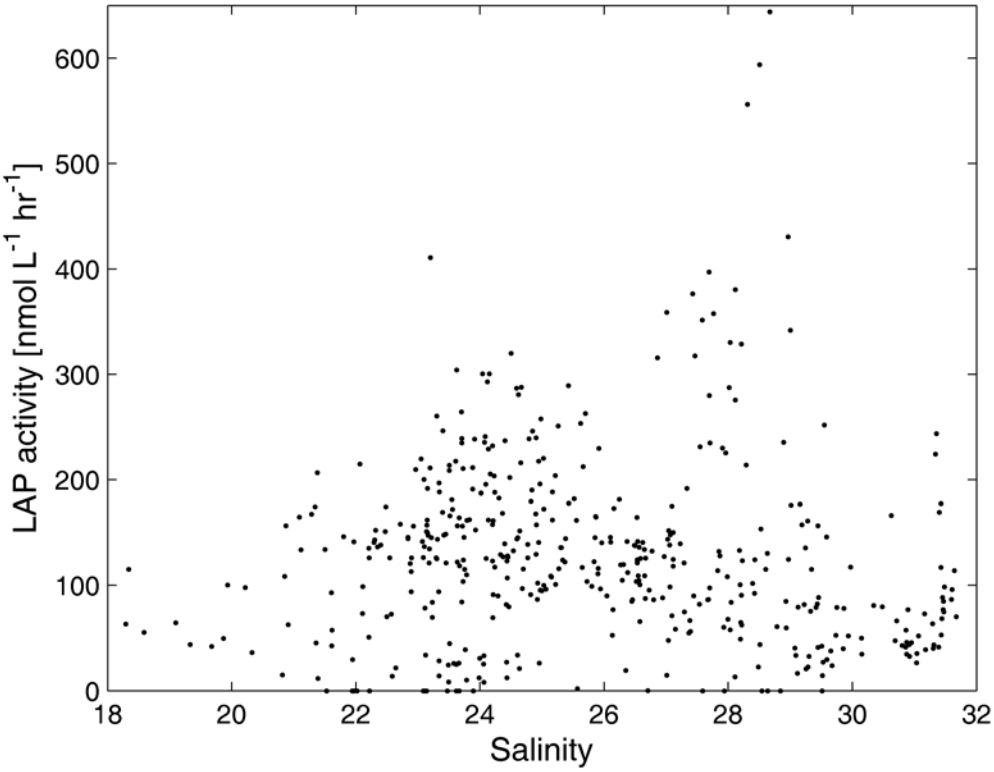

Figure 2.2 LAP activity distribution. Two major peaks are identified at salinities 24.5 and 28.5. The first peak is associated with the bulge, and the second with the coastal current.

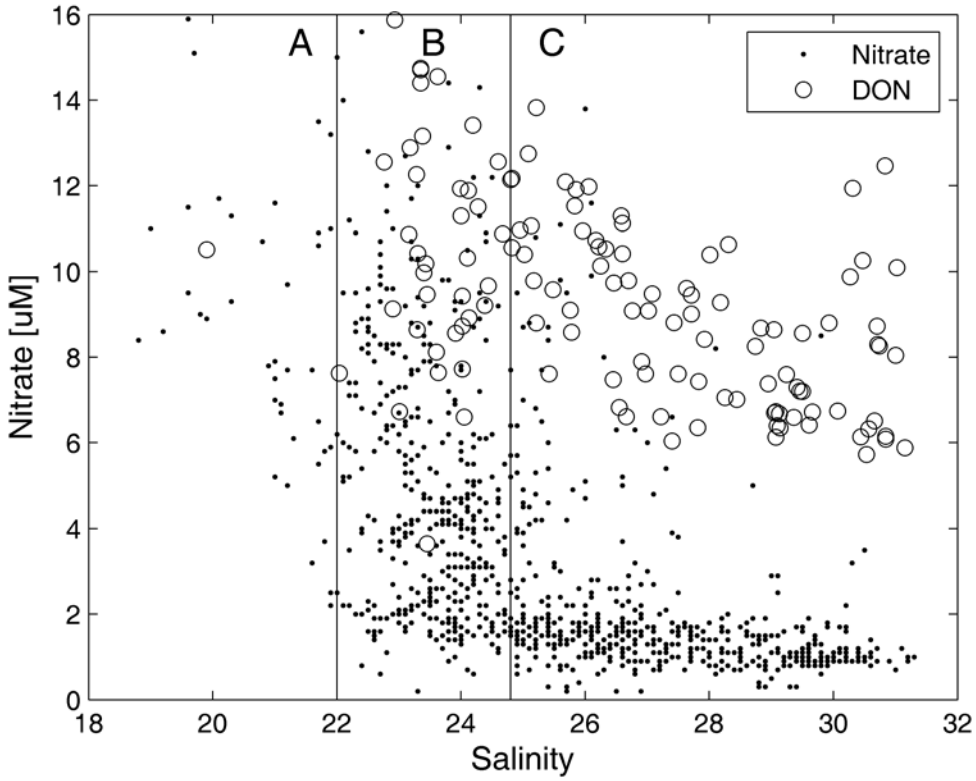

Figure 2.3 Nitrogen distribution. Black points are nitrate measurements, and the open circles are predicted dissolved organic nitrogen (DON). DON is predicted as the difference between measured total nitrogen and measured nitrate. Nitrate concentrations in section 'A' are presumed to be renewed by river input. Nitrate decreases strongly in Section 'B' from uptake, and decreases less quickly in Section 'C' as dilution becomes an increasingly important. The nitrate B/C boundary matches the salinity of the first LAP activity peak.

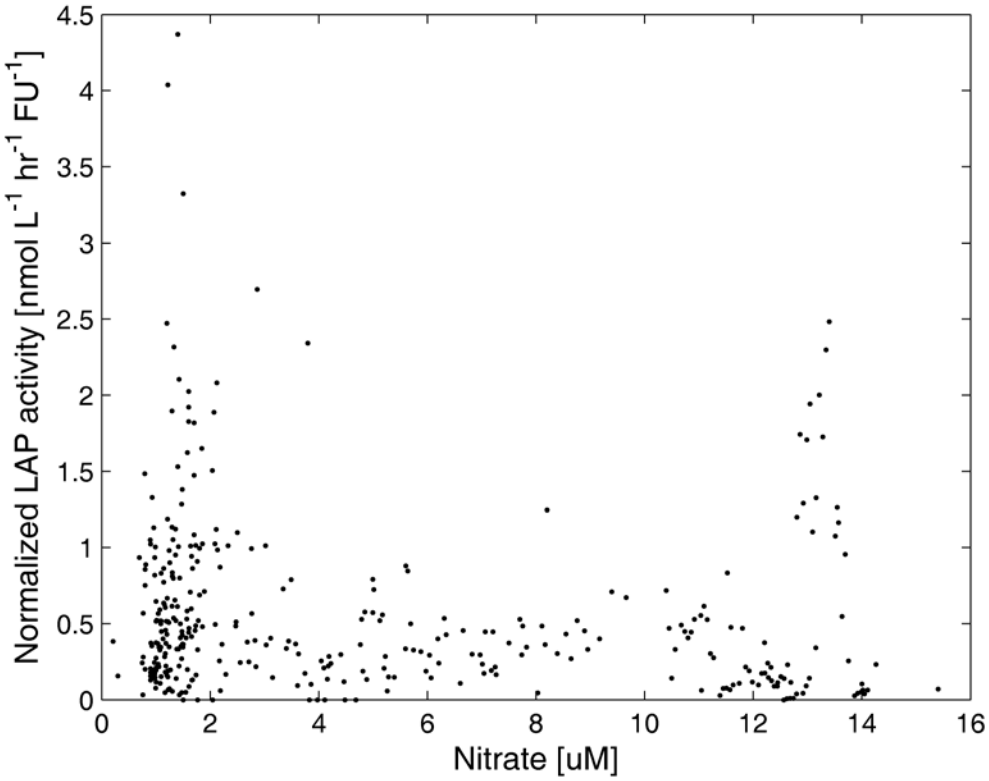

Figure 2.4 LAP and nitrate. LAP activity is normalized by fluorescence (in fluorescence units, FU) to highlight the activity due to nutrient stress. The shape is similar to an induction curve, where activity is low in the presence of high nutrient concentrations, and increases sharply when nutrients are below a certain threshold. Non-normalized activity has a similar distribution though with higher relative LAP activities in the mid-nitrate range.

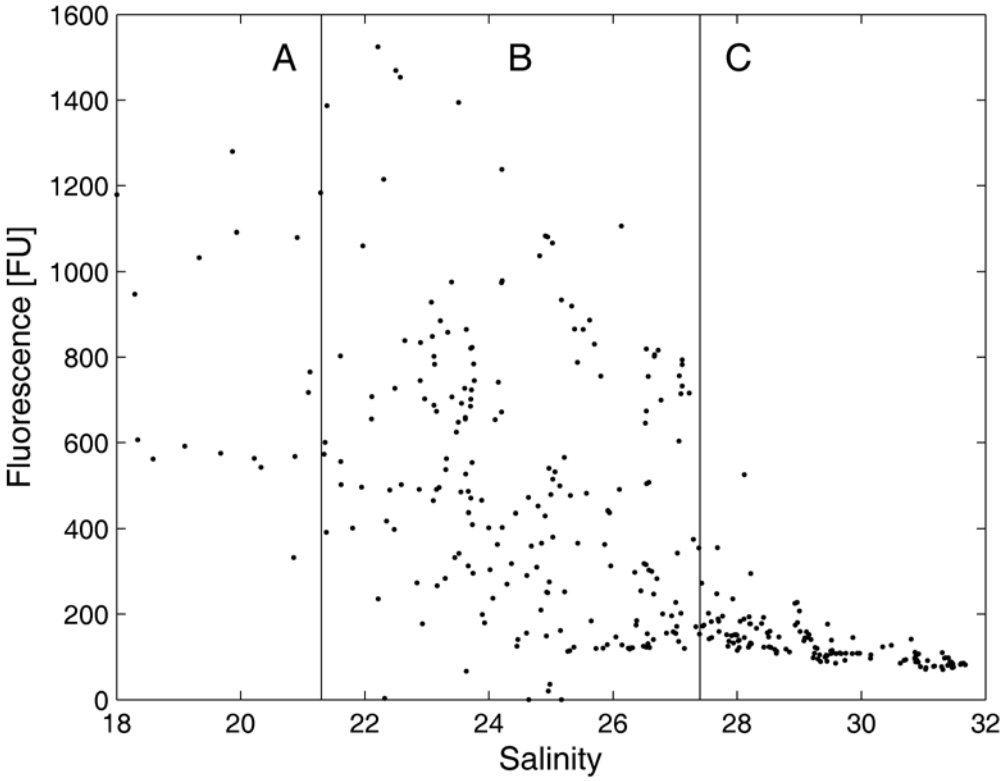

Figure 2.5 Fluorescence distribution. Section 'A' is dominated by the river and does not exhibit a trend, Section 'B' shows a steeply declining phytoplankton population, and Section 'C' shows a much milder decline. The general trends are reminiscent of that seen with nitrate (Figure 3). However, the Section B/C boundary is ~2.5 salinity units higher with fluorescence. The fluorescence B/C boundary matches the second LAP activity peak.

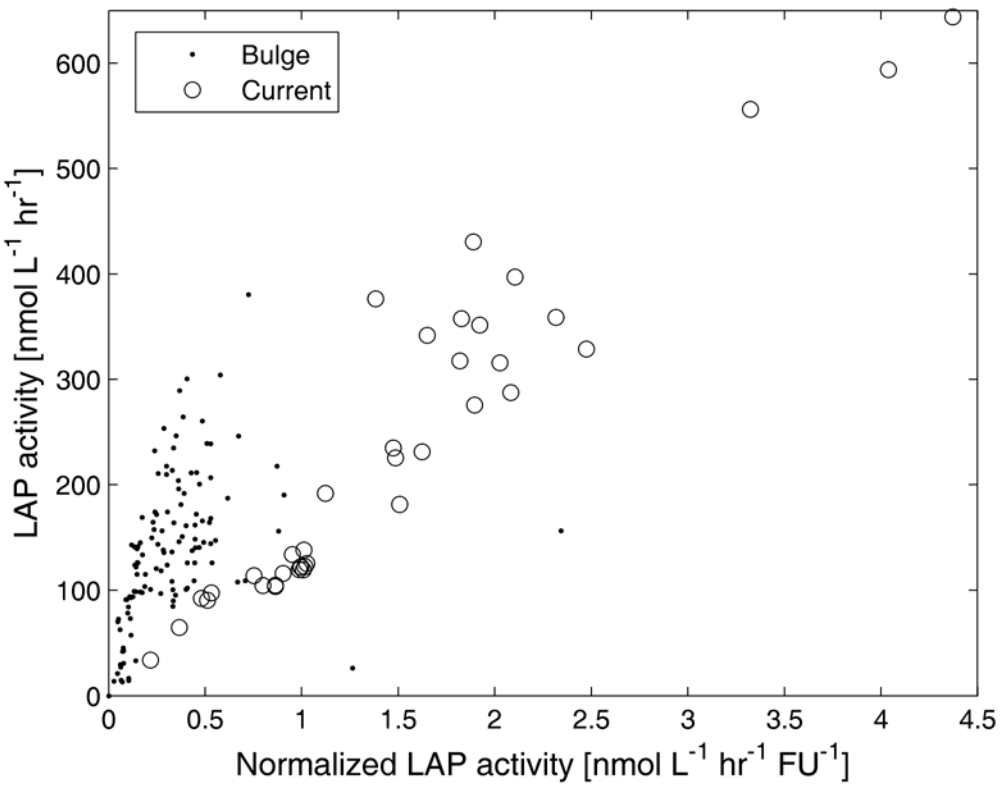

Figure 2.6 Normalized vs. non-normalized LAP activity. LAP activity was normalized to fluorescence on the abscissa. Black dots are samples taken from within the bulge box, and open circles are samples from within the coastal current box. For any given LAP activity, a smaller normalized LAP activity is seen in the bulge samples, suggesting more of the LAP activities are due to phytoplankton in the bulge.

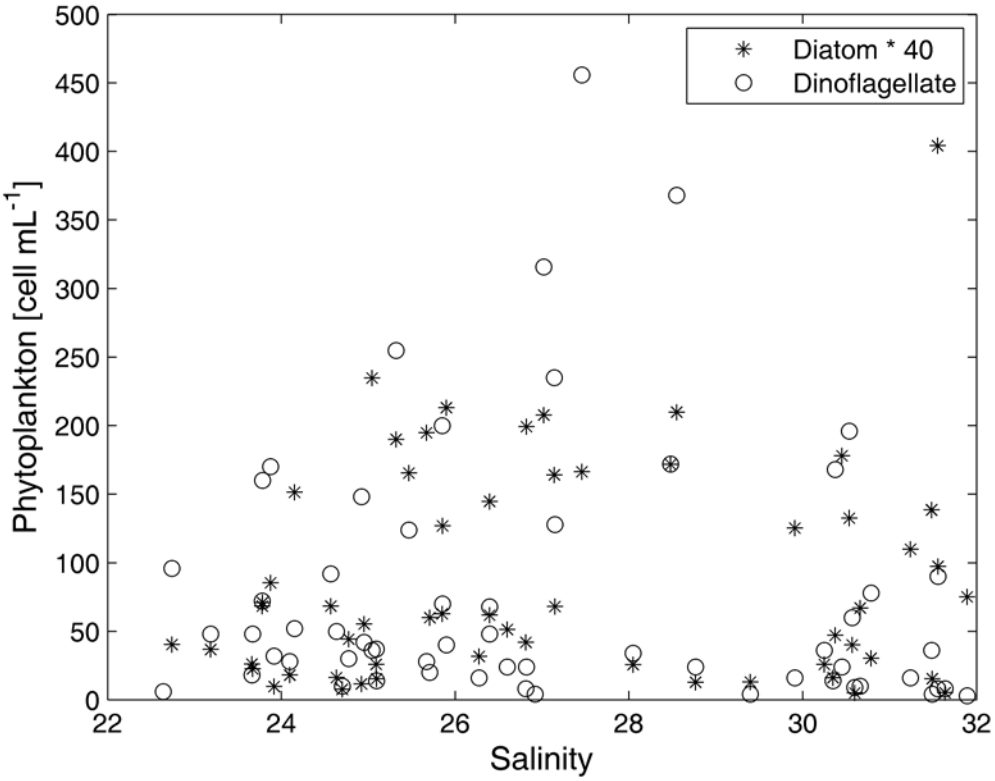

Figure 2.7 Flow cytometry. For diatom numbers, the listed value on the ordinate axis needs to be multiplied by 40 (e.g. 150 diatoms mL^{-1} on the plot is actually 600 counted diatoms). Two diatom samples are not shown, at salinity 22.6 and 26.9 and with counts of 2146 and 2269 cells mL^{-1} respectively.

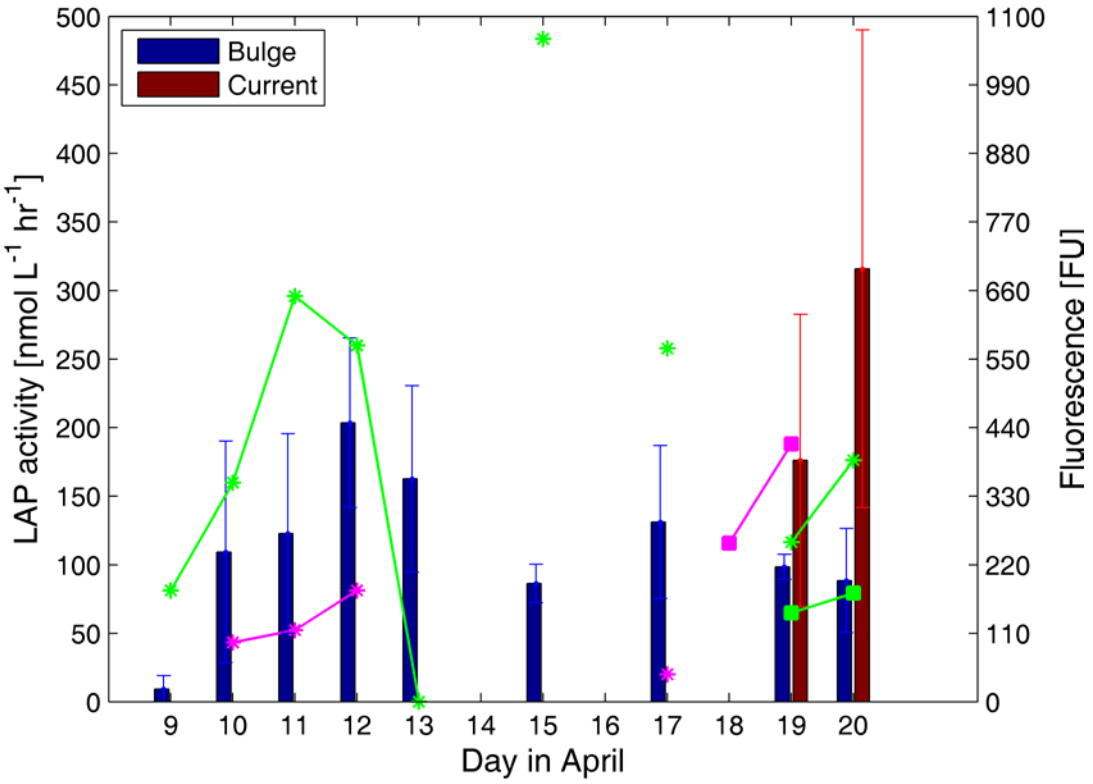

Figure 2.8 LAP activity time-series. LAP activities are the colored bars. Blue bars are LAP activities from the bulge box, and the red bars are from the coastal current box. Error bars are one standard deviation. Total fluorescence values are in green and use the right side ordinal axis. Dinoflagellate counts (cells mL^{-1}) are magenta, and share the left side ordinal scale with LAP activity. In both cases, asterisks are data from the bulge box, and squares are from the coastal current box.

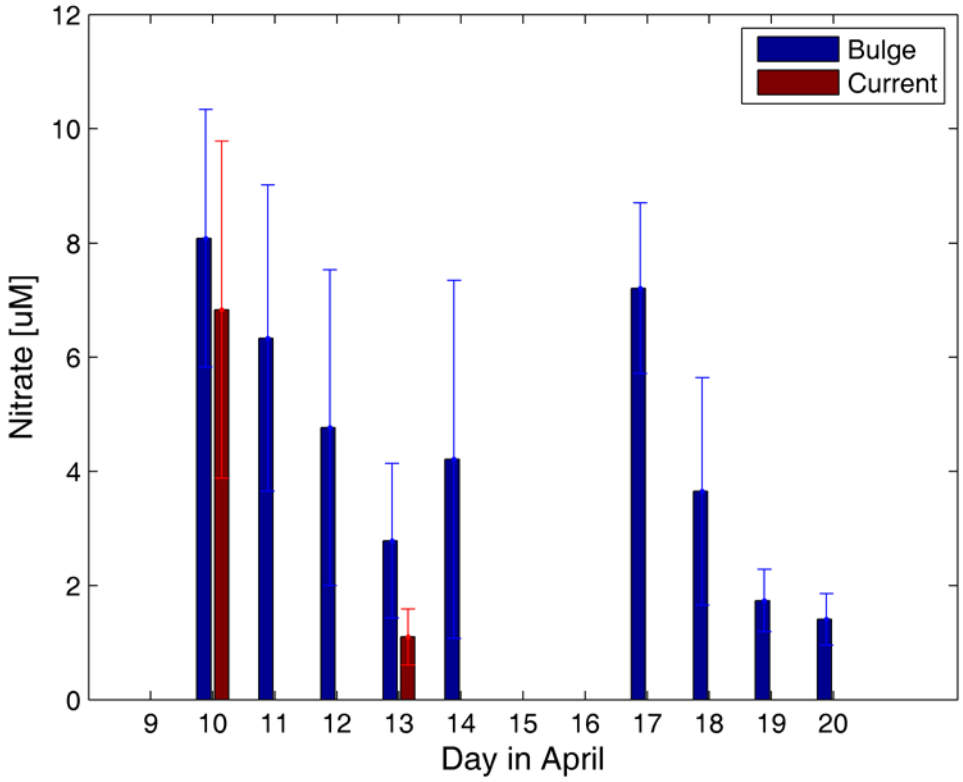

Figure 2.9 Nitrate time-series. Samples from the bulge box are blue; samples from the coastal current box are in red. Error bars are one standard deviation.

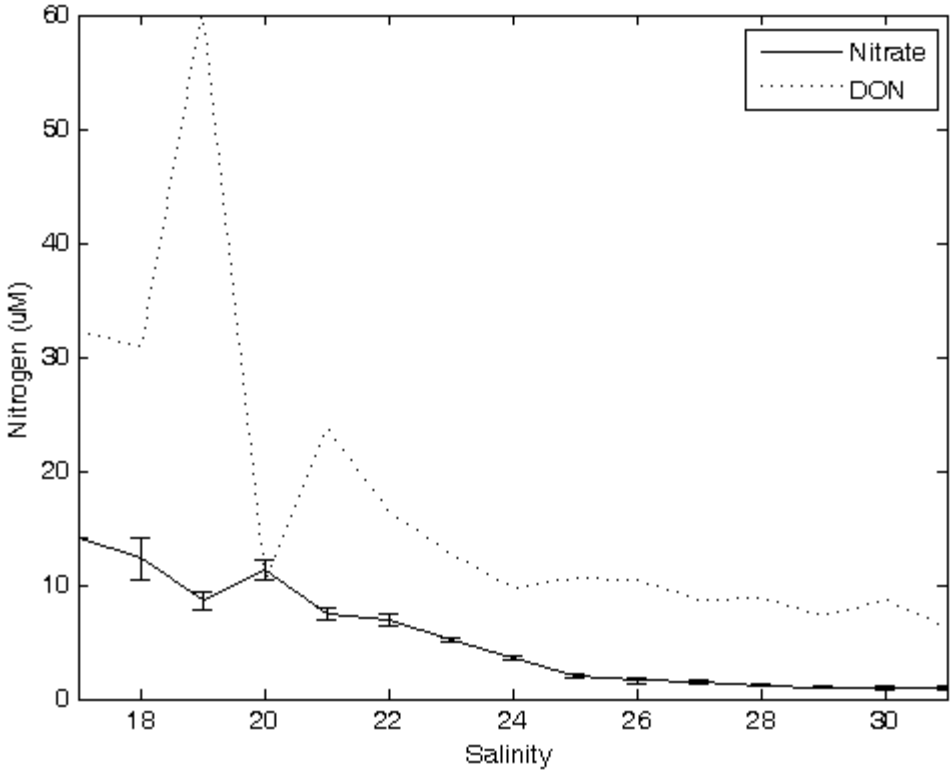

Figure 3.1 Nitrate and dissolved organic nitrogen (DON) concentrations. Each was binned by unit salinity and the median value taken of each salinity bin. Error bars in median nitrate are standard error. DON was calculated from median nitrate and interpolated median total nitrogen values.

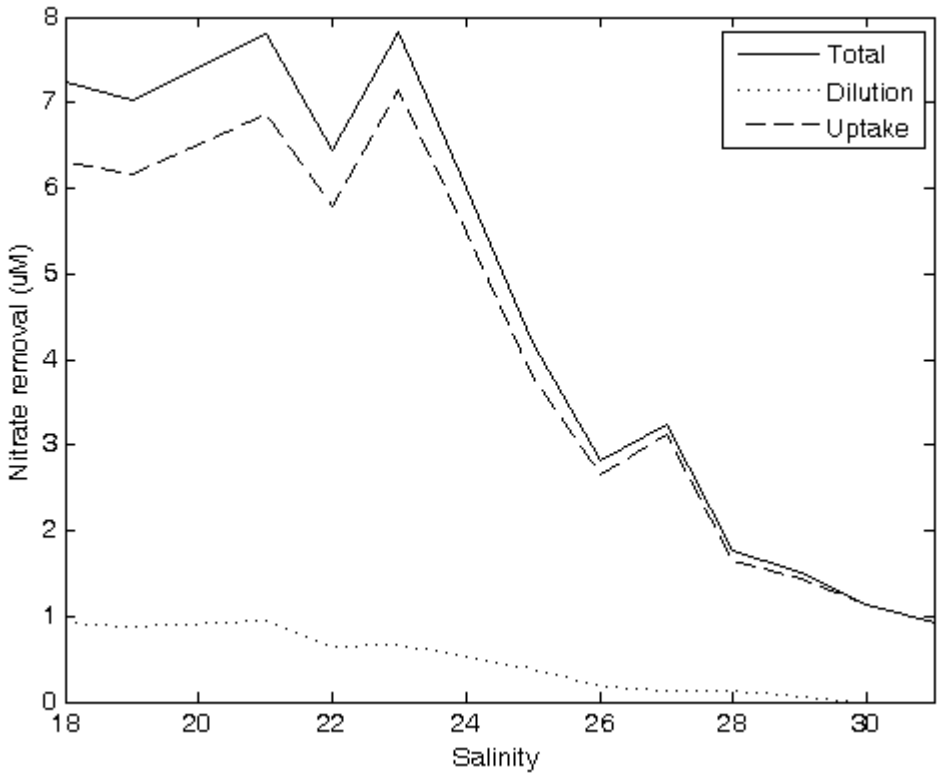

Figure 3.2 Nitrate removal processes. Dilution and uptake were calculated according to equations 1 and 2. Total removal, referred to as the *predicted removal*, is the sum of the dilution and uptake curves. All removal processes are positive, with the understanding that their effect will be to lower existing nitrate concentrations.

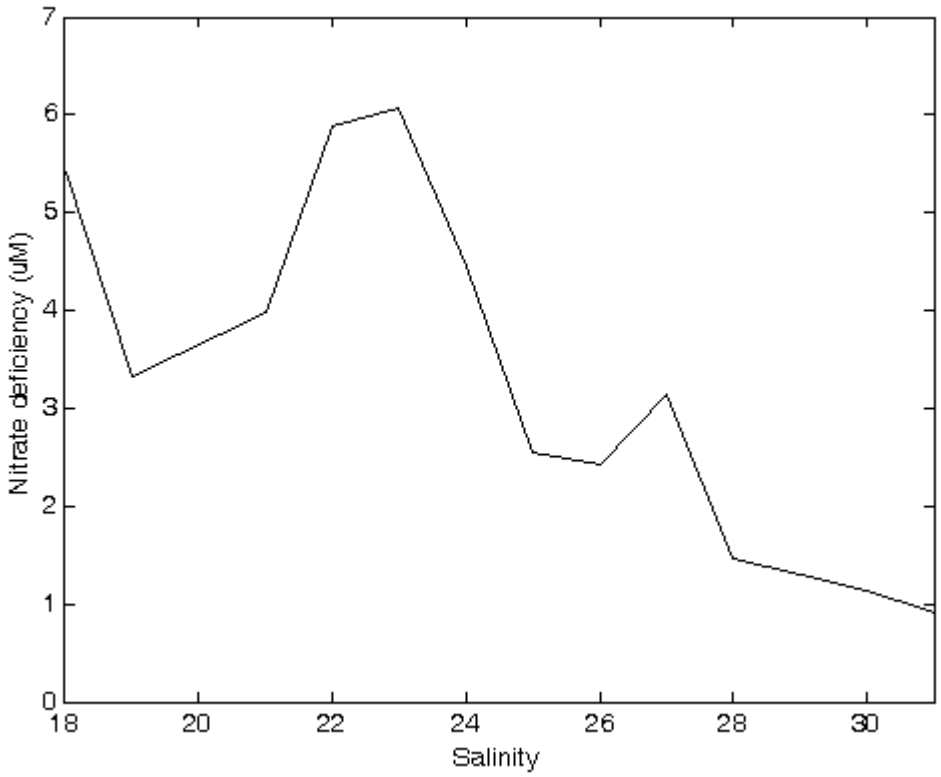

Figure 3.3 Nitrate deficiency. The deficiency is the difference between the predicted removal of nitrate and the measured difference. A positive deficiency indicates an in situ source of nitrate or nitrate equivalents. A nitrate deficit is not calculated for salinity 20 due to a positive change in median nitrate.

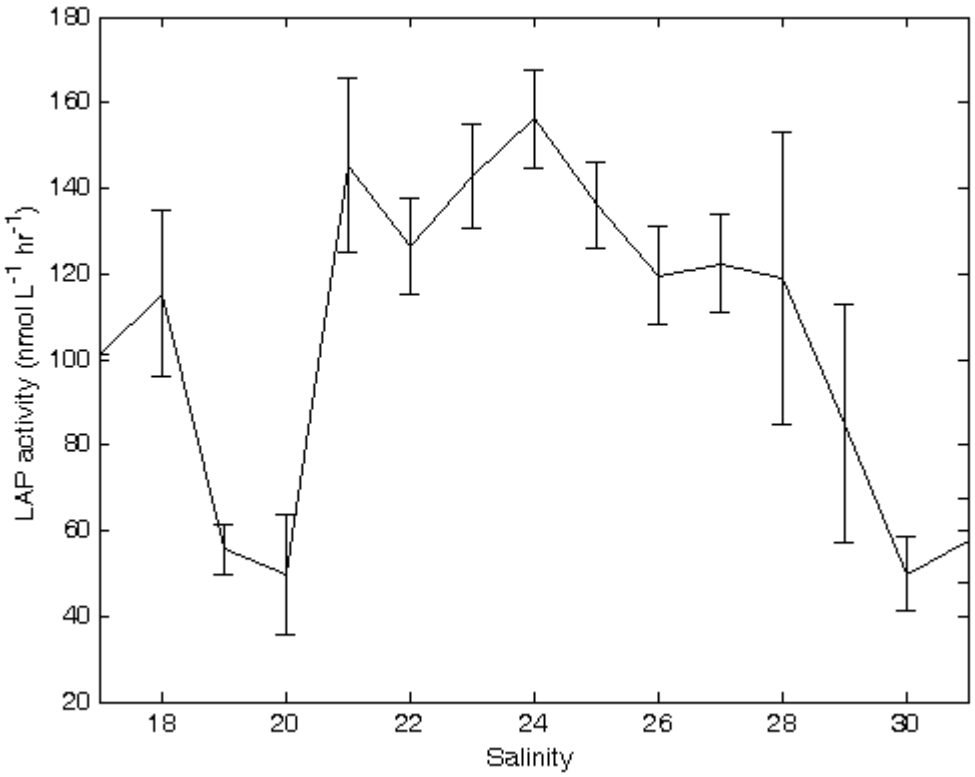

Figure 3.4 LAP activity. The values are median LAP, and the error bars are standard error.

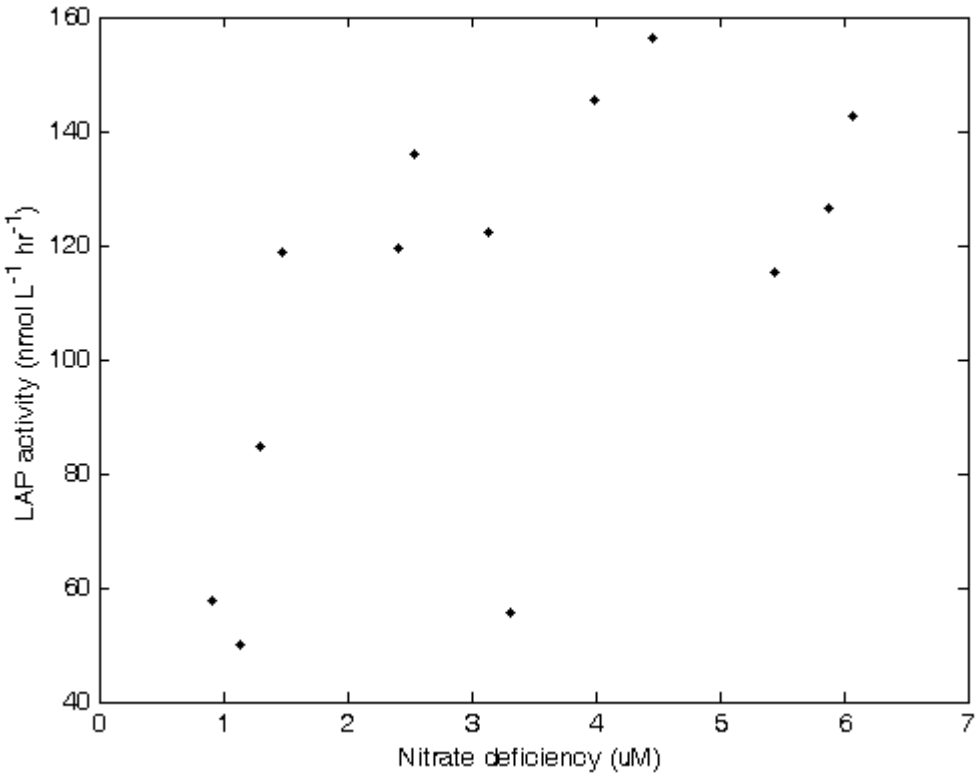

Figure 3.5 LAP activity and nitrate deficiency. Unlike the exponential increase of most ectoenzyme induction curves, LAP activity increases logarithmically with nitrate deficiency.

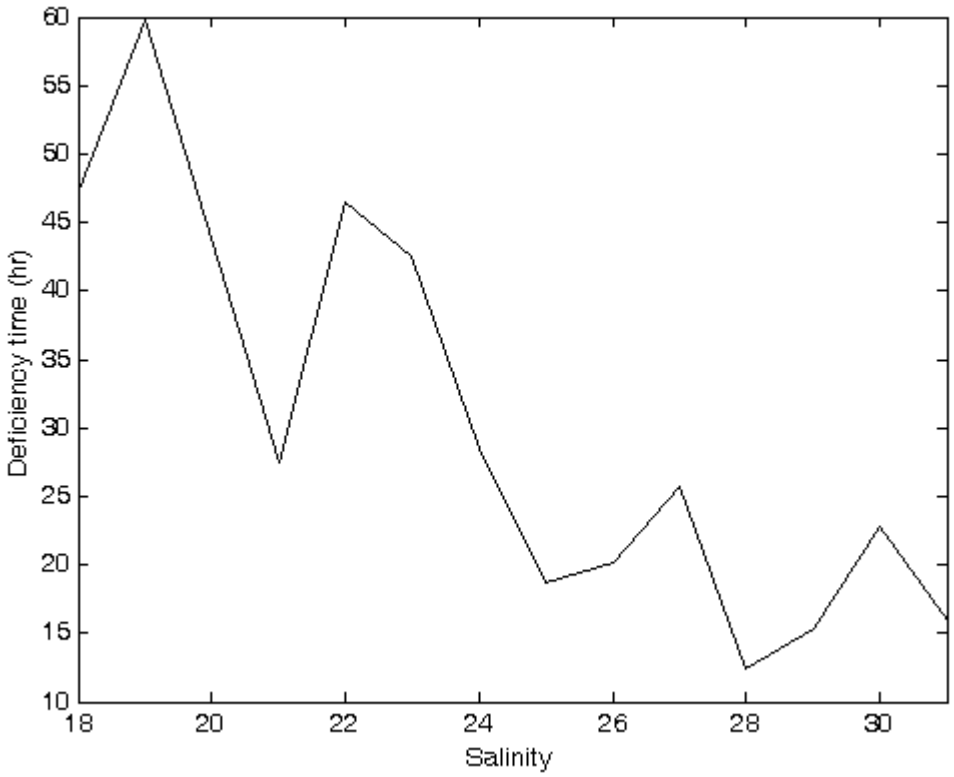

Figure 3.6 Deficiency time. The deficiency time is the number of hours required for LAP activity in a given salinity bin to produce enough nitrate equivalents to offset the calculated deficiency. For instance, if a salinity bin had a nitrate deficiency of 1 uM nitrate, and LAP activity in that bin were 100 nmol L^{-1} hr^{-1}, it would take 10 hours for LAP activity to create 1 uM of nitrate equivalents.

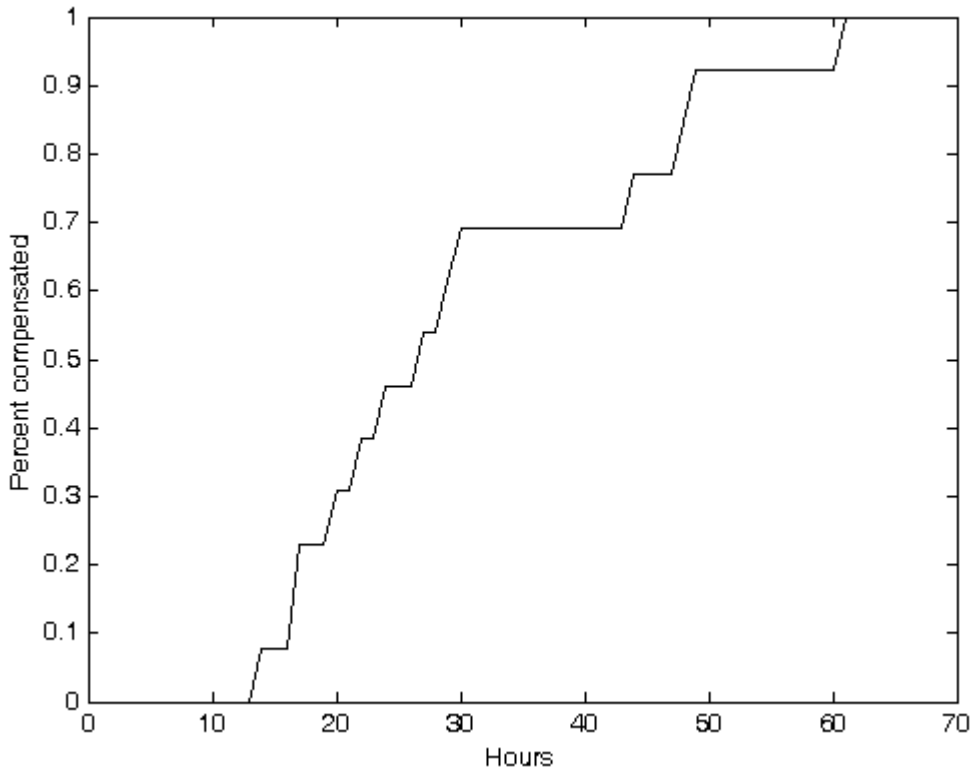

Figure 3.7 Percent compensation. Given sufficient time, LAP activity can generate any quantity of nitrate equivalents. When enough nitrate equivalents have been produced by LAP activity to equal the nitrate deficiency, the deficiency has been compensated for. For each hour of nitrate equivalent production by LAP, the percentage of salinity bins which have been compensated for (nitrate equivalent production = nitrate deficiency) is recorded as the percent complete.

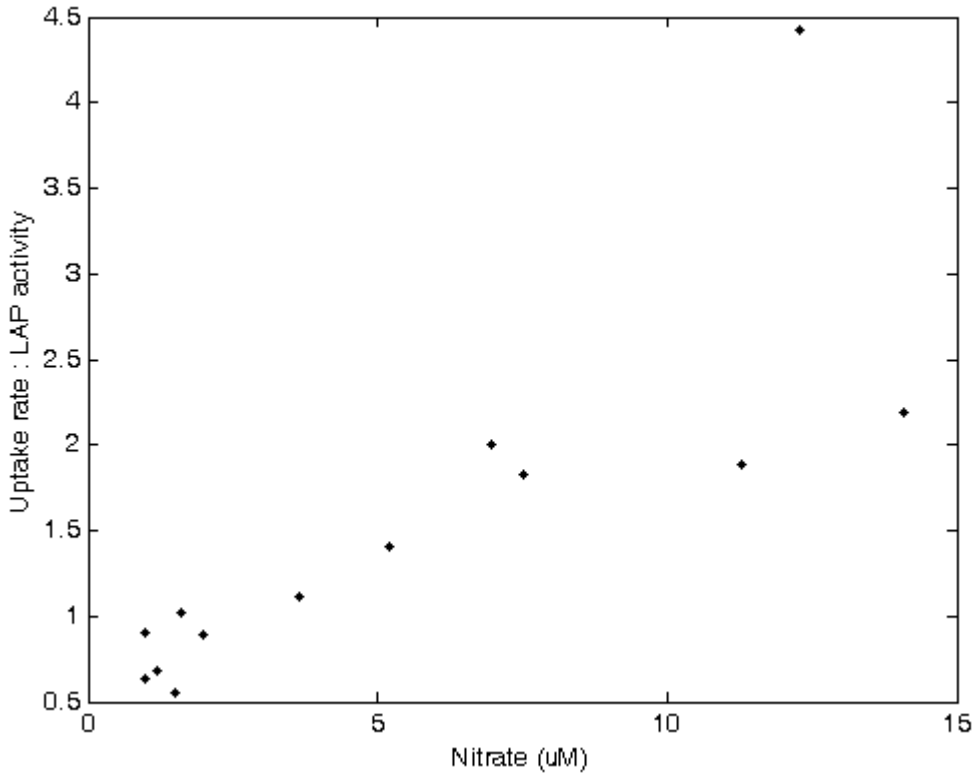

Figure 3.8 Uptake rate : LAP activity ratio. The uptake rate : LAP activity ratio is an indication of the coupling strength. A small ratio suggests more nitrate equivalents are being produced than used, and those equivalents are then available for non-LAP-producing organisms.

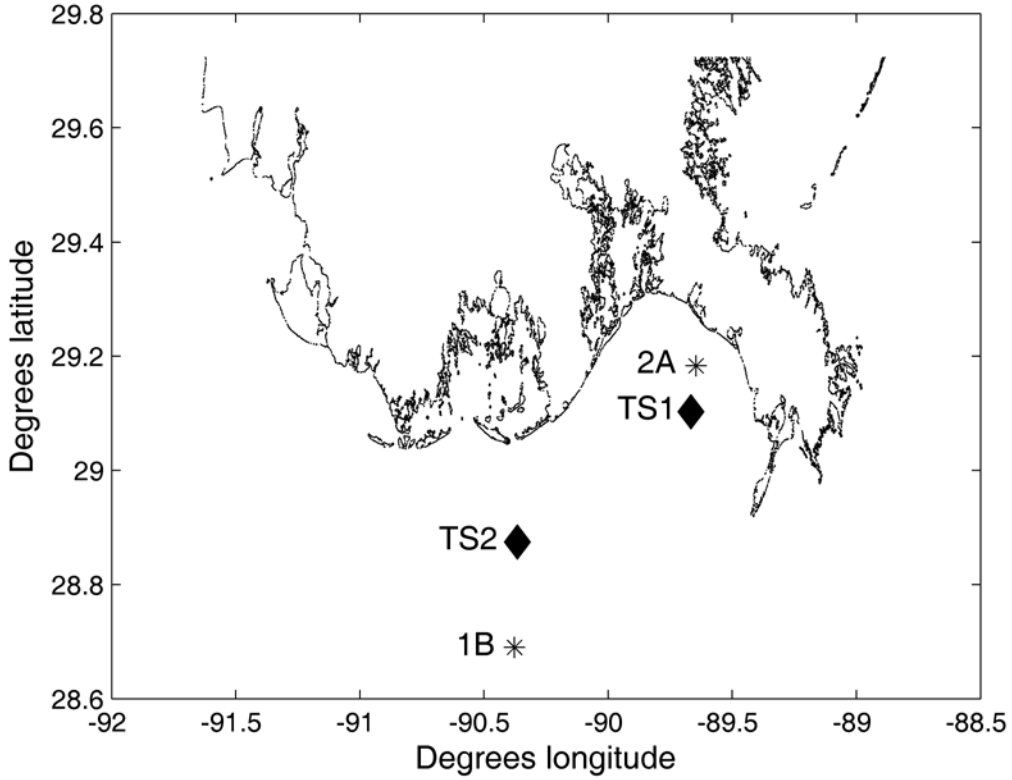

Figure 4.1 Louisiana shelf. The black diamonds are the locations of the two time-series stations described in this work. Stations TS1 and TS2 correspond geographically with stations 2A and 1B (asterisks) from Sylvan et al (2006). Both stations TS1 and 2A are located south of Barrataria Bay, while TS2 and 1B are south of Terrebonne Bay.

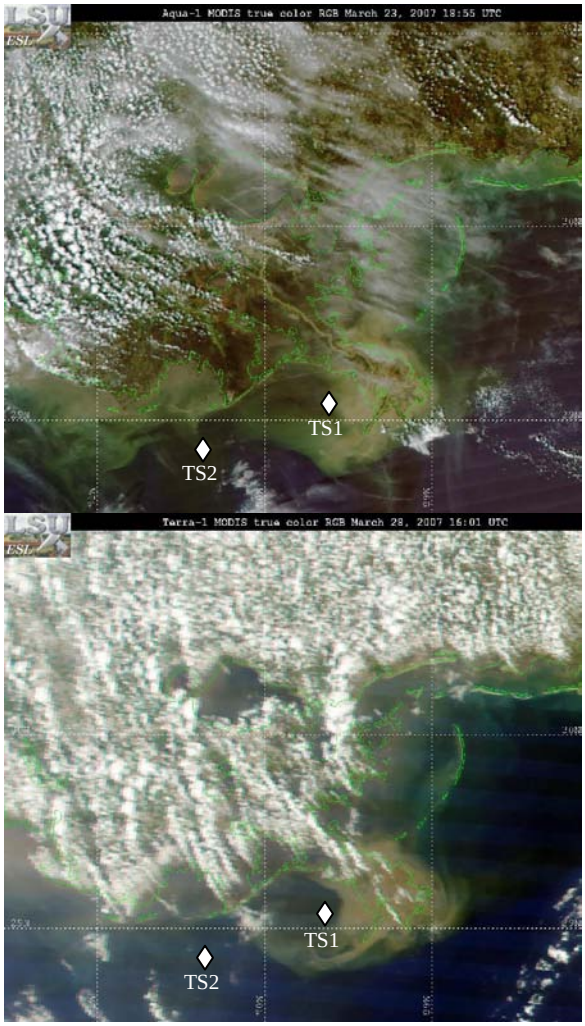

Figure 4.2 Satellite imagery. Left image is from the 23 March 2007 during TS1 measurement, and the right image is from 28 March 2007 during TS2 sampling. Approximate locations of TS2 and TS2 are marked by white diamonds. Images are from the LSU Earth Scan Laboratory.

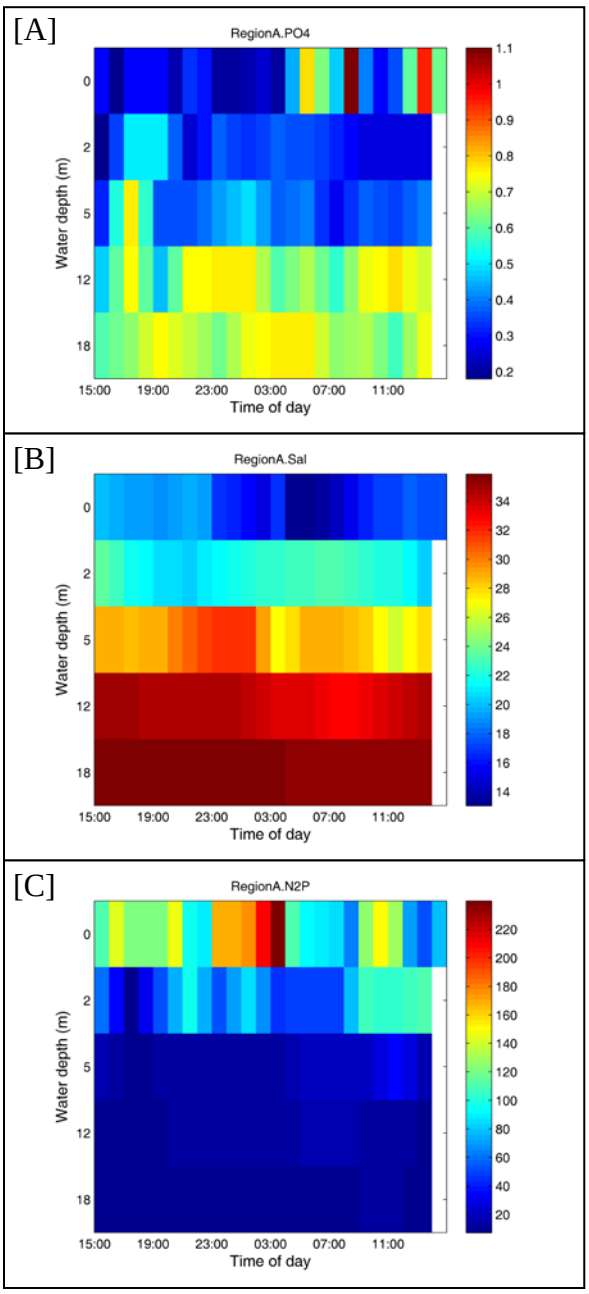

Figure 4.3 Environmental variables at station TS1. The variables are: SRP (A), salinity (B), DIN : SRP ratio (C). In each plot, the abscissa is the time of day (GMT, local + 6hr), and the ordinal axis is water depth in meters. Depths are discrete; there is no correction for mixing between the depths. The color scale is the magnitude of each environmental variable.

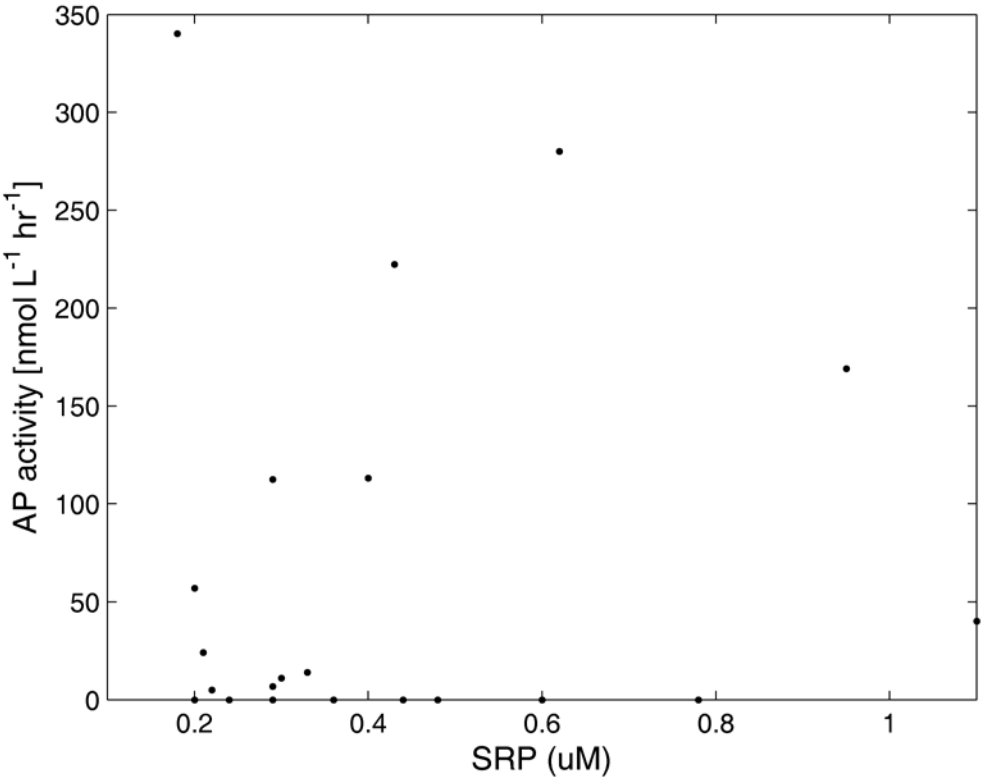

Figure 4.4 AP activity and SRP at TS1. Both values are taken in surface waters.

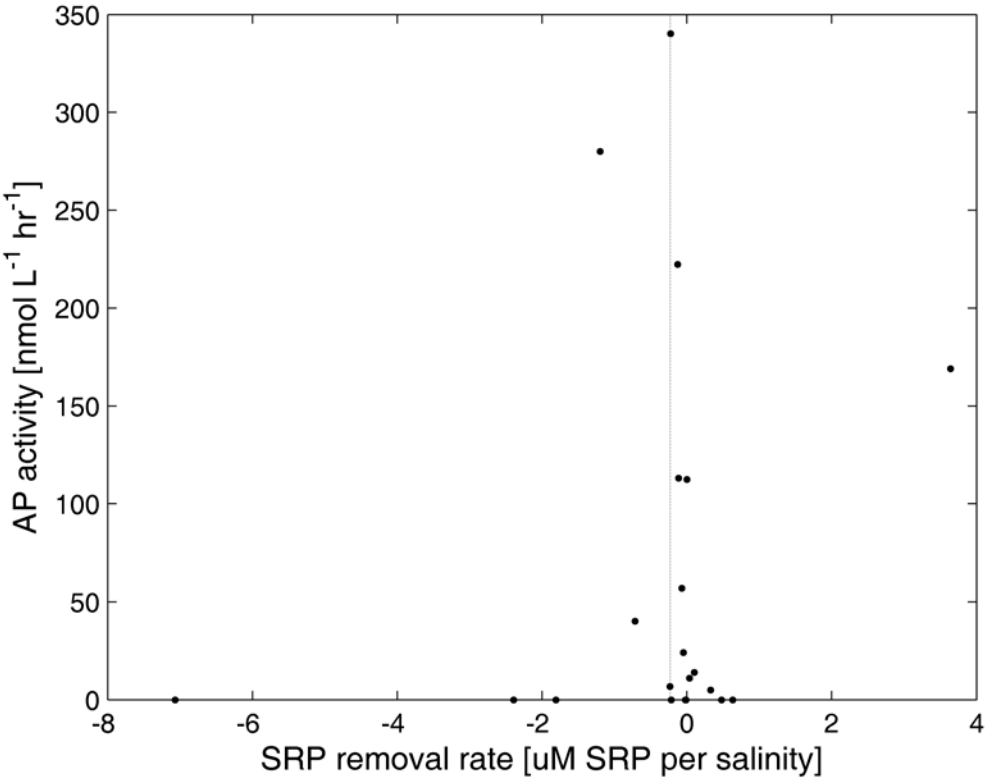

Figure 4.5 AP activity and SRP removal rate at TS1. The abscissa is the difference in surface SRP per unit salinity. The conservative mixing line between SRP and salinity has a slope of -0.047 uM SRP per salinity unit. Positive SRP removal rates imply the addition of SRP; negative rates decrease SRP. Values above this imply a source of SRP. A linear trend is seen between -0.05 and -0.2 uM per salinity unit, which is the range just below the conservative mixing value. The lower boundary of -0.2 uM per salinity unit is marked by a vertical dotted line.

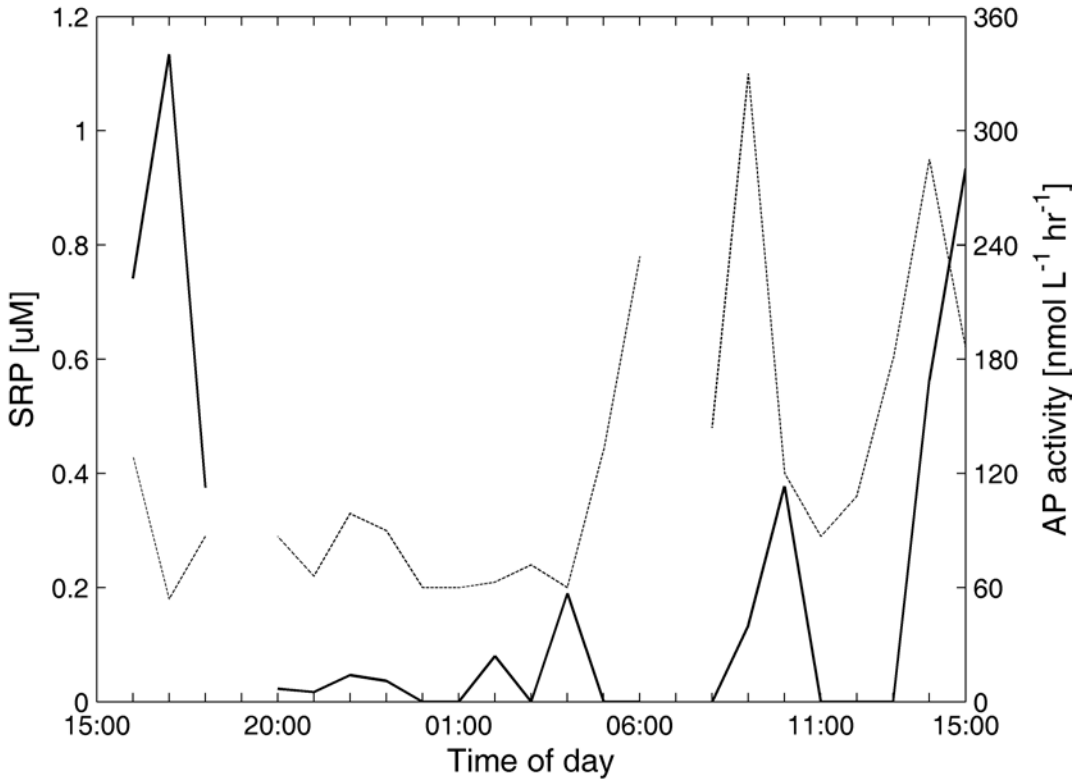

Figure 4.6 Time-series of SRP and AP activity at TS1. The dashed line is for SRP and corresponds with the left ordinal axis, which the solid line is for AP activity on the right axis. Gaps exist when cast data was not available. The high SRP value at 09:00 is a single point and should be viewed with suspicion.

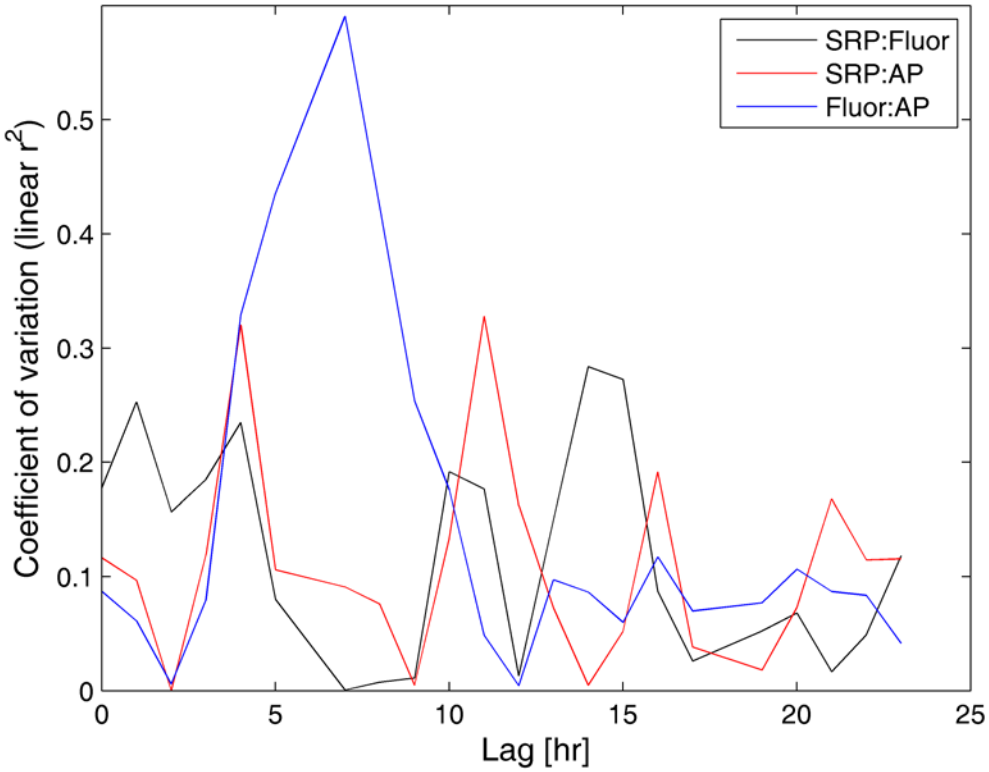

Figure 4.7 Environmental parameter lag at TS1. The coefficient of variation (r^2) using a linear fit was calculated between SRP and fluorescence (SRP : Fluor), SRP and AP activity (SRP : AP), and between fluorescence and AP activity (Fluor : AP). The second variable in each grouping was then lagged by one hour and the r^2 recalculated; this is similar to a cross-correlation analysis. This technique is specifically designed to look for linearity created by the time lag, even though initial relationships between SRP and fluorescence and SRP and AP activity are have a decaying exponential form. The r^2 for SRP : AP considers data only where SRP $\leq$ 0.3 uM (where AP induction is likely to occur).

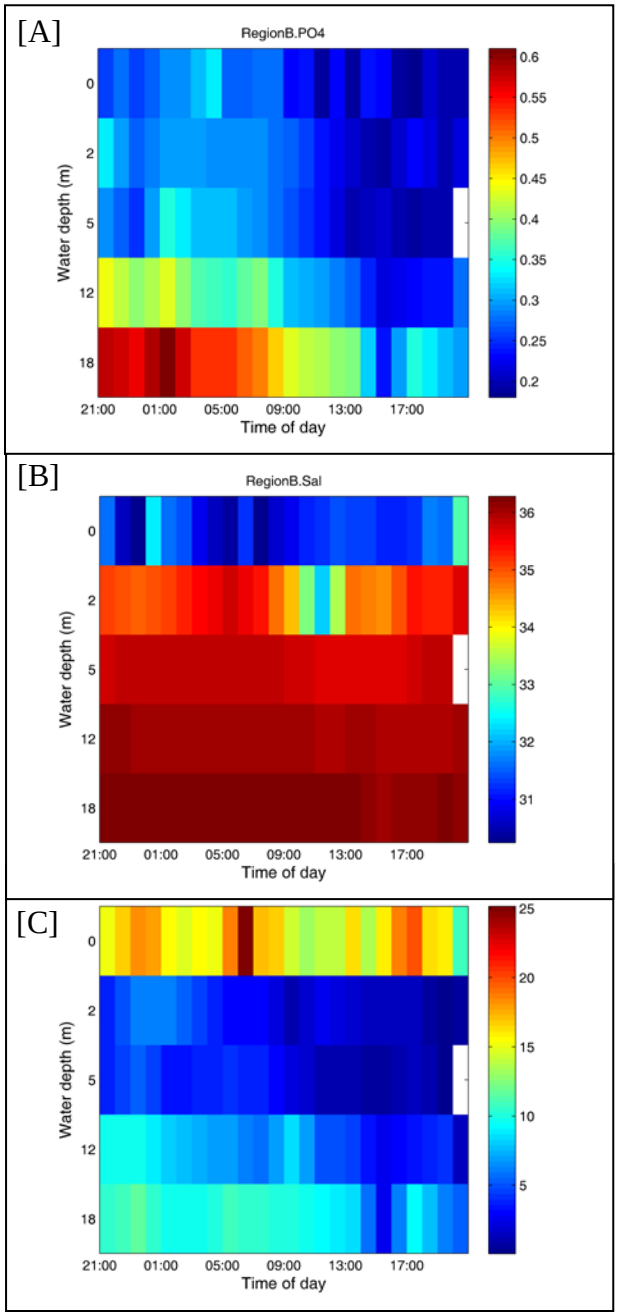

Figure 4.8 Environmental variables at station TS2. The variables are: SRP (A), salinity (B), DIN : SRP ratio (C). In each plot, the abscissa is the time of day (GMT, local + 6hr), and the ordinal axis is water depth. Depths are discrete; there is no correction for mixing between the depths. The color scale is the magnitude of each environmental variable.

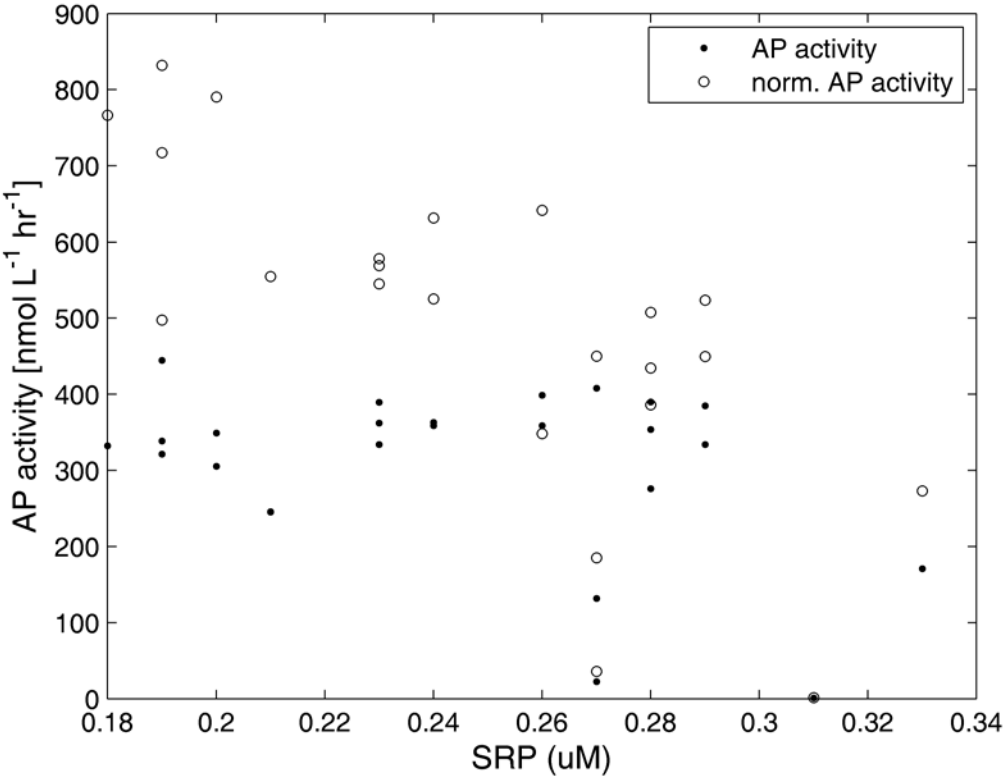

Figure 4.9 AP activity and SRP at TS2. Both values are taken in surface waters. Closed circles are values of AP activity plotted against SRP concentration. Open circles are AP activity normalized by fluorescence, plotted against SRP concentration. Note the different direction in the slope of the two data. One data point at (0.20, 2813) is not displayed to improve image scaling.

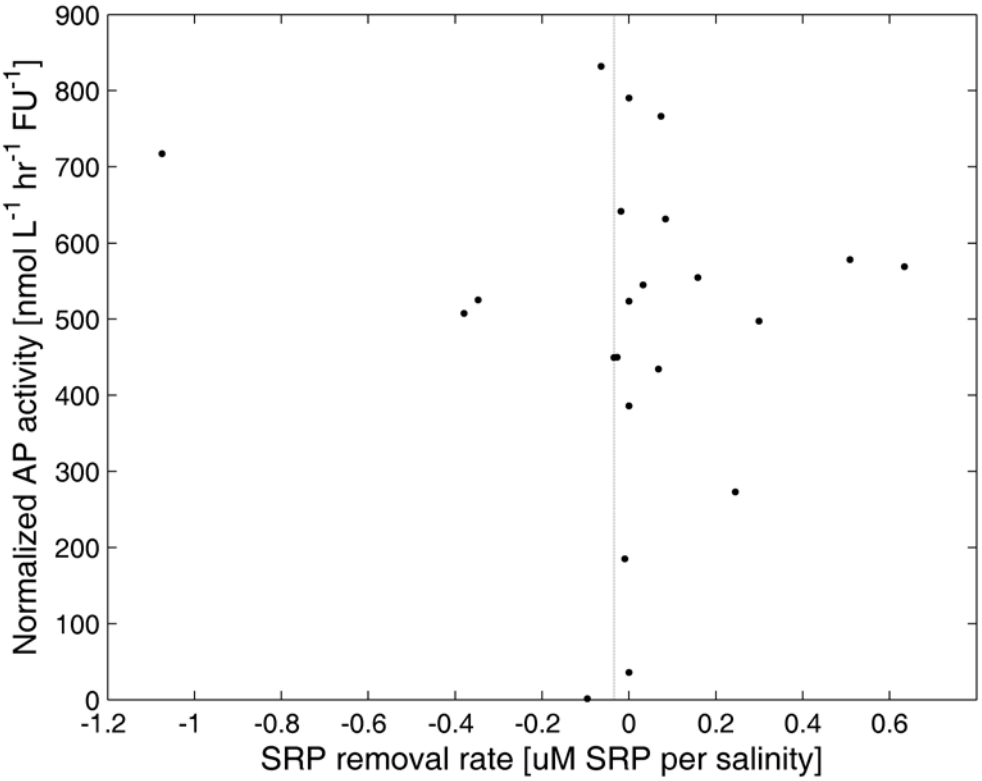

Figure 4.10 Normalized AP activity and SRP removal rate at TS2. The abscissa is the change in surface SRP per unit salinity. The conservative mixing line between SRP and salinity has a slope of -0.034 uM SRP per salinity unit. Positive SRP removal rates imply the addition of SRP; negative rates decrease SRP. The removal rate of the conservative mixing line is marked by the vertical dotted line. One data point at (-0.041, 2813) is not displayed to improve image scaling.

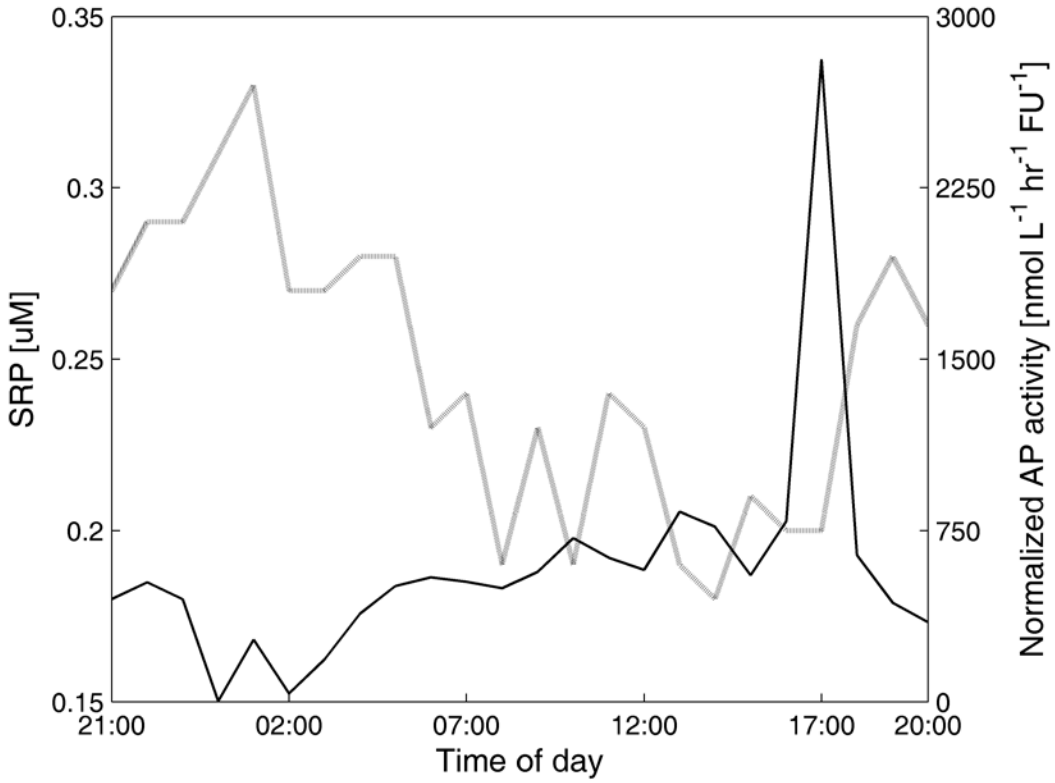

Figure 4.11 Time-series of SRP and AP activity at TS2. The dashed line is for SRP and corresponds with the left ordinal axis, which the solid line is for AP activity on the right axis. AP activity is normalized by fluorescence to account for the change in direction with respect to SRP (see text for details).

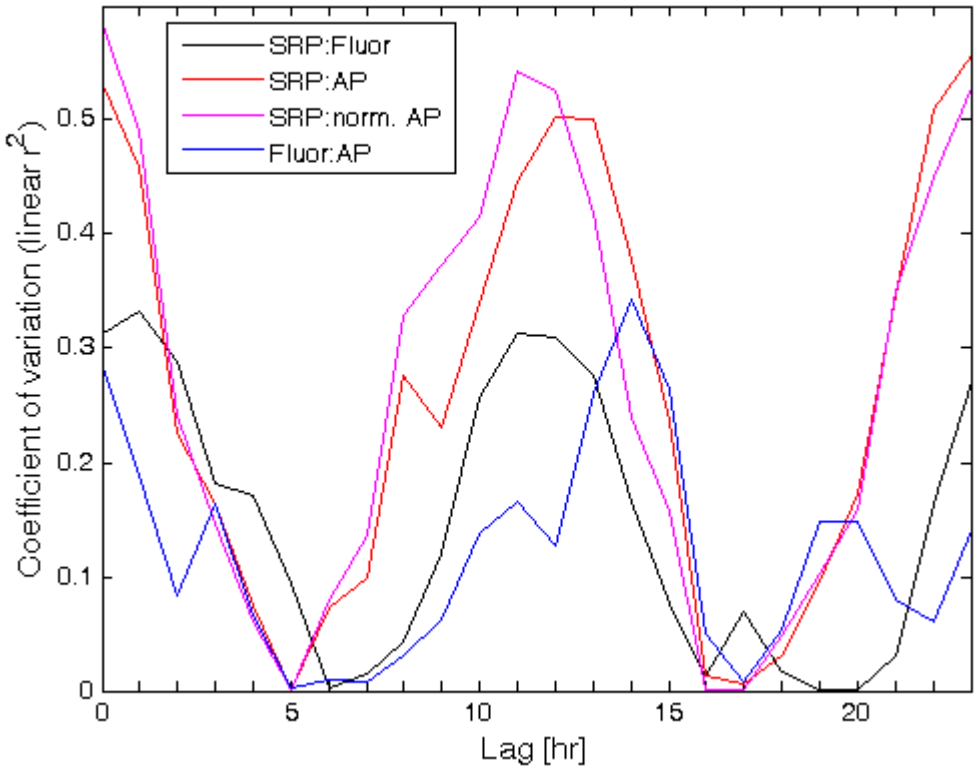

Figure 4.12 Environmental parameter lag at TS2. The coefficient of variation (r^2) using a linear fit was calculated between SRP and fluorescence (SRP : Fluor), SRP and AP activity (SRP : AP), and between fluorescence and AP activity (Fluor : AP). The second variable in each grouping was then lagged by one hour and the r^2 recalculated; this is similar to a cross-correlation analysis. This technique is specifically designed to look for linearity created by the time lag, even though initial relationships between SRP and fluorescence and SRP and AP activity are have a decaying exponential form. The r^2 for SRP : AP considers data only where SRP $\leq$ 0.3 uM (where AP induction is likely to occur).

APPENDIX OF MATLAB CODE

Main_Program

```
FileName = uigetfile('*.dat','Select the FiaLab file');
display(FileName)
Fid=fopen(FileName);
%Fid=fopen('test1.dat');
%FileName='test1.dat';
%Yes, there needs to be two of these
Header=fgetl(Fid);
Header=fgetl(Fid);

%parse data header from time/date
temp=Header;
for n=1:2
    [parse,temp]=strtok(temp,',');
    HeaderIndex(n,:)=str2double(parse);
end
Date=sscanf(temp,'%*2c%19c');

%Rearrange for datenum
Date=datenum([str2double(Date(1:4)),str2double(Date(6:7)),s
tr2double(Date(9:10))...

str2double(Date(12:13)),str2double(Date(15:16)),str2double(
Date(18:19))]);

%Gets names and indices, removes dead data, concatenates
indices
[NameTime,Name,LineIndexA,LineIndexB]=textread(FileName,'%f
%q %u %u %*[^\n]',HeaderIndex(1,1)*2-
1,'headerlines',3,'delimiter',',');
LineIndex=[LineIndexA(1:2:end),LineIndexB(1:2:end),floor(Li
neIndexA(1:2:end)+(LineIndexB(1:2:end)-
LineIndexA(1:2:end))*.75),...
    LineIndexB(1:2:end)];
%LineIndex=[LineIndexA(1:2:end),LineIndexA(1:2:end)+39,Line
IndexA(1:2:end)+22,LineIndexB(1:2:end)];

Name=Name(1:2:end);
NameTime=Date+NameTime(1:2:end)/86400;

%main_program2 correction- removal of last row when last
sample is short
if
LineIndex(end,3)>LineIndex(end,4)||LineIndex(end,2)>LineInd
ex(end,4)
```

```
    LineIndex=LineIndex(1:end-1,:);
    Name=Name(1:end-1);
end

%Gets data from first 2 columns (time and fluorescence of
channel 1)
[Time,FU]=textread(FileName,'%f%f%*[^\n]',HeaderIndex(2,1),
'headerlines',HeaderIndex(1,1)*2+2,'delimiter',',');
Time2=Date+Time/86400;

%Arrange data according to variable
%determine distance between killed controls
StdIndex=strmatch(' Stand',Name);
BlkIndex=strmatch(' B',Name);
DFIndex=strmatch(' D',Name);
KCIndex=strmatch(' K',Name);
ISIndex=strmatch(' I',Name);
SampIndex=strmatch(' Samp',Name);

KCspread=KCIndex(2)-KCIndex(1)-2;

%Calculate standard slope
Conc=3000;

for n=1:length(StdIndex)

StdAvg(n,1)=mean(FU(LineIndex(StdIndex(n),3):LineIndex(StdI
ndex(n),2)));
end
BlkAvg=mean(FU(LineIndex(BlkIndex,3):LineIndex(BlkIndex,2))
);
DFAvg=max(FU(LineIndex(DFIndex,3):LineIndex(DFIndex,2)));

DF=DFAvg/StdAvg;
StdSlope=polyfit([0 Conc/DF],[BlkAvg StdAvg],1);
StdSlope=StdSlope(1,1);

%Calculate slope and R of samples
for n=1:length(SampIndex)

temp=[LineIndex(SampIndex(n),3):LineIndex(SampIndex(n),2)]'
;
    SampAvg(n)=mean(FU(temp));
    SampSlope(n,:)=polyfit(Time(temp),FU(temp),1);
    tSampR=corrcoef(Time(temp),FU(temp));
    SampR(n,1)=abs(tSampR(1,2));
end
```

```
SampSlope=SampSlope(:,1);

%Create standard correction using internal standards
%subtract killed control slope from sample slope
for n=1:length(ISIndex)

ISAvg(n,1)=mean(FU(LineIndex(ISIndex(n),3):LineIndex(ISInde
x(n),2)));

temp=[LineIndex(KCIndex(n),3):LineIndex(KCIndex(n),2)]';
    KCSlope(n,:)=polyfit(Time(temp),FU(temp),1);
    if KCSlope(n,1)<0
        KCSlope2(n,1)=0;
    else KCSlope2(n,1)=KCSlope(n,1);
    end
    KCAvg(n,1)=mean(FU(temp));
    SampSlopeKC(n*KCspread-(KCspread-
1):n*KCspread,1)=SampSlope(n*KCspread-(KCspread-
1):n*KCspread,1)-KCSlope(n,1);
    SampSlopeKC2(n*KCspread-(KCspread-
1):n*KCspread,1)=SampSlope(n*KCspread-(KCspread-
1):n*KCspread,1)-KCSlope2(n,1);
end
if length(SampSlopeKC)<length(SampSlope)
    SampSlopeKC=[SampSlopeKC;SampSlope((n*KCspread)+1:end)-
KCSlope(n,1)];

SampSlopeKC2=[SampSlopeKC2;SampSlope((n*KCspread)+1:end)-
KCSlope2(n,1)];
end

KCSlope=KCSlope(:,1);
StdSlopeIS=StdSlope*(ISAvg/StdAvg(end));
StdSlopeIS=interp1([NameTime(StdIndex(end));NameTime(ISInde
x)],[StdSlope;StdSlopeIS],NameTime,'linear',StdSlopeIS(end)
);
StdSlopeIS=StdSlopeIS(SampIndex);

%Calculate activities of all samples without KC or IS
correction
SampAct=SampSlope/StdSlope*3600;

%Calculate activities of all samples with KC correction
SampActKC=SampSlopeKC/StdSlope*3600;
SampActKC2=SampSlopeKC2/StdSlope*3600;

%Calculate activities of all samples with IS correction
```

```
SampActIS=SampSlope./StdSlopeIS*3600;

%Calculate activities of all samples with KC and IS
correction
SampActKCIS=SampSlopeKC./StdSlopeIS*3600;
SampActKC2IS=SampSlopeKC2./StdSlopeIS*3600;

%Calculate activities of samples with KC and IS correction
with R2 values >0.85
R2Index=find(SampR>=sqrt(0.85));
```

LAP_Model

```
%load data
load NO3_vars
load Shuttle_vars
load age_dist
load HPLC

%to plot or not to plot
Plot=1;

%Remove data where fluoro=0
F=find(Fluoro~=0&Act>0);
Act=Act(F);
Sal=Sal(F);
Fluoro=Fluoro(F);

%calculate FU:NO3 ratio
F=find(Sal>29);
Slope1=polyfit(Sal(F),Fluoro(F),1);
F2=find(NO3Sal>29&NO3<=2);
Slope2=polyfit(NO3Sal(F2),NO3(F2),1);
Chl2NO3=mean((Slope1(1,1)*[29:0.5:32]+Slope1(1,2))./(Slope2
(1,1)*[29:0.5:32]+Slope2(1,2)));

%adjust NO3, FW, and Shuttle TN values
i=1;
for n=17:31
    T=find(NO3Sal>=n-0.5&NO3Sal<=n+0.5);
    T3=find(ShuttleSal>=n-0.5&ShuttleSal<=n+.5);
    T4=find(NO3ModelSal>=n-0.5&NO3ModelSal<=n+0.5);
    NO3med(i,1)=median(NO3(T));
    NO3std(i,1)=std(NO3(T));
    NO3sterr(i,1)=NO3std(i,1)/sqrt(length(T));
    TNmed(i,1)=median(ShuttleTN(T3));
    binSal(i,1)=n;
    i=i+1;
end

%fill in NaNs
TNmed=interp1(binSal(find(~isnan(TNmed))),TNmed(find(~isnan
(TNmed))),binSal);

%bin data by salinity units
%find mean,std of Fluoro
i=1;
for n=17:31
    T=find(Sal>=n-0.5&Sal<=n+0.5);
```

```
    Fluoromed(i,1)=median(Fluoro(T));
    Fluorostd(i,1)=std(Fluoro(T));
    Fluorosterr(i,1)=Fluorostd(i,1)/sqrt(length(T));
    Actmed(i,1)=median(Act(T));
    Actstd(i,1)=std(Act(T));
    Actsterr(i,1)=Actstd(i,1)/sqrt(length(T));
    i=i+1;
end

%Calculate Shuttle DON & replace NaNs
DONmed=TNmed-NO3med;
DONmed=interp1(binSal(find(~isnan(DONmed))),DONmed(find(~is
nan(DONmed))),binSal);

dNO3=diff(NO3med);
t=find(dNO3<=0);
dNO3=abs(dNO3(t));

plotSal=binSal(2:end);
plotSal=plotSal(t);
NO3med2=NO3med(1:end-1);
NO3med2=NO3med2(t);
Actmed2=Actmed(2:end);
Actmed2=Actmed2(t);

%Dilution prediction with changing conservative mixing
Uptake=Fluoromed/Chl2NO3;
Dilution=(min(NO3med)-NO3med)./(31-binSal);
Dilution2=(min(NO3med)-(NO3med-[Uptake(2:end);0]))./(31-
binSal);
Uptake=Uptake(2:end);
Uptake=Uptake(t);
UptakeRate=Uptake/25*1000;
Dilution=Dilution(1:end-1);
Dilution=abs(Dilution(t));
Dilution2=Dilution2(1:end-1);
Dilution2=abs(Dilution2(t));

pNO3=Dilution+Uptake;

%F=find(dNO3>Dilution(1:end-1));
%P=(dNO3-Dilution(1:end-1))./dNO3;
Dil2Uptake=Dilution./pNO3;
Excess=pNO3-dNO3;
R2=corrcoef(pNO3,dNO3);

RepleteTime=abs(Excess)./Actmed2*1e3;
```

```
DONmed2=DONmed(2:end);
DONmed2=DONmed2(t);
NoDON=find(.4*DONmed2<Excess);
AvailDON=min([.15*DONmed2 Excess],[],2);
LeftOver=Excess-AvailDON;

for n=0:max(ceil(RepleteTime))

Percent(n+1,1)=length(find(RepleteTime<=n))/length(RepleteT
ime);
end

if Plot==1
    %nitrate distribution
    figure(1)
    errorbar(binSal,NO3med,NO3sterr,NO3sterr,'k')
    xlabel('Salinity')
    ylabel('Nitrogen (uM)')
    xlim([17 31])
    hold on
    plot(binSal,DONmed,'k:')
    legend('Nitrate','DON')

    %nitrate removal mechanisms
    figure(2)
    plot(plotSal,pNO3,'k-
',plotSal,Dilution,'k:',plotSal,Uptake,'k--')
    xlabel('Salinity')
    ylabel('Nitrate removal (uM)')
    legend('Total','Dilution','Uptake')
    xlim([18 31])

    %nitrate deficiency
    figure(3)
    plot(plotSal,Excess,'k-')
    xlabel('Salinity')
    ylabel('Nitrate deficiency (uM)')
    xlim([18 31])

    %LAP distribution
    figure(4)
    errorbar(binSal,Actmed,Actsterr,Actsterr,'k')
    xlabel('Salinity')
    ylabel('LAP activity (nmol L^-^1 hr^-^1)')
    xlim([17 31])

    %Repletion time
```

```
    figure(6)
    plot(plotSal,RepleteTime,'k-')
    xlabel('Salinity')
    ylabel('Deficiency time (hr)')
    xlim([18 31])

    %Percent replete
    figure(7)
    plot(Percent,'k-')
    xlabel('Hours')
    ylabel('Percent compensated')

    %deficit vs activity
    figure(5)
    plot(Excess,Actmed2,'k.')
    xlabel('Nitrate deficiency (uM)')
    ylabel('LAP activity (nmol L^-^1 hr^-^1)')

    %uncoupling
    figure(8)
    plot(NO3med2,UptakeRate./Actmed2,'k.')
    xlabel('Nitrate (uM)')
    ylabel('Uptake rate : LAP activity')
end

%{
%Error propagation
%Equation: sqrt(sigma1^2+sigma2^2+cov(1,2))
Error=sqrt((sqrt(NO3std/sqrt(NO3std.^2).^2)+(sqrt(Fluorostd
.^2).^2))%+2*cov(NO3mean,Fluoromean));
Error=Error(2:end);
Error=ExcessNO3.*Error;

%HPLC data
F=find(~isnan(OscChl)&~isnan(OscSal));
plot(OscSal(F),(Diatom(F)./OscChl(F))/max(Diatom(F)./OscChl
(F)),'k.',...
OscSal(F),(Dino(F)./OscChl(F))/max(Dino(F)./OscChl(F)),'r.'
)
%}

%{
%the necessary plots
%%%%%%%%%%%%%%%%%%%%%%%%
%Nitrate distribution
plot(NO3Sal,NO3,'k.')
hold on
```

```
errorbar(binSal,NO3mean,NO3sterr,NO3sterr,'r-')
xlim([22 31])
xlabel('Salinity')
ylabel('Nitrate (uM)')

%%%%%%%%%%%%%%%%%%%%%%%%%
%Fluorescence distribution
plot(Sal,Fluoro,'k.')
hold on
errorbar(binSal,Fluoromean,Fluorosterr,Fluorosterr,'r-')
xlim([22 31])
xlabel('Salinity')
ylabel('Fluorescence (FU)')
%}
```

Curriculum Vitae
BRIAN M. GAAS

EDUCATION

2010 Ph.D. Oceanography, Rutgers University, New Brunswick, New Jersey
2006 M.S. Oceanography, Rutgers University, New Brunswick, New Jersey
2002 B.S. Biochemistry and Genetics, Texas A&M University, College Station, Texas

PUBLICATIONS

Ammerman, J.W., Gaas, B.M., and Sylvan, J.S. (2009) Nitrogen and phosphorus reduction goals in the new Gulf of Mexico Hypoxia Action Plan reflect new science and an emerging consensus. Submitted to EOS.

Jaeger, S.A., Gaas, B.M., Klinkhammer, G.P., and Ammerman, J.A. (2009) Multiple enzyme analyzer (MEA): steps toward the in situ detection of microbial community ectoenzyme activities. Limnology and Oceanography: Methods. 7: 716-729.

Gaas, B.M., and Ammerman, J.W. (2007) Automated high resolution ectoenzyme measurements: instrument development and deployment in three trophic regimes. Limnology and Oceanography: Methods. 5: 463-473.

Adams, H., Anderson, K., Feather, J., Gaas, B., Hodel, C., O'Donnell, K. (2003) Klickitat River Fish Barriers Survey. Washington Department of Fish and Wildlife.

PRINCIPLE OCCUPATIONS

2009-2010 Researcher
Spring 2009 Co-Instructor for “Current Topics in Oceanography”
2003-2009 Graduate Research Assistant